61. Top Quark

Revised September 2021 by T.M. Liss (City Coll. of New York), F. Maltoni (CP3 U. catholique de Louvain; Bologna U.) and A. Quadt (Göttingen U.).

61.1 Introduction

In the Standard Model (SM), the left-handed top quark is the $Q = 2/3$, $T_3 = +1/2$ member of the weak-isospin doublet containing the bottom quark, while the right-handed top is an $SU(2)_L$ singlet (see, e.g., the review "Electroweak Model and Constraints on New Physics" here). Its phenomenology is driven by its large mass. Being heavier than a W boson, it is the only quark that decays semi-weakly, i.e., into a real W boson and a b quark. This results in a lifetime that is shorter than the hadronization time. In addition, it is the only quark whose Yukawa coupling to the Higgs boson is of order unity. For these reasons, the top quark plays a special role in the Standard Model and in many extensions thereof. Top quark physics provides a unique laboratory where our understanding of the strong, both in the perturbative and non-perturbative regimes, and electroweak interactions can be tested. An accurate knowledge of its properties (mass, couplings, production cross sections, decay branching ratios, *etc.*) can bring key information on fundamental interactions at the electroweak symmetry-breaking scale and beyond. This review provides a concise discussion of the experimental and theoretical issues involved in the determination of the top-quark properties.

61.2 Top-quark production at the Tevatron and LHC

In hadron collisions, top quarks are produced dominantly in pairs through the processes $q\bar{q} \to t\bar{t}$ and $gg \to t\bar{t}$, at leading order in QCD. At the Tevatron ($p\bar{p}$ at 1.96 TeV) approximately 85% of the production cross section is from $q\bar{q}$ annihilation, with the remainder from gluon-gluon fusion. Conversely, at the LHC about 90% (80%) of $t\bar{t}$ production is from gluon-gluon fusion at $\sqrt{s} = 13$ TeV ($\sqrt{s} = 7$ TeV).

Predictions for the top-quark production total cross sections are available at next-to-next-to leading order (NNLO) [1, 2], also including next-to-next-to-leading-log (NNLL) soft gluon resummation. Assuming a top-quark mass of 173.3 GeV/c^2, close to the Tevatron + LHC combination [3], the resulting theoretical prediction of the top-quark pair cross-section at NNLO+NNLL accuracy at the Tevatron at $\sqrt{s} = 1.96$ TeV is $\sigma_{t\bar{t}} = 7.16^{+0.11+0.17}_{-0.20-0.12}$ pb where the first uncertainty is from scale dependence and the second from parton distribution functions. At the LHC, assuming a top-quark mass of 172.5 GeV/c^2 the cross sections are: $\sigma_{t\bar{t}} = 177.3^{+4.6+9.0}_{-6.0-9.0}$ pb at $\sqrt{s} = 7$ TeV, $\sigma_{t\bar{t}} = 252.9^{+6.4+11.7}_{-8.6-11.7}$ pb at $\sqrt{s} = 8$ TeV, $\sigma_{t\bar{t}} = 831.8^{+19.8+35.1}_{-29.2-35.1}$ pb at $\sqrt{s} = 13$ TeV, and $\sigma_{t\bar{t}} = 984.5^{+23.2+41.3}_{-34.7-41.3}$ pb at $\sqrt{s} = 14$ TeV [1].

Electroweak single top-quark production mechanisms, namely from $q\bar{q}' \to t\bar{b}$ [4], $qb \to q't$ [5], mediated by virtual s-channel and t-channel W-bosons, and Wt-associated production, through $bg \to W^-t$, lead to somewhat smaller cross sections. For example, t-channel production, while suppressed by the weak coupling with respect to the strong pair production, is kinematically enhanced, resulting in a sizeable cross section both at Tevatron and LHC energies. At the Tevatron, the t- and s-channel cross sections for top quarks are identical to those for antitop quarks , while at the LHC they are not, due to the charge-asymmetric initial state. NNLO cross sections for t-channel single top-quark production ($t + \bar{t}$) are calculated for $m_t = 173.2$ GeV/c^2 to be $2.08^{+0.04+0.08}_{-0.03-0.10}$ pb in $p\bar{p}$ collisions at $\sqrt{s} = 1.96$ TeV, where the first uncertainty is from scale dependence and the second from parton distribution functions. [6]. A calculation at NNLO accuracy for the t-channel cross section at the LHC has first appeared in [7], superseded by more recent calculations [6, 8] which predict ($m_t = 172.5$ GeV/c^2): $\sigma_{t+\bar{t}} = 64.0^{+0.77}_{-0.38}$ pb at $\sqrt{s} = 7$ TeV, $\sigma_{t+\bar{t}} = 84.6^{+1.0}_{-0.5}$ pb at

$\sqrt{s} = 8$ TeV, $\sigma_{t+\bar{t}} = 215^{+2.1}_{-1.3}$ pb at $\sqrt{s} = 13$ TeV, and $\sigma_{t+\bar{t}} = 245^{+2.7}_{-1.3}$ pb at $\sqrt{s} = 14$ TeV, where the quoted uncertainties are from scale variation only. For the s-channel, NNLO approximated calculations yield $1.03^{+0.05}_{-0.05}$ pb for the Tevatron [9]. An NLO calculation gives $4.3^{+0.13+0.14}_{-0.10-0.14}$ pb, $5.2^{+0.15+0.16}_{-0.12-0.16}$ pb, and $10.3^{+0.29+0.27}_{-0.24-0.27}$ pb for $\sqrt{s} = 7, 8, 13$ TeV at the LHC, respectively, with 64%, 64%, 62%, of top quarks. While negligible at the Tevatron, at LHC energies the Wt-associated production becomes relevant. At $\sqrt{s} = 7, 8, 13$ TeV, an approximate NNLO calculation gives $(t+\bar{t})$, $15.7^{+0.4+1.10}_{-0.4-1.14}$ pb , $22.4^{+0.6+1.40}_{-0.6-1.40}$ pb , $71.7^{+1.8+3.40}_{-1.8-3.40}$ pb , respectively, with an equal proportion of top and anti-top quarks [10].

Assuming $|V_{tb}| \gg |V_{td}|, |V_{ts}|$ (see the review "The CKM Quark-Mixing Matrix" for more information), the cross sections for single top production are proportional to $|V_{tb}|^2$, and no extra hypothesis is needed on the number of quark families or on the unitarity of the CKM matrix in extracting $|V_{tb}|$. Separate measurements of the s- and t-channel processes provide sensitivity to physics beyond the Standard Model [11].

With a mass above the Wb threshold, and $|V_{tb}| \gg |V_{td}|$, $|V_{ts}|$, the decay width of the top quark is expected to be dominated by the two-body channel $t \to Wb$. Neglecting terms of order m_b^2/m_t^2, α_s^2, and $(\alpha_s/\pi)M_W^2/m_t^2$, the width predicted in the SM at NLO is [12]:

$$\Gamma_t = \frac{G_F m_t^3}{8\pi\sqrt{2}} \left(1 - \frac{M_W^2}{m_t^2}\right)^2 \left(1 + 2\frac{M_W^2}{m_t^2}\right) \left[1 - \frac{2\alpha_s}{3\pi}\left(\frac{2\pi^2}{3} - \frac{5}{2}\right)\right], \tag{61.1}$$

where m_t refers to the top-quark pole mass. The width for a value of $m_t = 173.3$ GeV/c^2 is 1.35 GeV/c^2 (we use $\alpha_s(M_Z) = 0.118$) and increases with mass. With its correspondingly short lifetime of about 0.5×10^{-24} s, the top quark is expected to decay before top-flavored hadrons or $t\bar{t}$-quarkonium-bound states can form [13]. In fact, since the decay time is close to the would-be-resonance binding time, a peak will be visible in e^+e^- scattering at the $t\bar{t}$ threshold [14] and it is in principle present (yet very difficult to measure) in hadron collisions too [15, 16]. The order α_s^2 QCD corrections to Γ_t are also available [17], thereby improving the overall theoretical accuracy to better than 1%.

The final states for the leading pair-production process can be divided into three classes:

A. $t\bar{t} \to W^+ b\, W^- \bar{b} \to q\bar{q}'\, bq''\, \bar{q}'''\, \bar{b}$, (45.7%)
B. $t\bar{t} \to W^+ b\, W^- \bar{b} \to q\bar{q}'\, b\ell^- \bar{\nu}_\ell\, \bar{b} + \ell^+ \nu_\ell\, b\, q''\bar{q}'''\, \bar{b}$, (43.8%)
C. $t\bar{t} \to W^+ b\, W^- \bar{b} \to \ell^+ \nu_\ell\, b\, \ell'^- \bar{\nu}_{\ell'}\, \bar{b}$. (10.5%)

The quarks in the final state evolve into jets of hadrons. A, B, and C are referred to as the all-hadronic, lepton+jets (ℓ+jets), and dilepton ($\ell\ell$) channels, respectively. Their relative contributions, including hadronic corrections, are given in parentheses assuming lepton universality. While ℓ in the above processes refers to e, μ, or τ, most of the analyses distinguish the e and μ from the τ channel, which is more difficult to reconstruct. Therefore, in what follows, we will use ℓ to refer to e or μ, unless otherwise noted. Here, typically leptonic decays of τ are included. In addition to the quarks resulting from the top-quark decays, extra QCD radiation (quarks and gluons) from the colored particles in the event can lead to extra jets.

The number of jets reconstructed in the detectors depends on the decay kinematics, as well as on the algorithm for reconstructing jets used by the analysis. Information on the transverse momenta, p_T of the neutrinos is obtained from the imbalance in transverse momentum measured in each event (missing p_T, which is here also called missing transverse energy, E_T).

The identification of top quarks in the electroweak single top channel is much more difficult than in the QCD $t\bar{t}$ channel, due to a less distinctive signature and significantly larger backgrounds, mostly due to $t\bar{t}$ and W+jets production.

Fully exclusive predictions via Monte Carlo generators for the $t\bar{t}$ and single top production processes at NLO accuracy in QCD, including top-quark decays and possibly off-shell effects are available [18,19] through the MC@NLO [20] and POWHEG [21] methods. Very recently, the first Monte Carlo implementation of the NNLO computation has become available [22].

Besides fully inclusive QCD or EW top-quark production, more exclusive final states can be accessed at hadron colliders, whose cross sections are typically much smaller, yet can provide key information on the properties of the top quark. For all relevant final states (*e.g.*, $t\bar{t}V$, $t\bar{t}VV$ with $V = \gamma, W, Z$, $t\bar{t}H, t\bar{t}$+jets, $t\bar{t}b\bar{b}, t\bar{t}t\bar{t}$) automatic or semi-automatic predictions at NLO accuracy both in QCD and EW expansions, also in the form of event generators are available (see the review "Monte Carlo event generators" for more information).

61.3 Top-quark measurements

Since the discovery of the top quark, direct measurements of $t\bar{t}$ production have been made at six center-of-mass energies in pp or $p\bar{p}$ and in pPb collisions, providing stringent tests of QCD. The first measurements were made in Run I at the Tevatron at $\sqrt{s} = 1.8$ TeV. In Run II at the Tevatron relatively precise measurements were made at $\sqrt{s} = 1.96$ TeV. Finally, beginning in 2010, measurements have been made at the LHC at $\sqrt{s} = 7$ TeV, $\sqrt{s} = 8$ TeV, and $\sqrt{s} = 13$ TeV, and recently also in dedicated low energy runs at $\sqrt{s} = 5.02$ in pp and at 8.16 TeV in pPb collisions.

Production of single top quarks through electroweak interactions has now been measured with good precision at the Tevatron at $\sqrt{s} = 1.96$ TeV, and at the LHC at $\sqrt{s} = 7$ TeV, $\sqrt{s} = 8$ TeV, and also at $\sqrt{s} = 13$ TeV. Measurements at the Tevatron have managed to separate the s- and t-channel production cross sections, and at the LHC, the tW mechanism as well, though the t-channel is measured with best precision to date. The measurements allow an extraction of the CKM matrix element V_{tb}. Also more exclusive production modes and top-quark properties have been measured in single-top production.

With approximately 10 fb^{-1} of Tevatron data, and almost 5 fb^{-1} at 7 TeV, 20 fb^{-1} at 8 TeV and 139 fb^{-1} at 13 TeV at the LHC, many properties of the top quark have been measured with high precision. These include properties related to the production mechanism, such as $t\bar{t}$ spin correlations, forward-backward or charge asymmetries, and differential production cross sections, as well as properties related to the tWb decay vertex, such as the helicity of the W-bosons from the top-quark decay. Also studies of the $t\bar{t}b\bar{b}$, $t\bar{t}t\bar{t}$, $t\bar{t}\gamma$, $t\bar{t}Z$, $t\bar{t}h$, th, tZq or $t\gamma q$ processes and the corresponding vertices as well as contact interactions have been made, some yielding first observations, others strong evidence. Those processes probe genuinely new aspects of the top-quark such as electroweak couplings to neutral gauge bosons or possibly four-top-quark interactions. In addition, many searches for physics beyond the Standard Model are being performed with increasing reach in both production and decay channels.

In the following sections we review the current status of measurements of the characteristics of the top quark.

61.3.1 *Top-quark production*

61.3.1.1 *$t\bar{t}$ production*

Fig. 61.1 summarizes the $t\bar{t}$ production cross-section measurements from both, the Tevatron and LHC. Please note that some cross section measurements at the LHC have luminosity-related uncertainties which have improved in the meantime [23]. The latest measurement from DØ [24] ($p\bar{p}$ at $\sqrt{s} = 1.96$ TeV), combining the measurements from the dilepton and lepton plus jets final states in 9.7 fb^{-1}, is 7.26 ± 0.13 (stat.)$^{+0.57}_{-0.50}$ (syst.) pb (7.5%). From CDF the most precise measurement made [25] is in 8.8 fb^{-1} in the dilepton channel requiring at least one b-tag, yielding 7.09 ± 0.84 pb. Both of these measurements assume a top-quark mass of 172.5 GeV/c^2. The dependence of the cross-section measurements on the value chosen for the mass is less than that

of the theory calculations because it only affects the determination of the acceptance. In some analyses also the shape of topological variables might be modified.

Combining the recent cross section measurements with older ones in other channels yields $\sigma_{t\bar{t}} = 7.63 \pm 0.50$ pb (6.6%) for CDF, $\sigma_{t\bar{t}} = 7.56 \pm 0.59$ pb (7.8%) for DØ and $\sigma_{t\bar{t}} = 7.60 \pm 0.41$ pb (5.4%) for the Tevatron combination [26]. The contributions to the uncertainty are 0.20 pb from statistical sources, 0.29 pb from systematic sources, and 0.21 pb from the uncertainty on the integrated luminosity. The combined result is in good agreement with the SM expectation of $7.35^{+0.28}_{-0.33}$ pb at NNLO+NNLL in perturbative QCD [1] for a top mass of 172.5 GeV/c^2.

CDF has measured the $t\bar{t}$ production cross section in the dilepton channel with one hadronically decaying tau in 9.0 fb^{-1}, yielding $\sigma_{t\bar{t}} = 8.1 \pm 2.1$ pb. By separately identifying the single-tau and the ditau components, they measure the branching fraction of the top quark into the tau lepton, tau neutrino, and bottom quark to be $(9.6 \pm 2.8)\%$ [27]. CDF has also performed measurements of the $t\bar{t}$ production cross section normalized to the Z production cross section in order to reduce the impact of the luminosity uncertainty [28].

DØ has performed a measurement of differential $t\bar{t}$ cross sections in 9.7 fb^{-1} of lepton+jets data as a function of the transverse momentum, and absolute value of the rapidity of the top quarks as well as of the invariant mass of the $t\bar{t}$ pair [29]. Observed differential cross sections are consistent with SM predictions.

The LHC experiments ATLAS and CMS use similar techniques to measure the $t\bar{t}$ cross section in pp collisions. The most precise measurements come from the dilepton channel, and in particular the $e\mu$ channel. In order to test consistency of the cross-section measurements with some systematic uncertainties cancelling out while testing pQCD and PDFs, cross-section ratios between measurements at 7 TeV and at 8 TeV are performed and quoted in several cases. In other cases, the cross-section ratio between $t\bar{t}$- and Z-production is determined as that is independent of luminosity uncertainties, but keeps its sensitivity to the ratio of gluon versus quark PDFs. These experimental results should be compared to the theoretical calculations at NNLO+NNLL that yield $7.16^{+0.20}_{-0.23}$ pb for top-quark mass of 173.3 GeV/c^2 [1] at $\sqrt{s} = 1.96$ TeV, $68.2 \pm 4.8^{+1.9}_{-2.3}$ pb [30] for top-quark mass of 172.5 GeV/c^2 at $\sqrt{s} = 5$ TeV, and for top-quark mass of 173.3 GeV/c^2 $\sigma_{t\bar{t}} = 173.6^{+4.5+8.9}_{-5.9-8.9}$ pb at $\sqrt{s} = 7$ TeV, $\sigma_{t\bar{t}} = 247.7^{+6.3+11.5}_{-8.5-11.5}$ pb at $\sqrt{s} = 8$ TeV, and $\sigma_{t\bar{t}} = 816.0^{+19.4+34.4}_{-28.6-34.4}$ pb at $\sqrt{s} = 13$ TeV, at the LHC [1]. In a special run, ATLAS recorded 257 pb^{-1} at $\sqrt{s} = 5.02$ TeV. Using opposite charged dilepton events and counting the number of b-jets, they perform a fit including m_{ll} information to constrain Z+jets background, yielding a result of $\sigma_{t\bar{t}} = 66.0 \pm 4.9$ pb, giving a total uncertainty of 7.5% [31]. CMS has measured the $t\bar{t}$ production cross section at $\sqrt{s} = 5.02$ TeV, accumulating 27.4 pb^{-1}. The measurement is performed by analyzing events with at least one charged lepton. The measured cross section is $\sigma_{t\bar{t}} = 69.5 \pm 8.4$ pb [32], in agreement with the expectation from the Standard Model. Recently, they performed a measurement in opposite-sign $e\mu$-dilepton events with at least two jets using 304 pb^{-1}. They obtain a Drell-Yan scale factor under the Z-boson mass to estimate the background and extract a cross section using a counting technique of $\sigma_{t\bar{t}} = 60.3 \pm 5.8$ pb. The combination of the two results yields $\sigma_{t\bar{t}} = 62.6 \pm 4.1(stat.) \pm 3.0(syst. + lumi.)$ pb with 7.9% total relative uncertainty [33]. At $\sqrt{s} = 7$ TeV, ATLAS uses 4.6 fb^{-1} of $e\mu$ events in which they select an extremely clean sample and determine the $t\bar{t}$ cross section simultaneously with the efficiency to reconstruct and tag b-jets, yielding $\sigma_{t\bar{t}} = 182.9 \pm 7.1$ pb, corresponding to 3.9% precision [34]. Other measurements by ATLAS at $\sqrt{s} = 7$ TeV, include a measurement in 0.7 fb^{-1} in the lepton+jets channel [35], in the dilepton channel [36], and in 1.02 fb^{-1} in the all-hadronic channel [37], which together yield a combined value of $\sigma_{t\bar{t}} = 177 \pm 3(stat.)^{+8}_{-7}(syst.) \pm 7(lumi.)$ pb (6.2%) assuming $m_t = 172.5$ GeV/c^2 [38]. Further analyses in the hadronic τ plus jets channel in 1.67 fb^{-1} [39] and the hadronic τ + lepton channel in 2.05 fb^{-1} [40], and the all-hadronic channel in 4.7 fb^{-1} [41] yield consistent albeit less precise results. Another simultaneous mea-

surement of the $t\bar{t}, W^+W^-$, and $Z/\gamma^* \to \tau\tau$ cross section using the full 7 TeV dataset with 4.6 fb^{-1} yields $\sigma_{t\bar{t}} = 181 \pm 11$ pb, corresponding to a 6% precision [42]. The most precise measurement from CMS at $\sqrt{s} = 7$ TeV is also obtained in the dilepton channel, where they measure $\sigma_{t\bar{t}} = 161.9 \pm 2.5(stat.)^{+5.1}_{-5.0}(syst.) \pm 3.6(lumi.)$ pb, corresponding to a 4.2% precision [43]. Other measurements at $\sqrt{s} = 7$ TeV from CMS include measurements with 2.3 fb^{-1} in the e/μ+jets channel [44], with 3.5 fb^{-1} in the all-hadronic channel [45], with 2.2 fb^{-1} in the lepton+τ channel [46], and with 3.9 fb^{-1} in the τ+jets channel [47]. ATLAS and CMS also provide a combined cross section at $\sqrt{s} = 7$ TeV of $173.3 \pm 2.3(stat.) \pm 7.6(syst.) \pm 6.3(lumi.)$ pb using slightly older results based on $0.7 - 1.1$ fb^{-1} [48]. At $\sqrt{s} = 8$ TeV, ATLAS measures the $t\bar{t}$ cross section with 20.3 fb^{-1} using $e\mu$ dilepton events, with a simultaneous measurement of the $b-$tagging efficiency, yielding $\sigma_{t\bar{t}} = 242.9 \pm 1.7(stat.) \pm 5.5(syst.) \pm 5.1(lumi.) \pm 4.2(beam\,energy)$ pb [49] assuming $m_t = 172.5$ GeV/c^2, which corresponds to a 3.6% precision. In the $\ell + jets$ channel, they measure $\sigma_{t\bar{t}} = 260 \pm 1(stat.)^{+20}_{-23}(syst.) \pm 8(lumi.) \pm 4(beam\,energy)$ pb [50] in 20.3 fb^{-1} using a likelihood discriminant fit and b-jet identification. Subsequently, ATLAS performed a new analysis in 20.2 fb^{-1} $\ell+jets$ events. They model the W+jets background using Z+jets data and employ neural networks in three jet-multiplicity and b-jet multiplicity regions for the signal and background separation, yielding $\sigma_{t\bar{t}} = 248.3 \pm 0.7(stat.) \pm 13.4(syst.) \pm 4.7(lumi.)$ pb [51]. ATLAS also performed a cross section measurement in the hadronic τ+jets channel yielding consistent, albeit less precise results [52]. CMS performs a template fit to the M_{lb} mass distribution using 19.6 fb^{-1} in the lepton+jets channel yielding $\sigma_{t\bar{t}} = 228.5 \pm 3.8(stat.) \pm 13.7(syst.) \pm 6.0(lumi.)$ pb [53,54], which corresponds to a 6.7% precision. These 8 TeV measurements are in agreement with QCD predictions up to NLO accuracy. In the $e\mu$ channel, initially using 5.3 fb^{-1} [54] and then using 19.7 fb^{-1}, the cross sections are extracted using a binned likelihood fit to multi-differential final state distributions related to identified b quark and other jets in the event, yielding $\sigma_{t\bar{t}} = 244.9 \pm 1.4(stat.)^{+6.3}_{-5.5}(sys.) \pm 6.4(lumi.)$ pb [55]. The cross section and its ratio between 7 TeV and 8 TeV measurements are found to be consistent with pQCD calculations. The cross section is also measured in the hadronic τ+jets channel, yielding $\sigma_{t\bar{t}} = 257 \pm 3(stat.) \pm 24(syst.) \pm 7(lumi.)$ pb [56] and in the all-hadronic final state giving $\sigma_{t\bar{t}} = 275.6 \pm 6.1(stat.) \pm 37.8(syst.) \pm 7.2(lumi.)$ pb [57]. In combination of the most precise $e\mu$ measurements in $5.3 - 20.3$ fb^{-1}, ATLAS and CMS together yield at 8 TeV $\sigma_{t\bar{t}} = 241.5 \pm 1.4(stat.) \pm 5.7(syst.) \pm 6.2(lumi.)$ pb [58], which corresponds to a 3.5% precision, challenging the precision of the corresponding theoretical predictions. The LHCb collaboration presented the first observation of top-quark production in the forward region in pp-collisions. The $W + b$ final state with $W \to \mu\nu$ is reconstructed using muons with a transverse momentum, p_T, larger than 25 GeV in the pseudorapidity range $2.0 < \eta < 4.5$. The b-jets are required to have 50 GeV $< \mathrm{p_T} <$ 100 GeV and $2.2 < \eta < 4.2$, while the transverse component of the sum of the muon and b-jet momenta must satisfy $p_T > 20$ GeV. The results are based on data corresponding to integrated luminosities of 1.0 and 2.0 fb^{-1} collected at center-of-mass energies of 7 and 8 TeV by LHCb. The inclusive top quark production cross sections in the fiducial region are $\sigma_{t\bar{t}} = 239 \pm 53(stat.) \pm 38(syst.)$ pb at 7 TeV, and $\sigma_{t\bar{t}} = 289 \pm 43(stat.) \pm 46(syst.)$ pb at 8 TeV [59]. ATLAS and CMS have also measured the $t\bar{t}$ production cross section with Run-II data at $\sqrt{s} = 13$ TeV. In the $e\mu$ events with at least one b-tag, ATLAS uses 78 pb^{-1} and obtains $\sigma_{t\bar{t}} = 825 \pm 114$ pb [60]. This measurement is updated with lepton identification and trigger efficiencies to give $\sigma_{t\bar{t}} = 829 \pm 50(stat.) \pm 56(syst.) \pm 83(lumi)$ pb [61]. In this note, ATLAS also presents a $t\bar{t}$ cross section measurement in the ee and $\mu\mu$ dilepton channel with one and two b-tags using a counting approach, yielding $\sigma_{t\bar{t}} = 749 \pm 57(stat.) \pm 79(syst.) \pm 74(lumi.)$ pb. The cross section measurement in the $e\mu$ channel counting events with one or with two b-tags is also repeated using 3.2 pb^{-1} and yields $\sigma_{t\bar{t}} = 818 \pm 8(stat.) \pm 27(syst.) \pm 19(lumi.) \pm 12(beam)$ pb [62], consistent with theoretical QCD calculations at NNLO. In 36.1 fb^{-1} of $e\mu$ data with one or two b-tags, ATLAS

measures the $t\bar{t}$ cross section to $\sigma_{t\bar{t}} = 826.4 \pm 3.6(stat.) \pm 11.5(syst.) \pm 15.7(lumi.) \pm 1.9(beam)$ pb, giving a total of 2.4%. This measurement is also used to determine the top quark pole mass and to derive ratios and double ratios of $t\bar{t}$ and Z cross-sections at different energies as well as absolute and normalised differential cross-sections as functions of single lepton and dilepton kinematic variables [63]. In the $\ell + jets$, using 85 pb^{-1}, the cross-section is extracted by counting the number of events with exactly one electron or muon and at least four jets, at least one of which is identified as originating from a b-quark, yielding $\sigma_{t\bar{t}} = 817 \pm 13(stat.) \pm 103(syst.) \pm 88(lumi.)$ pb, both assuming $m_t = 172.5$ GeV/c^2 [61]. Very recently, ATLAS measures the inclusive $t\bar{t}$ cross section in 139 fb^{-1} in the $\ell + jes$ through a profile-likelihood fit to be $\sigma_{t\bar{t}} = 830.4 \pm 0.4(stat.) \pm 36(syst.) \pm 14(lumi)$ pb, with a relative uncertainty of 4.6% [64]. The result is consistent with the theoretical calculations at NNLO order in QCD perturbation theory. CMS uses 43 pb^{-1} in the $e\mu$ channel to measure $\sigma_{t\bar{t}} = 746 \pm 58(stat.) \pm 53(syst.) \pm 36(lumi)$ pb, in agreement with the expectation from the standard model [65]. Using 2.2 fb^{-1} in the $e\mu$ channel with at least one b-jet, CMS measures $\sigma_{t\bar{t}} = 815 \pm 9(stat.) \pm 38(syst.) \pm 19(lumi.)$ pb (5.3%), in agreement with the expectation from the Standard Model [66]. Using 35.9 fb^{-1} of dilepton data, CMS measures the $t\bar{t}$ cross section using a likelihood fit $\sigma_{t\bar{t}} = 803 \pm 2(stat.) \pm 25(syst.) \pm 20(lumi.)$ pb (4.0%), in agreement with the expectation from the SM calculation at NNLO order. This result is also used to extract the top quark mass and the strong coupling constant [67]. Using the same dataset in the dilepton channel with a hadronically decaying τ, they measure $\sigma_{t\bar{t}} = 781 \pm 7(stat.) \pm 62(syst.) \pm 20(lumi.)$ pb (8.3%) [68]. A first measurement of the total inclusive and the normalized differential cross section in the $\ell + jets$ channel is made in 42 pb^{-1} yielding $\sigma_{t\bar{t}} = 836 \pm 27(stat.) \pm 88(syst.) \pm 100(lumi.)$ pb [69]. In 2.2 fb^{-1}, $\ell + jets$ events are categorized according to the accompanying jet multiplicity. From a likelihood fit to the invariant mass distribution of the isolated lepton and a b-jet, the cross section is measured to be $\sigma_{t\bar{t}} = 888 \pm 2(stat.)^{+26}_{-28}(syst.) \pm 20(lumi)$ pb, in agreement with the SM prediction [70]. This result is also used to extract the top-quark mass. Recently, CMS has used 137 pb^{-1} in four regions determined by top p_T and b-tag score to measure the cross section in the $\ell + jets$ channel. They employ a combined χ^2 fit considering the migration matrices. Most of the measured differential cross sections are well described by standard model predictions with the exception of some double-differential distributions. They obtain $\sigma_{t\bar{t}} = 791 \pm 1(stat.) \pm 21(syst.) \pm 14(lumi)$ pb (3.2%) [71]. In the all-hadronic channel, CMS uses 2.53 fb^{-1} of data, yielding a cross section of $\sigma_{t\bar{t}} = 834 \pm 25(stat.)^{+118}_{-104}(syst.) \pm 23(lumi.)$ pb [72]. Also differential cross sections as a function of the leading top quark transverse momentum are measured. As general feature across channels, it is found that the measured top quark p_T spectrum is significantly softer than the NLO+PS theory predictions considered in the corresponding publications. CMS also performed a measurement of top-quark pair production in pPb heavy ion collisions at $\sqrt{s} = 8.16$ TeV in 174 nb^{-1} of lepton+jets events. They measure a cross section of $\sigma_{t\bar{t}} = 45 \pm 8$ nb, which is consistent with pQCD calculations and with the scaled pp data [73].

In Fig. 61.1, one sees the importance of $p\bar{p}$ at Tevatron energies where the valence antiquarks in the antiprotons contribute to the dominant $q\bar{q}$ production mechanism. At LHC energies, the dominant production mode is gluon-gluon fusion and the pp-$p\bar{p}$ difference nearly disappears. The excellent agreement of these measurements with the theory calculations is a strong validation of QCD and the soft-gluon resummation techniques employed in the calculations. The measurements reach high precision and provide stringent tests of pQCD calculations at NNLO+NNLL level including their respective PDF uncertainties.

Most of these measurements assume a $t \to Wb$ branching ratio of 100%. CDF and DØ have made direct measurements of the $t \to Wb$ branching ratio [74]. Comparing the number of events with 0, 1 and 2 tagged b jets in the lepton+jets channel, and also in the dilepton channel, using the known b-tagging efficiency, the ratio $R = B(t \to Wb)/\sum_{q=d,s,b} B(t \to Wq)$ can be extracted.

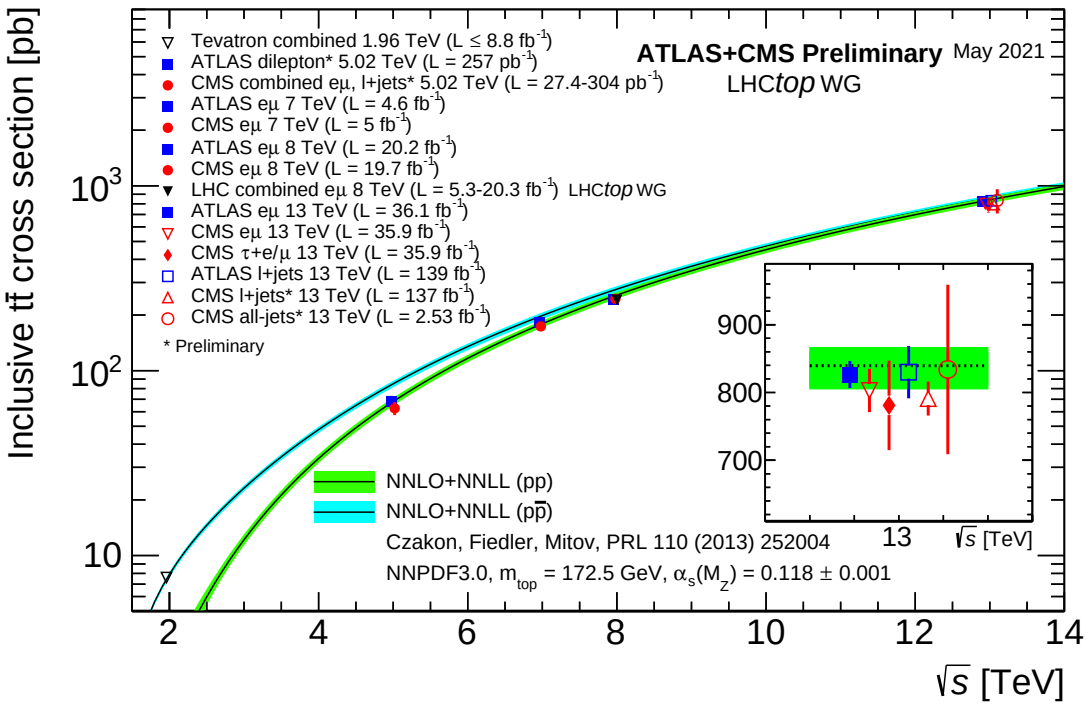

Figure 61.1: Measured and predicted $t\bar{t}$ production cross sections from Tevatron energies in $p\bar{p}$ collisions to LHC energies in pp collisions. The plot is kindly provided by the LHCtopWG working group, see https://twiki.cern.ch/twiki/bin/view/LHCPhysics/LHCTopWGSummaryPlots.

In 5.4 fb^{-1} of data, DØ measures $R = 0.90 \pm 0.04$, 2.5 standard deviations from unity. The currently most precise measurement was made by CMS in 19.7 fb^{-1} at $\sqrt{s} = 8$ TeV. They find $R = 1.014 \pm 0.003(stat.) \pm 0.032(syst.)$ and $R > 0.955$ at 95% C.L. [75]. A significant deviation of R from unity would imply either non-SM top-quark decay (for example a flavor-changing neutral-current decay), or a fourth generation of quarks. The latter is by other measurements.

Thanks to the large available event samples, the Tevatron and the LHC experiments also performed single-, double- or even triple-differential cross-section measurements in $t\bar{t}$ production. Such measurements are crucial, as they allow even more stringent tests of perturbative QCD as description of the production mechanism, allow along with other data the extraction of PDFs in PDF fits, and enhance the sensitivity to possible new physics contributions, especially now that NNLO predictions for the main differential observables in $t\bar{t}$ prediction have become available [76] and later confirmed [2]. Furthermore, such measurements reduce the uncertainty in the description of $t\bar{t}$ production as background in Higgs physics and searches for rare processes or beyond Standard Model physics. Differential cross sections are typically measured by a selection of candidate events, their kinematic reconstruction and subsequent unfolding of the obtained event counts in bins of kinematic distributions in order to correct for detector resolution effects, acceptance and migration effects. In some cases a bin-by-bin unfolding is used, while other analyses use more sophisticated techniques. Experiments at Tevatron and LHC measure the differential cross section with respect to the $t\bar{t}$ invariant mass, $d\sigma/dM_{t\bar{t}}$. The spectra are fully corrected for detector efficiency and resolution effects and are compared to several Monte Carlo simulations as well as selected theoretical calculations. Using 9.45 fb^{-1}, CDF measured $d\sigma/dM_{t\bar{t}}$, in the lepton+jets channel providing sen-

sitivity to a variety of exotic particles decaying into $t\bar{t}$ pairs [77]. In 9.7 fb^{-1} of lepton+jets data, DØ measured the differential $t\bar{t}$ production cross section with respect to the transverse momentum and absolute rapidity of the top quarks as well as of the invariant mass of the $t\bar{t}$ pair [29], which are all found to be in good agreement with the SM predictions. ATLAS measured the differential $t\bar{t}$ production cross section with respect to the top-quark transverse momentum, and of the mass, transverse momentum and rapidity of the top quark, the antitop quark as well as the $t\bar{t}$ system in up to 4.6 fb^{-1} at $\sqrt{s} = 7$ TeV in the lepton+jets channel [78–80]. It is found that data is softer than all predictions for higher values of the mass of the $t\bar{t}$ system as well as in the tail of the top-quark p_T spectrum beginning at 200 GeV, particularly in the case of the `Alpgen`+`Herwig` generator. The $M_{t\bar{t}}$ spectrum is not well described by NLO+NNLL calculations and there are also disagreements between the measured rapidity of the $t\bar{t}$ system spectrum and the `MC@NLO`+`Herwig` and `POWHEG`+`Herwig` generators, both evaluated with the CT10 PDF set. All distributions show a preference for HERAPDF1.5 when used for the NLO QCD predictions. In 5.0 fb^{-1} of $\sqrt{s} = 7$ TeV data in the lepton+jets and the dilepton channels, CMS measured normalised differential $t\bar{t}$ cross sections with respect to kinematic properties of the final-state charged leptons and jets associated to b-quarks, as well as those of the top quarks and the $t\bar{t}$ system. The data are compared with several predictions from perturbative QCD calculations and found to be consistent [81]. ATLAS uses 4.6 fb^{-1} of data at 7 TeV and 20.2 fb^{-1} at 8 TeV to measure the differential $t\bar{t}$ cross section in the dilepton final state as a function of the mass, the transverse momentum and the rapidity of the $t\bar{t}$ system [82]. The results are compared with different Monte Carlo generators and theoretical calculations of $t\bar{t}$ production and found to be consistent with the majority of predictions in a wide kinematic range. Using 20.3 fb^{-1} of $t\bar{t}$ events in the lepton+jets channel, ATLAS measures the normalized differential cross sections of $t\bar{t}$ production as a function of the top-quark, $t\bar{t}$ system and event-level kinematic observables [83]. The observables have been chosen to emphasize the $t\bar{t}$ production process and to be sensitive to effects of initial- and final-state radiation, to the different parton distribution functions, and to non-resonant processes and higher-order corrections. The results are in fair agreement with the predictions over a wide kinematic range. Nevertheless, most generators predict a harder top-quark transverse momentum distribution at high values than what is observed in the data. Predictions beyond NLO accuracy improve the agreement with data at high top-quark transverse momenta. Using the current settings in the Monte Carlo programs and parton distribution functions, the rapidity distributions are not well modelled by any generator under consideration. However, the level of agreement is improved when more recent sets of parton distribution functions are used. Using 20.3 fb^{-1} of 8 TeV data, ATLAS performed a dedicated differential $t\bar{t}$ cross-section measurement of highly boosted top quarks in the lepton+jets channel, where the hadronically decaying top quark has a transverse momentum above 300 GeV [84]. Jet substructure techniques are employed to identify top quarks, which are reconstructed with an anti-k_t jet with a radius parameters $R = 1.0$. The predictions of NLO and LO matrix element plus parton shower Monte Carlo generators are found to generally overestimate the measured cross sections. Using 5.0 fb^{-1} of data at 7 TeV and 19.7 fb^{-1} at 8 TeV in the lepton+jets channel, CMS reports measurements of normalized differential cross sections for $t\bar{t}$ production with respect to four kinematic event variables: the missing transverse energy; the scalar sum of the jet transverse momentum (p_T); the scalar sum of the p_T of all objects in the event; and the p_T of leptonically decaying W bosons from top quark decays [85]. No significant deviations from the predictions of several SM event generators are observed. Using the full 19.7 fb^{-1} data in the $e\mu$ channel, CMS measures normalized double-differential cross sections for $t\bar{t}$ production as a function of various pairs of observables characterizing the kinematics of the top quark and $t\bar{t}$ system [86]. The data are compared to calculations using perturbative QCD at NLO and approximate NNLO orders. They are also compared to predictions of Monte Carlo event generators that complement fixed-order com-

putations with parton showers, hadronization, and multiple-parton interactions. Overall agreement is observed with the predictions, which is improved when the latest global sets (as determined here by CMS) of proton parton distribution functions are used. The inclusion of the measured $t\bar{t}$ cross sections in a fit of parametrized parton distribution functions is shown to have significant impact on the gluon distribution [86]. Another analysis at high transverse momentum regime for the top quarks, is performed by the CMS collaboration in 19.7 fb^{-1} at $\sqrt{s} = 8$ TeV [87]. The measurement is performed for events in $e/\mu + jets$ final states where the hadronically decaying top quark is reconstructed as a single large-radius jet and identified as a top candidate using jet substructure techniques. The integrated cross section is measured at particle-level within a fiducial region resembling the detector-level selection as well as at parton-level. At particle-level, the fiducial cross section is measured to be $\sigma_{t\bar{t}} = 0.499 \pm 0.035(stat. + syst.) \pm 0.095(theo) \pm 0.013(lumi)$ pb for $p_T >$ 400 GeV. At parton-level, it translates to $\sigma_{t\bar{t}} = 1.44 \pm 0.10(stat. + syst.) \pm 0.29(theo.) \pm 0.04(lumi.)$ pb. At parton-level, interactions between incoming partons (quarks or gluons) are considered via a gauge interaction yielding final state partons. While such interactions can be well described theoretically, partons are not visible in the detector. At the particle-level, visible and measurable hadrons, i.e. bound states of quarks and anti-quarks, are considered to form jets. The hadronisation process takes us from one level to the other. In 19.7 fb^{-1} at $\sqrt{s} = 8$ TeV, CMS repeated those measurements in the lepton+jets and in the dilepton channels [88]. While the overall precision is improved, no significant deviations from the Standard Model are found, yet a softer spectrum for the top quark at high p_T with respect to theoretical available predictions has been observed. This behaviour has been also observed in the all-hadronic final state [89], where a total cross section measurement is performed, yielding $\sigma_{t\bar{t}} = 275.6 \pm 6.1(stat.) \pm 37.8(syst.) \pm 7.2(lumi)$ pb. At $\sqrt{s} = 13$ TeV, in 3.2 fb^{-1}, ATLAS measured the differential $t\bar{t}$ cross section as a function of the transverse momentum and absolute rapidity of the top quark, and of the transverse momentum, absolute rapidity and invariant mass of the $t\bar{t}$ system [90]. The measured differential cross sections are compared to predictions of NLO generators matched to parton showers and the measurements are found to be consistent with all models within the experimental uncertainties with the exception of the `Powheg-Box+ Herwig++` predictions, which differ significantly from the data in both the transverse momentum of the top quark and the mass of the $t\bar{t}$ system. Using 3.2 fb^{-1} of data in the lepton+jets channel, ATLAS measured the differential cross sections of $t\bar{t}$ production in fiducial phase-spaces as a function of top-quark and $t\bar{t}$ system kinematic observables [91]. Two separate selections are applied that each focus on different top-quark momentum regions, referred to as resolved and boosted topologies of the $t\bar{t}$ final state. The measured spectra are corrected for detector effects and are compared to several Monte Carlo simulations by means of calculated χ^2 and p-values.

ATLAS presents a measurement of the boosted top quark differential cross section in the all-hadronic decay mode [92]. They require two top-quark candidates, one with $p_T > 500$ GeV and a second with $p_T > 350$ GeV, with each candidate reconstructed as an anti-k_T jet with radius parameter $R = 1.0$. The top-quark candidates are separated from the multijet background using the jet substructure and the presence of a b-quark tag in each jet. The observed kinematic distributions are unfolded to recover the differential cross sections in a limited phase-space region and compared with SM predictions, showing agreement. In 36 fb^{-1}, ATLAS measures the single- and double-differential $t\bar{t}$ cross-section in the lepton + jets channel at particle and parton level. Two topologies, resolved and boosted, are considered and the results are presented as a function of several kinematic variables characterising the top and $t\bar{t}$ system and jet multiplicities. Overall, there is good agreement between the theoretical predictions and the data [93]. In 36.1 fb^{-1} of dilepton events, ATLAS measures the differential $t\bar{t}$ cross section as a function of several lepton kinematic variables [63]. The NLO+PS predictions give a good description of several observables. However,

POWHEG predicts a harder spectrum for lepton p_T variables than observed. In 139 fb^{-1} of data in the $\ell+jets$ channel in a boosted topology with at least one large-R "top-jet" from a hadronic decay with high-p_T, ATLAS employs a parameter sensitive to the top mass to reduce the jet uncertainties and measures the differential $t\bar{t}$ cross section as a function of kinematic variables characterising the $t\bar{t}$ system and also as a function of variables that characterise the additional radiation in the events [94]. The measured distribution of the top-quark transverse momentum, which is measured to be softer than expected, is used to set limits on the Wilson coefficients describing physics beyond the standard model. The modelling of the additional radiation events show some mild disagreements to the data. In the all-hadronic channel with six separately resolved jet, using 36.1 fb^{-1}, ATLAS measures single- and double-differential cross sections at particle and parton level as a function of various kinematic variables [95]. The rapidities of t and $t\bar{t}$ are found to be well modelled while discrepancies between theoretical predictions and data are found in the p_T distributions of the three leading jets, the top and the $t\bar{t}$ system. In 42 pb^{-1}, CMS measures the differential cross section at $\sqrt{s} = 13$ TeV as a function of kinematic properties of the top quarks and the $t\bar{t}$ system, as well as of the jet multiplicity in the event. Several predictions from perturbative QCD calculations are confronted with the data and are found to describe them well [96]. In 2.1 fb^{-1} at $\sqrt{s} = 13$ TeV, CMS measures the normalized differential cross sections for $t\bar{t}$ production in the dilepton channels as a function of the kinematic properties of the leptons, jets from bottom quark hadronization, top quarks, and top quark pairs at the particle and parton levels [97]. The results are compared to several Monte Carlo generators that implement calculations up to NLO in perturbative QCD interfaced with parton showering, and also to fixed-order theoretical calculations of top quark pair production up to NNLO, showing agreement. In 2.3 fb^{-1} of events in the lepton+jets channel, CMS measures the differential and double-differential cross sections for the $t\bar{t}$ production as a function of jet multiplicity and of kinematic variables of the top quarks and the $t\bar{t}$ system [98]. The differential cross sections are presented at particle level, within a phase space close to the experimental acceptance, and at parton level in the full phase space. The results are compared to several SM predictions. Using 35.9 fb^{-1}, CMS measures the differential $t\bar{t}$ cross section in the single-lepton decay channel, as a function of a number of kinematic event variables. The data are compared to a variety of state-of-the-art LO and NLO simulations [99]. In 35.8 fb^{-1}, CMS measures the differential and double-differential $t\bar{t}$ cross sections in the $\ell + jets$ channel as a function of kinematic variables of the top quarks and the top quark-antiquark ($t\bar{t}$) system. In addition, kinematic variables and multiplicities of jets associated with the $t\bar{t}$ production are measured. The kinematic variables of the top quarks and the $t\bar{t}$ system are reasonably described in general, though none predict all the measured distributions. In particular, the transverse momentum distribution of the top quarks is more steeply falling than predicted. The kinematic distributions and multiplicities of jets are adequately modeled by certain combinations of NLO calculations and parton shower models [100]. In the dilepton channel, CMS measures differential $t\bar{t}$ cross sections in 35.9 fb^{-1} as functions of kinematic observables of the top quarks and their decay products, the $t\bar{t}$ system, and the total number of jets in the event. All results are compared with SM predictions from Monte Carlo simulations with NLO accuracy in QCD at matrix-element level interfaced to parton-shower simulations. Where possible, parton-level results are compared to calculations with beyond-NLO precision in QCD. Significant disagreement is observed between data and all predictions for several observables. The measurements are used to constrain the top quark chromomagnetic dipole moment in an effective field theory framework at NLO in QCD and to extract $t\bar{t}$ and leptonic charge asymmetries [101]. In 35.9 fb^{-1} of dilepton events, CMS measures normalised multi-differential $t\bar{t}$ cross sections as a function of the kinematic properties of the top quark and of the $t\bar{t}$ system at parton level in the full phase space. A triple-differential measurement is performed as a function of the invariant mass and rapidity of the $t\bar{t}$ system and the multiplicity of additional jets at particle level.

The data are compared to predictions of Monte Carlo event generators that complement NLO QCD calculations with parton showers. The measurement is used to extract the strong coupling constant and the top-quark pole mass and parton distribution functions [102]. In 137 fb^{-1} of $\ell + jets$ data, arranged in four regions according to the top p_T, boosted vs. resolved, and the b-tagging score, CMS measures the single- and double-differential $t\bar{t}$ cross sections [71]. Here also the longitudinal momentum is measured well into the TeV range in one measurement starting in the resolved regime. Most of the measured differential cross sections are well described by standard model predictions with the exception of some double-differential distributions. The top p_T and $m_{t\bar{t}}$ is found to be softer than predicted. In 35.9 fb^{-1} of all-hadronic and $\ell + jets$ events in a boosted topology with at least two large-R jets with a b-tag inside and $p_T > 400$ GeV or one large-R jet, respectively, CMS measures the differential cross section as a function of kinematic variables of individual top quarks or of the $t\bar{t}$ system [103]. The observed absolute cross sections are significantly lower than the predictions from theory, while the normalized differential measurements are well described.

61.3.1.2 *Other $t\bar{t}$ production processes*

Further cross-section measurements are performed by ATLAS for $t\bar{t}$+heavy flavour [104] and $t\bar{t}$+jets production as well as the differential measurement of the jet multiplicity in $t\bar{t}$ events by ATLAS [105] and by CMS [106]. Here, `MC@NLO+Herwig` MC is found to predict too few events at higher jet multiplicities. In addition, CMS measured the cross-section ratio $\sigma_{t\bar{t}b\bar{b}}/\sigma_{t\bar{t}jj}$ using 19.6 fb^{-1} of 8 TeV data [107]. This is of high relevance for top quark production as background to searches, for example for measurements of $t\bar{t}h$ production and ongoing searches for 4-top quark production. Later, ATLAS also measured the $t\bar{t}$ production cross section along with the branching ratios into channels with leptons and quarks using 4.6 fb^{-1} of 7 TeV data [108]. They find agreement with the standard model at the level of a few percent.

Using 139 fb^{-1} of $t\bar{t} \to$ dilepton events, ATLAS distinguishes in a dedicated analysis muons originating from $W \to \mu\nu$ decays and those from $W \to \tau\nu \to \mu\nu\nu\nu$ decays via their transverse momentum spectrum and the impact parameter of the muon track, that reflects the tau lifetime, yielding high sensitivity. The measured ratio of $R(\tau/\mu) = 0.992 \pm 0.013$ is in agreement with the hypothesis of universal lepton couplings [109].

Using 36 fb^{-1} of dilepton events at 13 TeV, ATLAS also measures differential cross sections with respect to high-resolution variables, constructed to characterize the longitudinal and transverse momentum distributions of the b-hadron within the b-jets [110]. They are used to test the heavy-quark-fragmentation modelling.

Using 137 fb^{-1} of dilepton events at 13 TeV, CMS measures differential cross sections with respect to the mass of the $t\bar{t}$ system and the rapidity difference of the top-quark and antiquark [111]. Exploiting their sensitivity to the top-quark Yukawa coupling yields a best fit value of $Y_t = 1.16^{+0.24}_{-0.35}$, bounding $Y_t < 1.54$ at a 95% confidence level.

In 36.1 fb^{-1}, ATLAS measures the $t\bar{t}b\bar{b}$ cross section in the dilepton and the $\ell + jets$ channels. Results are presented at particle level in the form of inclusive cross-sections of $t\bar{t}$ final states with three and four b-jets as well as differential cross-sections as a function of global event properties and properties of b-jet pairs. The measured inclusive fiducial cross-sections generally exceed the $t\bar{t}b\bar{b}$ predictions from various NLO matrix element calculations matched to a parton shower, but are compatible within the total uncertainties [112]. In 2.3 fb^{-1}, CMS measures the $t\bar{t}b\bar{b}$ cross section in the dilepton channel [113]. They also determine the cross section ratio $\sigma_{t\bar{t}b\bar{b}}/\sigma_{t\bar{t}jj}$. In 35.9 fb^{-1}, CMS recently measured the cross section $t\bar{t}b\bar{b}$ as well as the cross section ratio $\sigma_{t\bar{t}b\bar{b}}/\sigma_{t\bar{t}jj}$ in the dilepton and the lepton+jets channel [114]. They fit the distribution of the b-tagging discriminant variable of the two jets that do not belong to the $t\bar{t}$ decay. In the same dataset, CMS measures the $t\bar{t}b\bar{b}$ cross section in the all-jet channel by selecting events containing at least eight jets, of

which at least two are identified as b-jets. A combination of multivariate analysis techniques is used to reduce the large background from multijet events not containing a top quark pair, and to help discriminate between jets originating from top quark decays and other additional jets. The measured cross sections are found to be larger than theoretical predictions by a factor of 1.5-2.4, corresponding to 1-2 standard deviations [115]. Recently, CMS measured the $t\bar{t}+b\bar{b}$ cross section in 35.9 fb^{-1} of dilepton and $\ell+jets$ events [114]. The cross section is extracted from the cross section ratio $R(t\bar{t}+b\bar{b})$ in order to reduce systematic uncertainties. The assignment of jets to the top or to the additional jets is based on b-tagging scores in the dilepon channel and on a kinematic fit in the $\ell+jets$ channel. Using the same data set in the all-hadronic channel, CMS measured the $t\bar{t}+b\bar{b}$ cross section to $\approx 25\%$ precision employing a multivariate analysis technique and a 2-dimensional likelihood fit [116]. Very recently, CMS also measured the $t\bar{t}+c\bar{c}$ cross section using 41.5 fb^{-1} of events with dileptonic final states [117]. A multi-class neural network is employed to separate $t\bar{t}+b\bar{b}$, $t\bar{t}+c\bar{c}$ and $t\bar{t}+ll$. The results are compatible with the prediction within $1-2\,\sigma$.

The production of four top-quarks is an interesting test of QCD and at the same time sensitive to the top quark Yukawa coupling and to production mechanisms with new mediators with strong couplings to top quarks. The latest cross section calculation yields $\sigma_{t\bar{t}t\bar{t}} = 12.0$ fb $\pm$ 20% [118]. Using the full Run-II data set of 139 fb^{-1}, ATLAS measures the four-tops cross section in the two-lepton same sign or three-lepton channel with 13% branching ratio and dominant $t\bar{t}V$ background as $\sigma_{t\bar{t}t\bar{t}} = 24^{+7}_{-6}$ fb [119]. Using the same data set in the one-lepton or two-lepton opposite-sign channel with 57% branching ratio and dominant $t\bar{t}$ + heavy flavor background, they measure $\sigma_{t\bar{t}t\bar{t}} = 26^{+17}_{-15}$ fb [120]. The combination yields $\sigma_{t\bar{t}t\bar{t}} = 24^{+7}_{-6}$ fb [120], corresponding to an observed (expected) significance of 4.7 (2.6) σ significance. CMS measures the four-top cross section in the two-lepton same sign or thee-lepton channel in 137 fb^{-1} to $\sigma_{t\bar{t}t\bar{t}} = 12.6^{+5.8}_{-5.2}$ fb [121], corresponding to an observed (expected) significance of 2.6 (2.7) σ significance. Using 35.8 fb^{-1}, they also study the one-lepton or two-lepton opposite-sign channel and obtain an upper limit of $\sigma_{t\bar{t}t\bar{t}} < 48$ fb at 95% CL [122]. The results are also interpreted in terms of the top-Yukawa coupling and various scenarios of physics beyond the standard model via effective field theory fits.

61.3.1.3 *Single-top production*

Single-top quark production was first observed in 2009 by DØ [123] and CDF [124, 125] at the Tevatron. The production cross section at the Tevatron is roughly half that of the $t\bar{t}$ cross section, but the final state with a single W-boson and typically two jets is less distinct than that for $t\bar{t}$ and much more difficult to distinguish from the background of W+jets and other sources. A comprehensive review of the first observation and the techniques used to extract the signal from the backgrounds can be found in [126].

The dominant production at the Tevatron is through s-channel and t-channel W-boson exchange. Associated production with a W-boson (tW production) has a cross section that is too small to observe at the Tevatron. The t-channel process is $qb \to q't$, while the s-channel process is $q\overline{q'} \to t\bar{b}$. The s- and t-channel productions can be separated kinematically. This is of particular interest because potential physics beyond the Standard Model, such as fourth-generation quarks, heavy W and Z bosons, flavor-changing-neutral-currents [11], or a charged Higgs boson, would affect the s- and t-channels differently. However, the separation is difficult and initial observations and measurements at the Tevatron by both experiments were of combined s+t-channel production. The two experiments combined their measurements for maximum precision with a resulting s+t-channel production cross section of $2.76^{+0.58}_{-0.47}$ pb [127]. The measured value assumes a top-quark mass of 170 GeV/c^2. The mass dependence of the result comes both from the acceptance dependence and from the $t\bar{t}$ background evaluation. Also the shape of discriminating topological variables is sensitive to m_t. The dependence on m_t is therefore not necessarily a simple linear dependence but amounts

to only a few tenths of picobarns over the range $170 - 175$ GeV/c^2. The measured value agrees well with the theoretical calculation at $m_t = 173$ GeV/c^2 of $\sigma_{s+t} = 3.12^{+0.00}_{-0.04}(scale) \pm 0.18(pdf)$ pb (including both top and anti-top production) [9,128].

Using the full Run-II data set of up to 9.7 fb^{-1}, CDF and DØ have measured the t-channel single-top quark production to be $\sigma_{t+\bar{t}} = 2.25^{+0.29}_{-0.31}$ pb [129,130]. In the same publication, they also present the simultaneously measured $s-$ and $t-$channel cross sections and the $s+t$ combined cross section measurement resulting in $\sigma_{s+t} = 3.30^{+0.52}_{-0.40}$ pb, without assuming the SM ratio of σ_s/σ_t. The modulus of the CKM matrix element obtained from the $s+t$-channel measurement is $|V_{tb}| = 1.02^{+0.06}_{-0.05}$ and its value is used to set a lower limit of $|V_{tb}| > 0.92$ at 95% C.L. Those results are in good agreement with the theoretical value at the mass 172.5 GeV/c^2 of $\sigma_t = 2.08 \pm 0.13$ pb [128]. It should be noted that the theory citations here list cross sections for t or $\bar{t}$ alone, whereas the experiments measure the sum. At the Tevatron, these cross sections are equal. The theory values quoted here already include this factor of two.

Using datasets of 9.7 fb^{-1} each, CDF and DØ combine their analyses and report the first observation of single-top-quark production in the s-channel, yielding $\sigma_s = 1.29^{+0.26}_{-0.24}$ pb [131]. The probability of observing a statistical fluctuation of the background of the given size is 1.8×10^{-10}, corresponding to a significance of 6.3 standard deviations.

At the LHC, the t-channel cross section is expected to be more than three times as large as s-channel and tW production, combined. Both ATLAS and CMS have measured single top production cross sections at $\sqrt{s} = 7$ TeV in pp collisions (assuming $m_t = 172.5$ GeV/c^2 unless noted otherwise). Using 4.59 fb^{-1} of data at $\sqrt{s} = 7$ TeV, ATLAS measures the t-channel single-top quark cross section in the lepton plus 2 or 3 jets channel with one b-tag by fitting the distribution of a multivariate discriminant constructed with a neural network, yielding $\sigma_t = 46 \pm 6$ pb, $\sigma_{\bar{t}} = 23 \pm 4$ pb with a ratio $R_t = \sigma_t/\sigma_{\bar{t}} = 2.04 \pm 0.18$ and $\sigma_{t+\bar{t}} = 68 \pm 8$ pb, consistent with SM expectations [132,133]. CMS follows two approaches in 1.6 fb^{-1} of lepton plus jets events. The first approach exploits the distributions of the pseudorapidity of the recoil jet and reconstructed top-quark mass using background estimates determined from control samples in data. The second approach is based on multivariate analysis techniques that probe the compatibility of the candidate events with the signal. They find $\sigma^{t-channel}_{t+\bar{t}} = 67.2 \pm 6.1$ pb, and $|V_{tb}| = 1.020 \pm 0.046(exp.) \pm 0.017(th.)$ [134].

At $\sqrt{s} = 8$ TeV, both experiments repeat and refine their measurements. ATLAS uses 20.2 fb^{-1} of data. Total, fiducial and differential cross-sections are measured for both top-quark and top-antiquark production [135]. An artificial neural network is employed to separate signal from background. The fiducial cross-section is measured with a precision of 5.8% (top quark) and 7.8% (top antiquark), respectively. The total cross-sections are measured to be $\sigma_t^{t-channel}(tq) = 56.7^{+4.3}_{-3.8}$ pb for top-quark production and $\sigma_{\bar{t}}^{t-channel}(\bar{t}q) = 32.9^{+3.0}_{-2.7}$ pb for top-antiquark production, in agreement with the SM prediction. In addition, the ratio of top-quark to top-antiquark production cross-sections is determined to be $R_t = 1.72 \pm 0.09$. The total cross-section is used to extract the Wtb coupling: $f_{LV} \cdot |V_{tb}| = 1.029 \pm 0.048$, which corresponds to $|V_{tb}| > 0.92$ at the 95% confidence level, when assuming $f_{LV} = 1$ and restricting the range of $|V_{tb}|$ to the interval $[0,1]$. The differential cross-sections as a function of the transverse momentum and rapidity of both the top quark and the top antiquark are measured at both the parton and particle levels. The transverse momentum and rapidity differential cross-sections of the accompanying jet from the t-channel scattering are measured at particle level. All measurements are compared to various Monte Carlo predictions as well as to fixed-order QCD calculations where available. The SM predictions provide good descriptions of the data. Using the same dataset, ATLAS probes the Wtb vertex structure from polarization observables in t-channel single-top quark events. The polarization observables are extracted from asymmetries in angular distributions measured with

respect to spin quantisation axes appropriately chosen for the top quark and the W-boson. The asymmetry measurements are performed at parton level by correcting the observed angular distributions for detector effects and hadronisation after subtracting the background contributions. The measured top-quark and W-boson polarization values are in agreement with the Standard Model predictions [136]. CMS uses 19.7 fb^{-1} in the electron or muon plus jets channel, exploiting the pseudorapidity distribution of the recoil jet. They find $\sigma_t = 53.8 \pm 1.5(stat.) \pm 4.4(syst.)$ pb and $\sigma_{\bar{t}} = 27.6 \pm 1.3(stat.) \pm 3.7(syst.)$ pb, resulting in an inclusive t-channel cross section of $\sigma_{t+\bar{t}} = 83.6 \pm 2.3(stat.) \pm 7.4(syst.)$ [137]. They measure a cross section ratio of $R_t = \sigma_t/\sigma_{\bar{t}} = 1.95 \pm 0.10(stat.) \pm 0.19(syst.)$, in agreement with the SM. The CKM matrix element V_{tb} is extracted to be $|V_{tb}| = 0.998 \pm 0.038(exp.) \pm 0.016(th.)$. Later, CMS has also provided a fiducial cross section measurement for t-channel single top at $\sqrt{s} = 8$ TeV with 19.7 fb^{-1} of data in signal events with exactly one muon or electron and two jets, one of which is associated with a b-hadron [138]. The definition of the fiducial phase space follows closely the constraints imposed by event-selection criteria and detector acceptance. The total fiducial cross section is measured using different generators at next-to-leading order plus parton-shower accuracy. Using as reference the `aMC@NLO` MC predictions in the four-flavour scheme $\sigma_t^{\text{fid}} = 3.38 \pm 0.25(exp.) \pm 0.20(th.)$ pb is obtained, in good agreement with the theory predictions. At 13 TeV, ATLAS uses 3.2 fb^{-1} to measure the t-channel cross section. Using a binned maximum-likelihood fit to the discriminant distribution of a neural network, the cross-sections are determined to be $\sigma_t(tq) = 156 \pm 5(stat.) \pm 27(syst.) \pm 3(lumi.)$ pb and $\sigma(\bar{t}q) = 91 \pm 4(stat.) \pm 18(syst.) \pm 2(lumi.)$ pb [139]. The cross-section ratio is measured to be $R_t = \sigma_t/\sigma_{\bar{t}} = 1.72 \pm 0.09(stat.) \pm 0.18(syst.)$. All results are in agreement with SM predictions. A measurement of the t-channel single top-quark cross section is also available at 13 TeV with the CMS detector, corresponding to an integrated luminosity of 2.2 fb^{-1}. Fits to the transverse W-mass and the output of an artificial neural network allow the determination of the background and the signal contribution. The measured cross-section is $\sigma_t = 238 \pm 13(stat.) \pm 29(syst.)$ pb [140]. The CKM matrix element is determined to $|V_{tb}| = 1.05 \pm 0.07(exp.) \pm 0.02(th.)$. Using 35.9 fb^{-1} of data, CMS performs measurements of the t-channel cross sections of single top quarks and antiquarks in the t channel, and their ratio. Events with one muon or electron are selected, and different categories of jet and b-jet multiplicity and multivariate discriminators are applied to separate the signal from the background, resulting in $\sigma_t(tq) = 130 \pm 1(stat) \pm 19(syst)$ pb and $\sigma_t(\bar{t}q) = 77 \pm 1(stat) \pm 12(syst)$ pb, respectively, and their ratio is $1.68 \pm 0.02(stat) \pm 0.05(syst)$. The results are in agreement with the predictions from the Standard Model [141]. Recently, CMS used the same dataset to measure the CKM matrix elements from their t-channel single-top quark production cross section. In the standard model hypothesis of CKM unitarity, a lower limit of $|V_{tb}| > 0.970$ is measured at the 95% confidence level. Several theories beyond the standard model are considered, and by releasing all constraints among the involved parameters, the values $|V_{tb}| = 0.988 \pm 0.024$, and $|V_{td}|^2 + |V_{ts}|^2 = 0.06 \pm 0.06$, where the uncertainties include both statistical and systematic components, are measured [142].

The predicted cross section for the tW process at the LHC $\sqrt{s} = 7$ TeV is 15.6 ± 1.2 pb [10]. This is of interest because it probes the Wtb vertex in a different kinematic region than s- and t-channel production, and because of its similarity to the associated production of a charged-Higgs boson and a top quark. The signal is difficult to extract because of its similarity to the $t\bar{t}$ signature. Furthermore, it is difficult to uniquely define because at NLO a subset of diagrams has the same final state as $t\bar{t}$ and the two interfere [143]. The cross section is calculated using the *diagram removal* technique [144] to define the signal process. In the diagram removal technique the interfering diagrams are removed, at the amplitude level, from the signal definition (an alternative technique, *diagram subtraction* removes these diagrams at the cross-section level and yields similar results [144]). These techniques work provided the selection cuts are defined such that the interference effects are small, which is

usually the case.

Both, ATLAS and CMS, also provide evidence for the associate tW production at $\sqrt{s} = 7$ TeV [145,146]. ATLAS uses 2.05 fb^{-1} in the dilepton plus missing E_T plus jets channel, where a template fit to the final classifier distributions resulting from boosted decision trees as signal to background separation is performed. The result is incompatible with the background-only hypothesis at the 3.3σ (3.4σ expected) level, yielding $\sigma_{tW} = 16.8 \pm 2.9(stat.) \pm 4.9(syst.)$ pb and $|V_{tb}| = 1.03^{+0.16}_{-0.19}$ [145]. CMS uses 4.9 fb^{-1} in the dilepton plus jets channel with at least one b-tag. A multivariate analysis based on kinematic properties is utilized to separate the $t\bar{t}$ background from the signal. The observed signal has a significance of 4.0σ and corresponds to a cross section of $\sigma_{tW} = 16^{+5}_{-4}$ pb [146].

Both experiments repeated their tW-analyses at $\sqrt{s} = 8$ TeV. ATLAS uses 20.3 fb^{-1} to select events with two leptons and one central b-jet. The tW signal is separated from the backgrounds using boosted decision trees, each of which combines a number of discriminating variables into one classifier. Production of tW events is observed with a significance of 7.7σ. The cross section is extracted in a profile likelihood fit to the classifier output distributions. The tW cross section, inclusive of decay modes, is measured to be $\sigma_{tW} = 23.0 \pm 1.3(stat.)^{+3.2}_{-3.5}(syst.) \pm 1.1(lumi.)$ pb, yielding a value for the CKM matrix element $|V_{tb}| = 1.01 \pm 0.10$ and a lower limit of 0.80 at the 95% C.L. [147]. A fiducial cross section is also measured. ATLAS and CMS also combine their early measurements and obtain $\sigma_{tW} = 16.3 \pm 4.1$ pb [148], in agreement with the NLO+NNLL expectation. Very recently, ATLAS used 20.2 fb^{-1} in the single-lepton channel with at least three jets to measure the Wt production cross section. A neural network is trained to separate the tW signal from the dominant $t\bar{t}$ background. The cross-section is extracted from a binned profile maximum-likelihood fit to a two-dimensional discriminant built from the neural-network output and the invariant mass of the hadronically decaying W boson. The measured cross section is $\sigma_{tW} = 26 \pm 7$ pb, in good agreement with the Standard Model expectation [149]. CMS uses 12.2 fb^{-1} in events with two leptons and a jet originating from a b-quark. A multivariate analysis based on kinematic properties is utilized to separate the signal and background. The tW associate production signal is observed at the level of 6.1σ, yielding $\sigma_{tW} = 23.4 \pm 5.4$ pb and $|V_{tb}| = 1.03 \pm 0.12(exp.) \pm 0.04(th.)$ [150]. ATLAS and CMS also combine their early measurements and obtain $\sigma_{tW} = 23.1 \pm 3.6$ pb [148], in agreement with the NLO+NNLL expectation. The product of a form factor with the CKM matrix element V_{tb} is determined to be $|V_{tb}| = 1.02 \pm 0.04(meas.) \pm 0.02(theo.) > 0.79$. At 13 TeV in the tW-channel, ATLAS uses 3.2 fb^{-1} of events with two opposite sign isolated leptons and at least one jet; they are separated into signal and control regions based on their jet multiplicity and the number of jets with b-tags. Signal is separated from background in two regions using boosted decision trees. The cross section is extracted by fitting templates to the data distributions, and is measured to be $\sigma_{tW} = 94 \pm 10(stat.)^{+28}_{-22}(syst.) \pm 2(lumi.)$ pb [151]. The measurement is in agreement with the SM prediction. CMS uses 36 fb^{-1} of events with two opposite sign isolated leptons, one tight and one loose jet and one b-tag. Signal and background is separated in categories depending on the number of jets and the subset of b-tagged jets using a boosted decision tree. A maximum likelihood fits yields $\sigma_{tW} = 63.1 \pm 1.8(stat.) \pm 6.4(syst.) \pm 2.1(lumi.)$ pb [152]. Very recently, CMS uses 36 fb^{-1} in the single-lepton channel, where a boosted decision tree is used to separate the tW signal from the dominant $t\bar{t}$ background, whilst the subleading W+jets and multijet backgrounds are constrained using data-based estimates. This result is the first observation of the tW process in final states containing a muon or electron and jets, with a significance exceeding 5 standard deviations. The cross section is determined to be $\sigma_{tW} = 89 \pm 4(stat) \pm 12(syst)$ pb, consistent with the Standard Model [153].

The s-channel production cross section is expected to be 4.6 ± 0.3 pb for $m_t = 173$ GeV/c^2 at $\sqrt{s} = 7$ TeV [9]. At ATLAS, a search for s-channel single top quark production is performed in 0.7 fb^{-1} at 7 TeV using events containing one lepton, missing transverse energy and two b-jets.

Using a cut-based analysis, an observed (expected) upper limit at 95% C.L. on the s-channel cross-section of $\sigma_s < 26.5$ (20.5) pb is obtained [154]. At 8 TeV, ATLAS uses 20.3 fb^{-1} of data with one lepton, large missing transverse momentum and exactly two b-tagged jets. They perform a maximum-likelihood fit of a discriminant based on a Matrix Element Method and optimized in order to separate single top-quark s-channel events from the main background contributions which are top-quark pair production and W boson production in association with heavy flavor jets. They find $\sigma_s = 4.8 \pm 0.8(stat.)^{+1.6}_{-1.3}(syst.)$ pb with a signal significance of 3.2 standard deviations [155], which provides first evidence for s-channel single-top production at 8 TeV. The signal is extracted through a maximum-likelihood fit to the distribution of a multivariate discriminant defined using boosted decision trees to separate the expected signal contribution from background processes. At 7 TeV and 8 TeV, CMS uses 5.1 fb^{-1} and 19.3 fb^{-1}, respectively, and analyses leptonic decay modes by performing a maximum likelihood fit to a multivariate discriminant defined using a Boosted Decision Tree, yielding cross sections of $\sigma_s = 7.1 \pm 8.1$ pb and $\sigma_s = 13.4 \pm 7.3$ pb, respectively, and a best fit value of 2.0 ± 0.9 for the combined ratio of the measured σ_s values and the ones expected in the Standard Model [156]. The signal significance is 2.5 standard deviations. ATLAS and CMS present the combinations of their single-top-quark production cross-section measurements, using Run-I data corresponding to integrated luminosities of 1.17 to 5.1 fb^{-1} at $\sqrt{s} = 7$ TeV and 12.2 to 20.3 fb^{-1} at $\sqrt{s} = 8$ TeV. These combinations are performed per centre-of-mass energy and for each production mode: t-channel, tW, and s-channel. The combined t-channel cross-sections are 67.5 ± 5.7 pb and 87.7 ± 5.8 pb at $\sqrt{s} = 7$ and 8 TeV, respectively. The combined tW cross-sections are 16.3 ± 4.1 pb and 23.1 ± 3.6 pb at $\sqrt{s} = 7$ and 8 TeV, respectively. For the s-channel cross-section, the combination yields 4.9 ± 1.4 pb at $\sqrt{s} = 8$ TeV. The square of the magnitude of the CKM matrix element V_{tb} multiplied by a form factor f_{LV} is determined for each production mode and centre-of-mass energy, using the ratio of the measured cross-section to its theoretical prediction. All combined measurements are consistent with their corresponding SM predictions [157]. Both, ATLAS and CMS, also measured the electroweak production of single top-quarks in association with a Z-boson, see section 61.3.2.4 of this review.

Fig. 61.2 provides a summary of all single top cross-section measurements at the LHC as a function of the center-of-mass energy. All cross-section measurements are very well described by the theory calculation within their uncertainty.

Thanks to the large statistics now available at the LHC, both CMS and ATLAS experiments also performed differential cross-section measurements in single-top t-channel production [132], [158]. Such measurements are extremely useful as they test our understanding of both QCD and EW top-quark interactions. The CMS collaboration has measured differential single top quark t-channel production cross sections as functions of the transverse momentum and the absolute value of the rapidity of the top quark. The analysis is performed in the leptonic decay channels of the top quark, with either a muon or an electron in the final state, using data collected with the CMS experiment at the LHC at $\sqrt{s} = 8$ TeV and corresponding to an integrated luminosity of 19.7 fb^{-1}. Neural networks are used to discriminate the signal process from the various background contributions. The results are found to agree with predictions from Monte Carlo generators [158]. Using the same data set and under the assumption that the spin analyzing power of a charged lepton is 100% as predicted in the SM, they are also able to measure the polarization of the top quark $P_t = 0.82 \pm 0.12(stat.) \pm 0.32(syst.)$ [159]. At 13 TeV, using 35.9 fb^{-1}, CMS measures the differential t-channel cross sections, for the first time in single-top production, and charge ratios for t-channel single top quark production [160]. The results are found to be in agreement with SM predictions using various NLO event generators and sets of parton distribution functions. Additionally, the spin asymmetry, sensitive to the top quark polarization, is determined from the differential distribution of the polarization angle at parton level to be 0.439 ± 0.062, in agreement with the SM prediction.

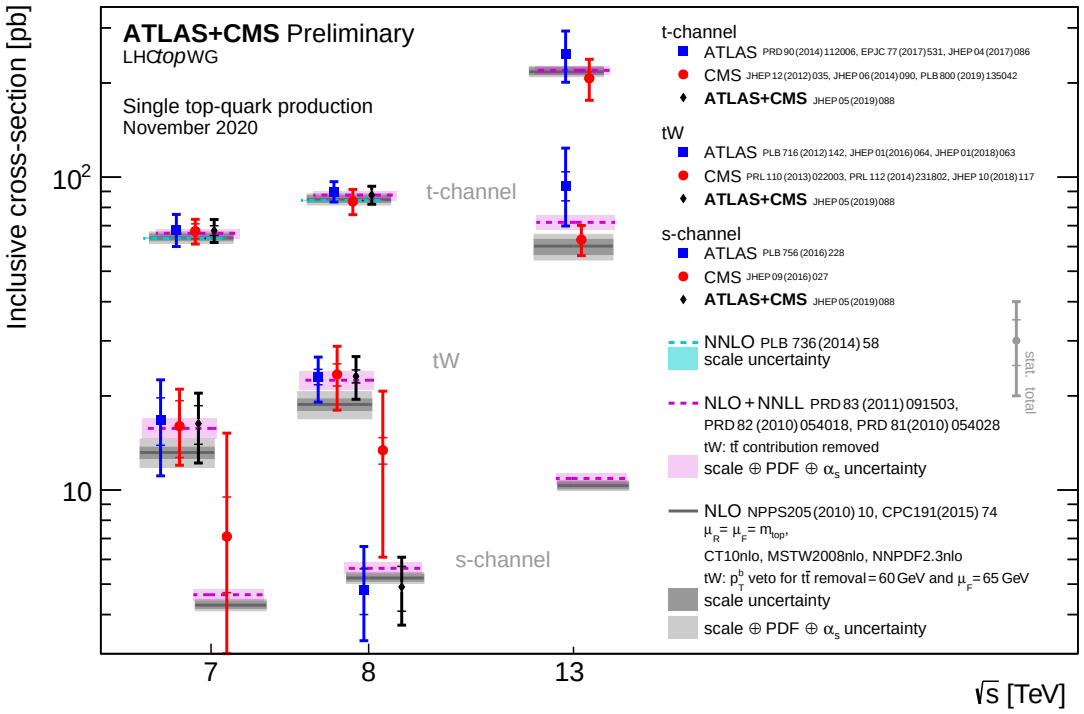

Figure 61.2: Measured and predicted single top production cross sections at LHC energies in pp collisions. The recent CMS measurement of the tW production cross section at 13 TeV in the l+jets channel is not yet shown here. The plot is kindly provided by the LHCtopWG working group, see https://twiki.cern.ch/twiki/bin/view/LHCPhysics/LHCTopWGSummaryPlots.

This disfavours the results obtained at 8 TeV. ATLAS has measured the differential tW cross section in 36.1 fb^{-1} at 13 TeV with respect to the energy of the b-jet, the energy of the system of the two leptons and b-jet, and the transverse mass or mass of combinations of leptons, the b-jet and neutrinos [161]. Using 35.9 fb^{-1} of $e\mu$ events, CMS to measure the differential tW cross section. A fiducial region is defined according to the detector acceptance, and the requirement of exactly one b-tagged jet. The resulting distributions are unfolded to particle-level and compared with predictions calculated at next-to-leading order in perturbative QCD. Within current uncertainties, all the predictions agree with the data [162].

61.3.1.4 *Top-Quark Asymmetries*

A forward-backward asymmetry in $t\bar{t}$ production at a $p\bar{p}$ collider arises starting at order α_S^3 in QCD from the interference between the Born amplitude $q\bar{q} \to t\bar{t}$ with 1-loop box production diagrams and between diagrams with initial- and final-state gluon radiation. The asymmetry, A_{FB}, is defined by

$$A_{FB} = \frac{N(\Delta y > 0) - N(\Delta y < 0)}{N(\Delta y > 0) + N(\Delta y < 0)}, \tag{61.2}$$

where $\Delta y = y_t - y_{\bar{t}}$ is the rapidity difference between the top- and the anti-top quark. Calculations at α_S^3 predict a measurable A_{FB} at the Tevatron. The most recent calculations up to order α_S^4, including electromagnetic and electroweak corrections, yield a predicted asymmetry of $\approx(9.5\pm0.7)\%$ [163]. This is about 10% higher than the previous calculation at NLO [164, 165], and improves the agreement with experiment.

Both CDF and DØ measured asymmetry values in excess of the SM prediction, fueling spec-

ulation about exotic production mechanisms (see, for example, [166] and references therein). The first measurement of this asymmetry by DØ in 0.9 fb^{-1} [167] found an asymmetry at the detector level of $(12 \pm 8)\%$. The first CDF measurement in 1.9 fb^{-1} [168] yielded $(24 \pm 14)\%$ at parton level. Both values were higher, though statistically consistent with the SM expectation. With the addition of more data, the uncertainties have been reduced, and the central values, if somewhat smaller, have remained consistent with the first measurements. At the same time, the improved calculations from theory have increased the predicted asymmetry values, improving the agreement between theory and experiment.

CDF and DØ have now combined results using the full Tevatron dataset at $\sqrt{s} = 1.96$ TeV [169]. Three combined asymmetries are reported: $A_{FB}^{t\bar{t}}$ as defined in Eq. 2 for fully-reconstructed $t\bar{t}$ events, a single-lepton asymmetry, A_{FB}^{ℓ} defined as in Eq. 2 but with Δy replaced by the product of the lepton charge and pseudo-rapidity, and a dilepton asymmetry, $A_{FB}^{\ell\ell}$, defined as in Eq. 2 but with Δy replaced by $\Delta\eta$ between the two leptons. The combined results are $A_{FB}^{t\bar{t}} = 0.128 \pm 0.021 \pm 0.014$, $A_{FB}^{\ell} = 0.073 \pm 0.016 \pm 0.012$, and $A_{FB}^{\ell\ell} = 0.108 \pm 0.043 \pm 0.016$, where the first uncertainty is statistical and the second systematic. These are to be compared to SM predictions at NNLO QCD and NLO electroweak of $A_{FB}^{t\bar{t}} = 0.095 \pm 0.007$ [163], $A_{FB}^{\ell} = 0.038 \pm 0.003$, and $A_{FB}^{\ell\ell} = 0.048 \pm 0.004$ [165], respectively. Both experiments have also measured differential asymmetries, in bins of $M_{t\bar{t}}$, Δy, $q_\ell \times \eta_\ell$, and $\Delta\eta_{\ell\ell}$, with consistent results, though the growth of $A_{FB}^{t\bar{t}}$ with increasing $M_{t\bar{t}}$ and Δy appears somewhat more rapid than the SM prediction [169].

At the LHC, where the dominant $t\bar{t}$ production mechanism is the charge-symmetric gluon-gluon fusion, the measurement is more difficult. For the sub-dominant $q\bar{q}$ production mechanism, the symmetric pp collision does not define a forward and backward direction. Instead, the charge asymmetry, A_C, is defined in terms of a positive versus a negative $t - \bar{t}$ rapidity difference, Δy

$$A_C^{t\bar{t}} = \frac{N(\Delta|y| > 0) - N(\Delta|y| < 0)}{N(\Delta|y| > 0) + N(\Delta|y| < 0)}. \tag{61.3}$$

Both CMS and ATLAS have measured A_C in the LHC dataset. Using lepton+jets events in 4.7 fb^{-1} of data at $\sqrt{s} = 7$ TeV, ATLAS measures $A_C^{t\bar{t}} = (0.6 \pm 1.0)\%$ [170]. ATLAS has reported on the same measurement performed at $\sqrt{s} = 8$ TeV with 20.3 fb^{-1} of data, with a result of $A_C^{t\bar{t}} = (0.9 \pm 0.5)\%$ [171]. In the dilepton channel at $\sqrt{s} = 8$ TeV, ATLAS measures [172] $A_C^{t\bar{t}} = (2.1 \pm 1.6)\%$, and $A_C^{\ell\ell} = (0.8 \pm 0.6)\%$ (defined in terms of the $\Delta\eta$ of the two leptons) in agreement with the SM predictions of $(1.11 \pm 0.04)\%$ and $(0.64 \pm 0.03)\%$, respectively [165]. Using lepton+jets events CMS has measured A_C at both $\sqrt{s} = 7$ and 8 TeV. They measure $A_C^{t\bar{t}} = (0.4 \pm 1.5)\%$ and $A_C^{t\bar{t}} = (0.33 \pm 0.26(stat.) \pm 0.33(syst.))\%$ in 5.0 fb^{-1} at $\sqrt{s} = 7$ TeV and In 19.7 fb^{-1} at $\sqrt{s} = 8$ TeV, respectively [173, 174]. Both measurements are consistent with the SM expectations of $A_C^{t\bar{t}} = (1.23 \pm 0.05)\%$ at $\sqrt{s} = 7$ TeV and $(1.11 \pm 0.04)\%$ at $\sqrt{s} = 8$ TeV [165], although the uncertainties are still too large for a precision test. In 19.5 fb^{-1} of dilepton events at $\sqrt{s} = 8$ TeV, CMS measures $A_C^{t\bar{t}} = (1.1 \pm 1.3)\%$ and $A_C^{\ell\ell} = (0.3 \pm 0.7)\%$ [175], consistent with SM expectations [176].

In their 7 and 8 TeV analyses ATLAS and CMS also provide differential measurements as a function of $M_{t\bar{t}}$ and the transverse momentum p_T and rapidity y of the $t\bar{t}$ system. To reduce model-dependence, the CMS collaboration has performed a measurement in a reduced fiducial phase space [177], with a result of $A_C = (-0.35 \pm 0.72(stat.) \pm 0.31(syst.))\%$, in agreement with SM expectations.

To specifically address the dependence of the asymmetry on $M_{t\bar{t}}$, ATLAS has performed a measurement in boosted $t\bar{t}$ events [178]. In 20.3 fb^{-1} of data at $\sqrt{s} = 8$ TeV, in events with $M_{t\bar{t}} > 0.75$ TeV, and $|(\Delta|y|)| < 2$, ATLAS measures $A_C^{t\bar{t}} = (4.2 \pm 3.2)\%$ compared to a NLO SM

prediction of $(1.60 \pm 0.04)\%$. The measurement is also presented in three bins of $M_{t\bar{t}}$, each in agreement, though with large uncertainties, with the SM expectations.

Both ATLAS and CMS have measured asymmetries in the distribution of leptons from $t\bar{t}$ decays. ATLAS, in 4.6 fb^{-1} of $\sqrt{s} = 7$ TeV data, has measured $A^{\ell\ell} = (2.4 \pm 1.5(\text{stat.}) \pm 0.9(\text{sys.}))\%$ in dilepton events [179]. Using a neutrino weighting technique in the same dataset to reconstruct the top quarks, ATLAS measures $A_C = (2.1 \pm 2.5\ (\text{stat.}) \pm 1.7\ (\text{sys.}))\%$. CMS, in 5.0 fb^{-1} of $\sqrt{s} = 7$ TeV data, uses dilepton events to measure $A_C = (1.0 \pm 1.5\ (\text{stat.}) \pm 0.6\ (\text{sys.}))\%$, where a matrix weighting technique is used to reconstruct the top quarks, and $A^{\ell\ell} = (0.9 \pm 1.0\ (\text{stat.}) \pm 0.6\ (\text{sys.}))\%$ [180]. An earlier result using lepton+jets events from the same CMS dataset found $A_C = (0.4 \pm 1.0 \pm 1.1)\%$ [173]. Combined results from ATLAS and CMS have now been released [181]. At $\sqrt{s} = 7$ TeV the combined result is $A_C = (0.5 \pm 0.7\ (\text{stat.}) \pm 0.6\ (\text{sys.}))\%$, and at $\sqrt{s} = 8$ TeV it is $A_C = (0.55 \pm 0.23 \pm 0.25)\%$. These results are all consistent, within their large uncertainties, with the SM expectations of $A^{\ell\ell} = (0.70 \pm 0.03)\%$ and $A_C = (1.23 \pm 0.05)\%$ [165].

ATLAS has released a charge asymmetry measurement at $\sqrt{s} = 13$ TeV using the full 139 fb^{-1} dataset. A Bayesian unfolding procedure is used in lepton plus jets events, combining both resolved and boosted topologies, to infer the asymmetry at parton level, correcting for detector resolution and acceptance effects. The inclusive charge asymmetry is measured as $A_C = (0.60 \pm 0.15)\%$ (stat+syst.) [182]. In addition to the inclusive measurement, the result includes differential measurements in five bins of $M_{t\bar{t}}$, and four bins of longitudinal boost. Both inclusive and differential results are found consistent with Standard Model predictions at NNLO in QCD and NLO in electroweak theory.

A model-independent comparison of the Tevatron and LHC results is made difficult by the differing $t\bar{t}$ production mechanisms at work at the two accelerators and by the symmetric nature of the pp collisions at the LHC. A recent result from the CMS Collaboration [183] in 35.9 fb^{-1} of lepton plus jets events at $\sqrt{s} = 13$ TeV, uses a likelihood analysis to separate the $q\bar{q}$ process from production via gluon-gluon and gluon-quark interactions and extract $A_{FB} = (4.8^{+8.8}_{-8.4}\ (\text{stat.}) \pm 2.8\ (\text{sys.}))\%$. In addition, given a particular model of BSM physics, a comparison can be obtained through the resulting asymmetry predicted by the model at the two machines, see for example [178].

A new measurement from ATLAS explores a so-called 'energy asymmetry' in $t\bar{t}$ production in association with a high-p_T jet ($t\bar{t}j$ production). The energy asymmetry is defined as a difference between the top and anti-top quarks' energies, and is measured in ATLAS in three bins of the associated high-p_T jet angle, θ_j. Both the energies and jet angle are measured in the $t\bar{t}j$ rest frame. A Bayesian unfolding method corrects for resolution and acceptance effects. The measurement is in agreement with the Standard Model at NLO accuracy [184].

61.3.2 *Top-Quark Properties*

61.3.2.1 *Top-Quark Mass Measurements*

The most precisely studied property of the top quark is its mass. The top-quark mass has been measured in the lepton+jets, the dilepton, and the all-jets channel by all four Tevatron and LHC experiments, and now in single-top events at the LHC. The latest and/or most precise results are summarized in Table 61.1. The lepton+jets channel yields the most precise single measurements because of good signal to background ratio (in particular after b-tagging) and the presence of only a single neutrino in the final state. The momentum of a single neutrino can be reconstructed (up to a quadratic ambiguity) via the missing E_T measurement and the constraint that the lepton and neutrino momenta reconstruct to the known W boson mass. In the large data samples available at the LHC, measurements in the dilepton channel can be competitive and certainly complementary to those in the lepton+jets final state.

A large number of techniques have now been applied to measuring the top-quark mass. The orig-

inal 'template method' [185], in which Monte Carlo templates of reconstructed mass distributions are fit to data, has evolved into a precision tool in the lepton+jets channel, where the systematic uncertainty due to the jet energy scale (JES) uncertainty is controlled by a simultaneous, *in situ* fit to the $W \to jj$ hypothesis [186]. All the latest measurements in the lepton+jets and the all-jets channels use this technique in one way or another. In 20.2 fb^{-1} of data at $\sqrt{s} = 8$ TeV in the lepton+jets channel, ATLAS achieves a total uncertainty of 0.53% with a statistical component of 0.23% [187]. The measurement is based on a 3-dimensional template fit, determining the top-quark mass, the global jet energy scale and a b-to-light jet energy scale factor. The most precise CMS result in the lepton+jets channel uses an ideogram method and comes from a so-called 'hybrid' approach in which the prior knowledge about the jet energy scale is incorporated as a Gaussian constraint, with a width determined by the uncertainty on the jet energy corrections. In 19.7 fb^{-1} of $\sqrt{s} = 8$ TeV data, CMS achieves a total uncertainty of 0.30% with a statistical component of 0.09% with the hybrid approach [188]. Using this same method, CMS has released a top-mass measurement from $\sqrt{s} = 13$ TeV data. Using 35.9 fb^{-1} of lepton+jets events they measure the top mass with a precision of 0.36%, with a statistical component of 0.05% [189]. The measurements at $\sqrt{s} = 13$ TeV include, for the first time, an uncertainty due to 'color reconnection' [190,191]. In this same dataset, CMS has extracted a top mass from highly boosted top-quark decays by selecting events in which the hadronic-side top decay is reconstructed as a single jet with $P_T > 400$ GeV. The cross section as a function of jet mass is unfolded at the particle level to extract a top mass with a precision of 1.4% [192].

The template method is complemented by the 'matrix element' method. This method was first applied by the DØ Collaboration [193], and is similar to a technique originally suggested by Kondo *et al.* [194] and Dalitz and Goldstein [195] In the matrix element method a probability for each event is calculated as a function of the top-quark mass, using a LO matrix element for the production and decay of $t\bar{t}$ pairs. The *in situ* calibration of dijet pairs to the $W \to jj$ hypothesis is now also used with the matrix element technique to constrain the jet energy scale uncertainty. In the lepton+jets channel, DØ uses the full Tevatron dataset of 9.7 fb^{-1} and yields an uncertainty of about 0.43% [196].

In the dilepton channel, the signal to background is typically very good, but reconstruction of the mass is non-trivial because there are two neutrinos in the final state, yielding a kinematically unconstrained system. A variety of techniques have been developed to handle this. An analytic solution to the problem has been proposed [197], but this has not yet been used in the mass measurement. One of the most precise measurements in the dilepton channel comes from using the invariant mass of the charged lepton and b-quark system ($M_{\ell b}$), which is sensitive to the top-quark mass and avoids the kinematic difficulties of the two-neutrino final state. In 4.6 fb^{-1} of $\sqrt{s} = 7$ TeV data, ATLAS has measured the top-quark mass in the dilepton channel to a precision of 0.53% using a template fit to the $M_{\ell b}$ distribution [198]. Using 19.7 fb^{-1} of data at $\sqrt{s} = 8$ TeV, CMS has released [199] a mass measurement in the dilepton channel based on a simultaneous fit to $M_{\ell b}$ and a transverse-mass-like variable M_{T2} [200]. The most precise result in this analysis, which comes from a linear combination of fits with the jet energy scale fixed at its nominal value and one that simultaneously determines the top mass and jet energy scale, has a total uncertainty of 0.54%. At the LHC, because of their precision, these techniques have largely displaced a number of earlier techniques in the dilepton channel, though these techniques are still included, and described, in the combined results from CMS, reported in Ref. [188].

In the neutrino weighting technique, used by CDF to analyze the full Run 2 dilepton dataset of 9.1 fb^{-1}, a weight is assigned by assuming a top-quark mass value and applying energy-momentum conservation to the top-quark decay, resulting in up to four possible pairs of solutions for the neutrino and anti-neutrino momenta. The missing E_T calculated in this way is then compared to

Table 61.1: Measurements of top-quark mass from Tevatron and LHC. The results are a selection of both published and preliminary (not yet submitted for publication as of September 2021) measurements. For a complete set of published results see the Listings. Statistical uncertainties are listed first, followed by systematic uncertainties.

m_t (GeV/c^2)	Source	$\int \mathcal{L}$dt fb^{-1}	Ref.	Channel
$172.08 \pm 0.25 \pm 0.41$	ATLAS	20.2	[187]	ℓ+jets+$\ell\ell$+All jets
$172.44 \pm 0.13 \pm 0.47$	CMS	19.7	[188]	ℓ+jets+$\ell\ell$+All jets
$172.35 \pm 0.16 \pm 0.48$	CMS	19.7	[188]	ℓ+jets
$172.34 \pm 0.20 \pm 0.70$	CMS	35.9	[201]	$\ell\ell$
$173.72 \pm 0.55 \pm 1.01$	ATLAS	20.2	[202]	All jets
$172.25 \pm 0.08 \pm 0.62$	CMS	35.9	[189]	ℓ+jets
$172.6 \pm 0.4 \pm 2.4$	CMS	35.9	[192]	Boosted jets
$172.13 \pm 0.32^{+0.69}_{-0.70}$	CMS	35.9	[203]	Single top
$174.30 \pm 0.35 \pm 0.54$	CDF,DØ (I+II)	$\leq$9.7	[204]	publ. or prelim.
$173.34 \pm 0.27 \pm 0.71$	Tevatron+LHC	$\leq$8.7+$\leq$4.9	[3]	publ. or prelim.

the observed missing E_T to assign a weight [205]. The CDF result achieves a precision of 1.8% using a combination of neutrino weighting and an "alternative mass", which is insensitive to the jet energy scale [206]. The alternative mass depends on the angles between the leptons and the leading jets and the lepton four-momenta.

In the all-jets channel there is no ambiguity due to neutrino momenta, but the signal to background is significantly poorer due to the severe QCD multijets background. The emphasis therefore has been on background modeling, and reduction through event selection. The most recent measurement in the all-jets channel, by CMS in 35.9 fb^{-1} of $\sqrt{s} = 13$ TeV data [201], uses an ideogram method and a 2-dimensional simultaneous fit for m_t and the jet energy scale to extract the top-quark mass and achieves a precision of 0.36%. A measurement from ATLAS [202] uses a template fit to the ratio of three-jet (m_t) to two-jet (M_W) mass in the all-hadronic channel, the two-jet denominator provides an *in situ*, fit to the $W \to jj$ hypothesis. In 20.2 fb^{-1} of data at $\sqrt{s} = 8$ TeV, the result has a precision of 0.65%. A measurement from CDF in 9.3 fb^{-1} uses a two-dimensional template fit and achieves a precision of 1.1% [207].

The CMS Collaboration extracted a top-quark mass measurement from single-top events, something not previously done because of the poor signal to background ratio. The mass is extracted from the invariant mass of the muon, bottom quark, and missing transverse energy. The first measurement with 19.7 fb^{-1} of data at $\sqrt{s} = 8$ TeV, achieved a precision of 0.71% [208]. A more recent measurement in 35.9 fb^{-1} of data at $\sqrt{s} = 13$ TeV achieves 0.44% precision [203].

A dominant systematic uncertainty in these methods is the understanding of the jet energy scale, and so several techniques have been developed that have little sensitivity to the jet energy scale uncertainty. In addition to Reference [206] mentioned above, these include the measurement of the top-quark mass using the following techniques: Fitting of the lepton p_T spectrum of candidate events [209]; fitting of the transverse decay length of the b-jet (L_{xy}) [210]; fitting the invariant mass of a lepton from the W-decay and a muon from the semileptonic b decay [211,212], kinematic properties of secondary vertices from b-quark fragmentation [213], the invariant mass of the $J/\psi+\ell$ system in events in which a b-quark fragments to a J/ψ particle [214], fitting the b-jet energy peak [215], and dilepton kinematics in $e\mu$ events [216].

Several measurements have now been made in which the top-quark mass is extracted from the measured $t\bar{t}$ cross section using the theoretical relationship between the mass and the production

cross section. These determinations make use of predictions calculated at higher orders, where the top mass enters as an input parameter defined in a given scheme. At variance with the usual methods, which involve the kinematic properties of the final states and therefore the pole mass, this approach can also directly determine a short-distance mass, such as the $\overline{\text{MS}}$ mass [217]. With an alternative method ATLAS extracted the top-quark pole mass using $t\bar{t}$ events with at least one additional jet, basing the measurement on the relationship between the differential rate of gluon radiation and the mass of the quark [218]. A similar analysis by CMS used the differential cross section as a function of the invariant mass of the $t\bar{t}$ system and the leading jet not associated with the top decays [219].

Each of the experiments has produced a measurement combining its various results. The combined measurement from CMS with up to 19.7 fb^{-1} of data achieves statistical and systematic uncertainties of 0.08% and 0.27%, respectively [188]. The combined measurement from ATLAS, with up to 20.3 fb^{-1} yields statistical and systematic uncertainties of 0.14% and 0.24%, respectively [187]. CDF has combined measurements with up to 9.3 fb^{-1} [220] and achieves a statistical precision of 0.33% and a systematic uncertainty of 0.43%. DØ achieves a 0.33% statistical+JES and a 0.28% systematic uncertainty by combining results in 9.7 fb^{-1} [221].

Combined measurements from the Tevatron experiments and from the LHC experiments take into account the correlations between different measurements from a single experiment and between measurements from different experiments. The Tevatron average [204], using up to 9.7 fb^{-1} of data, now has a precision of 0.37%. The LHC combination, using up to 4.9 fb^{-1} of data, has a precision of 0.56% [222], where more work on systematic uncertainties is required. A Tevatron-LHC combination has been released, combining the results of all four experiments, using the full Tevatron dataset and the $\sqrt{s} = 7$ TeV LHC data, with a resulting precision of 0.44% [3]

The direct measurements of the top-quark mass, such as those shown in Table 61.1, correspond to the parameter used in the Monte Carlo generators, which is closely related to the pole mass [223]. The relation between the pole mass and short-distance masses, such as $\overline{\text{MS}}$, is affected by non-perturbative effects. Recent calculations evaluate the size of this ambiguity to be below 250 MeV and therefore still smaller than the current measurement uncertainty [224,225]. ATLAS has recently performed a 'calibration' of the top mass parameter in POWHEG + PYTHIA 8 with respect to the so-called 'MSR' mass scheme [226]. Using simulated lepton+jets events and the mass distribution of large-radius jets containing the three quarks from the hadronically decaying top quark, they find a mass difference between the Monte Carlo mass and the MSR mass of 80 MeV with large uncertainties [227].

As a result of renormalization at higher-orders in perturbation theory, the top quark mass depends on the scale at which it is evaluated. The CMS collaboration has made the first measurement of the so-called running of the top-quark mass in the $\overline{\text{MS}}$ scheme [228]. The running mass is extracted from a measurement of the differential cross section as a function of the $t\bar{t}$ invariant mass, unfolded back to the parton level, in $e\mu$ final states. The running mass varies by about 15% from $M_{t\bar{t}} = 400$ GeV to $M_{t\bar{t}} \approx 1$ TeV, in good agreement with the renormalization group calculation at one-loop level. Compared to the hypothesis of no running, the significance of the measured running is 2.6σ. However, caveats of such an interpretation have been raised as a result of the large theoretical uncertainties [229].

With the discovery of a Higgs boson at the LHC with a mass of about 125 GeV/c^2 [230, 231], the precision measurement of the top-quark mass takes a central role in the question of the stability of the electroweak vacuum because top-quark radiative corrections tend to drive the Higgs quartic coupling, λ, negative, potentially leading to an unstable vacuum. A calculation at NNLO [232] leads to the conclusion of vacuum stability for a Higgs mass satisfying $M_H \geq 129.4 \pm 5.6$ GeV/c^2 [233]. Given the uncertainty, a Higgs mass of 125 GeV/c^2 satisfies the limit, but the central values of the

Higgs and top-quark masses put the electroweak vacuum squarely in the metastable region. The uncertainty is dominated by the precision of the top-quark mass measurement and its interpretation as the pole mass. For more details, see the Higgs boson review in this volume.

As a test of the CPT-symmetry, the mass difference of top- and antitop-quarks $\Delta m_t = m_t - m_{\bar{t}}$, which is expected to be zero, can be measured. CDF measures the mass difference in 8.7 fb^{-1} of 1.96 TeV data in the lepton+jets channel using a template methode to find $\Delta m_t = -1.95 \pm 1.11(stat.) \pm 0.59(syst.)$ GeV/c^2 [234] while DØ uses 3.6 fb^{-1} of lepton+jets events and the matrix element method with at least one b-tag. They find $\Delta m_t = 0.8 \pm 1.8(stat.) \pm 0.5(syst.)$ GeV/c^2 [235]. In 4.7 fb^{-1} of 7 TeV data, ATLAS measures the mass difference in lepton+jets events with a double b-tag requirement and hence very low background to find $\Delta m_t = 0.67 \pm 0.61(stat.) \pm 0.41(syst.)$ GeV/c^2 [236]. CMS measures the top-quark mass difference in 5 fb^{-1} of 7 TeV data in the lepton+jets channel and finds $\Delta m_t = -0.44 \pm 0.46(stat.) \pm 0.27(syst.)$ GeV/c^2 [237]. They repeat this measurement with 19.6 fb^{-1} of 8 TeV data to find $\Delta m_t = -0.15 \pm 0.19(stat.) \pm 0.09(syst.)$ GeV/c^2 [238]. Now that the top mass has been measured in single-top events, the mass difference can be measured by tagging the top- or anti-top quark with the lepton charge. In 35.9 fb^{-1} of 13 TeV single-top candidate events CMS measures the mass ratio and difference to be $0.995^{+0.005}_{-0.006}$ and $0.83^{+0.77}_{-1.01}$ GeV, respectively [203]. All measurements are consistent with the SM expectation.

61.3.2.2 *Top-Quark Spin Correlations, Polarization, and Width*

One of the unique features of the top quark is that it decays before its spin can be flipped by the strong interaction. Thus the top-quark polarization is directly observable via the angular distribution of its decay products and it is possible to define and measure observables sensitive to the top-quark spin and its production mechanism. Although the top- and antitop-quarks produced by strong interactions in hadron collisions are essentially unpolarized, the spins of t and $\bar{t}$ are correlated. For QCD production at threshold, the $t\bar{t}$ system is produced in a $^3S_1$ state with parallel spins for $q\bar{q}$ annihilation or in a $^1S_0$ state with antiparallel spins for gluon-gluon fusion. The situations at the Tevatron, where the production is primarily from $q\bar{q}$ annihilation, and at the LHC, where the production is primarily from gluon-gluon fusion, are therefore somewhat complementary. However, at the LHC production of $t\bar{t}$ pairs at large invariant mass occurs primarily via fusion of gluons with opposite helicities, and the $t\bar{t}$ pairs so produced have parallel spins as in production at the Tevatron via $q\bar{q}$ annihilation. The direction of the top-quark spin is 100% correlated to the angular distributions of the down-type fermion (charged leptons or d-type quarks) in the decay. The joint angular distribution [239–241]

$$\frac{1}{\sigma}\frac{d^2\sigma}{d(\cos\theta_+)d(\cos\theta_-)} = \frac{1}{4}(1 + B_+\cos\theta_+ + B_-\cos\theta_- + \kappa\cdot\cos\theta_+\cdot\cos\theta_-), \tag{61.4}$$

where θ_+ and θ_- are the angles of the daughters in the top-quark rest frame with respect to a particular spin quantization axis (assumed here to be the same for θ_+ and θ_-), is a very sensitive observable. The maximum value for κ, 0.782 at NLO at the Tevatron [242], is found in the off-diagonal basis [239], while at the LHC the value at NLO is 0.326 in the helicity basis [242]. The coefficients B_+ and B_- are near zero in the SM because the top quarks are unpolarized in $t\bar{t}$ production. In place of κ, $A\alpha_+\alpha_-$ is often used, where α_i is the spin analyzing power, and A is the spin correlation coefficient, defined as

$$A = \frac{N(\uparrow\uparrow) + N(\downarrow\downarrow) - N(\uparrow\downarrow) - N(\downarrow\uparrow)}{N(\uparrow\uparrow) + N(\downarrow\downarrow) + N(\uparrow\downarrow) + N(\downarrow\uparrow)}, \tag{61.5}$$

where the first arrow represents the direction of the top-quark spin along a chosen quantization axis, and the second arrow represents the same for the antitop-quark. The spin analyzing power α_i

is +0.998 for positively charged leptons, -0.966 for down-type quarks from W decays, and -0.393 for bottom quarks [243]. The sign of α flips for the respective antiparticles. The spin correlation could be modified by a new $t\bar{t}$ production mechanism such as through a Z' boson, Kaluza-Klein gluons, a dark-matter mediator, or a Higgs boson.

The experiments typically use a Monte Carlo to provide templates for the measured distributions, or alternatively a matrix-element technique, and fit a parameter f, representing the fraction of events with the expected Standard Model correlation, with $(1-f)$ the fraction with no correlation. The correlation coefficient is extracted via $A_{\rm meas} = f \cdot A_{\rm SM}$. A 'fraction' $f > 1$ means that the measured correlation coefficient is larger than the Standard Model expectation.

CDF used 5.1 fb^{-1} in the dilepton channel to measure the correlation coefficient in the beam axis [244]. The measurement was made using the expected distributions of $(\cos\theta_+, \cos\theta_-)$ and $(\cos\theta_b, \cos\theta_{\bar{b}})$ of the charged leptons or the b-quarks in the $t\bar{t}$ signal and background templates to calculate a likelihood of observed reconstructed distributions as a function of assumed κ. They determined the 68% confidence interval for the correlation coefficient κ as $-0.52 < \kappa < 0.61$ or $\kappa = 0.04 \pm 0.56$ assuming $m_t = 172.5$ GeV/c^2.

CDF also analyzed lepton+jets events in 5.3 fb^{-1} [245] assuming $m_t = 172.5$ GeV/c^2. They form three separate templates - the same-spin template, the opposite-spin template, and the background template for the 2-dimensional distributions in $\cos(\theta_l)\cos(\theta_d)$ vs. $\cos(\theta_l)\cos(\theta_b)$. The fit to the data in the helicity basis returns an opposite helicity fraction of $F_{OH} = 0.74 \pm 0.24(stat.) \pm 0.11(syst.)$. Converting this to the spin correlation coefficient yields $\kappa_{helicity} = 0.48 \pm 0.48(stat.) \pm 0.22(syst.)$. In the beamline basis, they find an opposite spin fraction of $F_{OS} = 0.86 \pm 0.32(stat.) \pm 0.13(syst.)$ which can be converted into a correlation coefficient of $\kappa_{beam} = 0.72 \pm 0.64(stat.) \pm 0.26(syst.)$.

DØ performed a measurement of the ratio f of events with correlated t and $\bar{t}$ spins to the total number of $t\bar{t}$ events. Combining dilepton and lepton plus jets events, and using a matrix-element technique in 9.7 fb^{-1} of Tevatron data, DØ measures $f = 1.16 \pm 0.21$, corresponding to $A_{exp.} = 0.89 \pm 0.22(stat. + syst.)$ in the off-diagonal basis [246].

In Ref. [247] DØ presents a measurement of top-quark polarization in $t\bar{t}$ production at the Tevatron. In 9.7 fb^{-1} of $p\bar{p}$ collisions, DØ uses lepton angular distributions in lepton+jets events to measure polarization in the beam, helicity, and transverse bases. The measurements are, respectively, 0.081 ± 0.048, -0.102 ± 0.061 and, 0.040 ± 0.035, where the beam-basis result is a combination with an earlier DØ result in dilepton events [248]. These results are all consistent near-zero polarization, as predicted in the SM.

Spin correlations have been conclusively measured at the LHC by both the ATLAS and CMS collaborations. In the dominant gluon fusion production mode for $t\bar{t}$ pairs at the LHC, the angular distribution between the two leptons in $t\bar{t}$ decays to dileptons is sensitive to the degree of spin correlation [249].

Measurements have been made at 7, 8, and now 13 TeV. While there is some interest in the $\sqrt{s}$ dependence of the correlations as a test of the production mechanism ($q\bar{q}$ vs gluon-gluon and possible sensitivity to new physics) the earlier measurements at 7 and 8 TeV [250–255] had relatively large uncertainties and have now been overtaken by the high-statistics 13 TeV measurements, which we review here.

The most recent result from ATLAS, in 36.1 fb^{-1} at $\sqrt{s} = 13$ TeV, uses $\Delta\phi$, the azimuthal angle between the two charged leptons in $e\mu$ events in an analysis that also measures the differential cross sections in $\Delta\phi$ and $\Delta\eta$ between the two leptons [256]. The result, measured by comparison with NLO Monte Carlo generators, is $f = 1.249 \pm 0.024 \pm 0.061^{+0.067}_{-0.090}$, where the uncertainties are statistical, systematic, and theoretical, is again greater than 1.0. Whereas the previous results were statistically consistent with the Standard Model expectation of 1.0, this result is inconsistent at the level of 2.2σ. The NLO generators are NLO in QCD only (and only at the production level).

Including electroweak couplings produces an expected Standard Model distribution consistent with the data, but results in a large scale uncertainty, giving $f = 1.03 \pm 0.13$.

In 35.9 fb^{-1} of data at $\sqrt{s} = 13$ TeV, CMS has measured spin correlations in dilepton events using $\Delta\phi$ and found $f = 1.05 \pm 0.03 \pm 0.08^{+0.09}_{-0.12}$ [257], where the uncertainties are statistical, systematic, and theoretical. The correlation is also measured using the coefficient κ in Eq. 61.4 (called $-C_{ij}$ in Reference [257]) using three orthogonal spin quantization axes defined in Ref. [258]. All results are consistent with $f = 1$. Measurements of the coefficients B_i in Eq. 61.4 in this analysis, which are expected to be nearly zero in the SM, yield $B_+ = 0.005 \pm 0.023$ and $B_- = 0.007 \pm 0.023$, consistent with the SM predictions at NLO of $0.0040^{+0.0017}_{-0.0012}$ [258]. These results are part of a complete study of the top-quark spin density matrix at $\sqrt{s} = 13$ TeV, through the measurement of the coefficients of Eq. 61.4.

In a similar ATLAS measurement at $\sqrt{s} = 8$ TeV [259], the spin-correlation coefficient κ is measured in the helicity basis to be $\kappa = 0.296 \pm 0.093$ in good agreement with the SM expectation of 0.318 (corresponding to a central value of f of 0.931). The polarization coefficients, B, in Eq. 61.4 are measured, also in the helicity basis, to be $B_+ = -0.044 \pm 0.038$ and $B_- = -0.064 \pm 0.040$, consistent with the SM predictions of 0.0030 ± 0.0010 and 0.0034 ± 0.00104, respectively.

Observation of top-quark spin correlations requires a top-quark lifetime less than the spin decorrelation timescale [260]. The top-quark width, inversely proportional to its lifetime, is expected to be of order 1 GeV/c^2 (Eq. 1). Early measurements made at CDF [261] and CMS [262] established confidence-level intervals for the width, but did not have the sensitivity to make a direct measurement.

The first direct measurement comes from an ATLAS analysis that directly fits reconstructed lepton+jets events in 20.2 fb^{-1} of data at $\sqrt{s} = 8$ TeV. They find $\Gamma_t = 1.76 \pm 0.33^{+0.79}_{-0.68}$ GeV/c^2 [263]. A more recent measurement from ATLAS with 139 fb^{-1} of data at $\sqrt{s} = 13$ TeV [264], uses a template fit to the lepton-b-quark invariant mass in dilepton final states. The result, $\Gamma_t = (1.9 \pm 0.5)$ GeV/c^2, is the most precise measurement to date.

The total width of the top-quark can also be determined from the partial decay width $\Gamma(t \to Wb)$ and the branching fraction $B(t \to Wb)$. DØ obtains $\Gamma(t \to Wb)$ from the measured t-channel cross section for single top-quark production in 5.4 fb^{-1}, and $B(t \to Wb)$ is extracted from a measurement of the ratio $R = B(t \to Wb)/B(t \to Wq)$ in $t\bar{t}$ events in lepton+jets channels with 0, 1 and 2 b-tags. Assuming $B(t \to Wq) = 1$, where q includes any kinematically accessible quark, the result is: $\Gamma_t = 2.00^{+0.47}_{-0.43}$ GeV/c^2 which translates to a top-quark lifetime of $\tau_t = (3.29^{+0.90}_{-0.63}) \times 10^{-25}$ s. Assuming a high mass fourth generation b' quark and unitarity of the four-generation quark-mixing matrix, they set the first upper limit on $|V_{tb'}| < 0.59$ at 95% C.L. [265]. A similar analysis has performed by CMS in 19.7 fb^{-1} of $\sqrt{s} = 8$ TeV data. It provides a better determination of the total width with respect to the measurement by DØ giving $\Gamma_t = 1.36 \pm 0.02(stat.)^{+0.14}_{-0.11}(syst.)$ GeV/c^2 [75].

61.3.2.3 *W-Boson Helicity in Top-Quark Decay*

The Standard Model dictates that the top quark has the same vector-minus-axial-vector $(V-A)$ charged-current weak interactions $\left(-i\frac{g}{\sqrt{2}}V_{tb}\gamma^\mu\frac{1}{2}(1-\gamma_5)\right)$ as all the other fermions. In the SM, the fraction of top-quark decays to longitudinally polarized W bosons is proportional to its Yukawa coupling and hence enhanced with respect to the weak coupling. It is expected to be [266] $\mathcal{F}_0^{\rm SM} \approx x/(1+x)$, $x = m_t^2/2M_W^2$ ($\mathcal{F}_0^{\rm SM} \sim 70\%$ for $m_t = 173$ GeV/c^2). Fractions of left-handed, right-handed, or longitudinal W bosons are denoted as $\mathcal{F}_-$, $\mathcal{F}_+$, and $\mathcal{F}_0$ respectively. In the SM, $\mathcal{F}_-$ is expected to be $\approx 30\%$ and $\mathcal{F}_+ \approx 0\%$. Predictions for the W polarization fractions at NNLO in QCD are available [267].

The Tevatron and the LHC experiments use various techniques to measure the helicity of the

W boson in top-quark decays, in both the lepton+jets and in dilepton channels in $t\bar{t}$ production.

The first method uses a kinematic fit, similar to that used in the lepton+jets mass analyses, but with the top-quark mass constrained to a fixed value, to improve the reconstruction of final-state observables, and render the under-constrained dilepton channel solvable. Alternatively, in the dilepton channel the final-state momenta can also be obtained through an algebraic solution of the kinematics. The distribution of the helicity angle ($\cos\theta^*$) between the lepton and the b quark in the W rest frame provides the most direct measure of the W helicity. In a simplified version of this approach, the $\cos\theta^*$ distribution is reduced to a forward-backward asymmetry.

The second method (p_T^ℓ) uses the different lepton p_T spectra from longitudinally or transversely polarized W-decays to determine the relative contributions.

A third method uses the invariant mass of the lepton and the b-quark in top-quark decays ($M^2_{\ell b}$) as an observable, which is directly related to $\cos\theta^*$.

At the LHC, top-quark pairs in the dilepton channels are reconstructed by solving a set of six independent kinematic equations in the missing transverse energy in x- and in y-direction, two W-masses, and the two top/antitop-quark masses. In addition, the two jets with the largest p_T in the event are interpreted as b-jets. The pairing of the jets to the charged leptons is based on the minimization of the sum of invariant masses M_{min}. Simulations show that this criterion gives the correct pairing in 68% of the events.

Finally, the Matrix Element Method (MEM) has also been used [194], in which a likelihood is formed from a product of event probabilities calculated from the MEM for a given set of measured kinematic variables and assumed W-helicity fractions.

The results of recent CDF, DØ, ATLAS, and CMS analyses are summarized in Table 61.2. The datasets are now large enough to allow for a simultaneous fit of $\mathcal{F}_0$, $\mathcal{F}_-$ and $\mathcal{F}_+$, which we denote by '3-param' or $\mathcal{F}_0$ and $\mathcal{F}_+$, which we denote by '2-param' in the table. Results with either $\mathcal{F}_0$ or $\mathcal{F}_+$ fixed at its SM value are denoted '1-param'. For the simultaneous fits, the correlation coefficient between the two values is about -0.8. A complete set of published results can be found in the Listings. All results are in agreement with the SM expectation.

CDF and DØ combined their results based on $2.7 - 5.4$ fb^{-1} [268] for a top-quark mass of 172.5 GeV/c^2. ATLAS presents results from 1.04 fb^{-1} of $\sqrt{s} = 7$ TeV data using a template method for the $\cos\theta^*$ distribution and angular asymmetries from the unfolded $\cos\theta^*$ distribution in the lepton+jets and the dilepton channel [269]. CMS performs a similar measurement based on template fits to the $\cos\theta^*$ distribution with 5.0 fb^{-1} of 7 TeV data in the lepton+jets final state [270]. As the polarization of the W bosons in top-quark decays is sensitive to the Wtb vertex Lorentz structure and anomalous couplings, both experiments also derive limits on anomalous contributions to the Wtb couplings. CMS and ATLAS collaborations have also combined their results from 7 TeV data to obtain values on the helicity fractions as well as limits on anomalous couplings [271].

At 8 TeV, ATLAS came out with a measurement of the W-helicity fractions in 20.2 fb^{-1} in lepton+jets events with at least one b-tag [272]. Using 19.8 fb^{-1} of 8 TeV data, CMS measured the W-helicity in lepton + 4 jet events with two b-tags [273]. In $t\bar{t}$ events with two opposite-sign leptons (electron or muon) in the final state in this dataset, CMS applied six kinematic constraints on the kinematics of the produced particles [274]. Also, using the same dataset a first measurement of the W-boson helicity in top-quark decays was made in electroweak single top production [275], yielding similarly precise and consistent results. The 8 TeV results obtained in $t\bar{t}$ and single-top events by ATLAS and CMS have also been combined recently [276]. These results are in agreement with the standard model predictions at next-to-next-to-leading order in perturbative QCD and represent an improvement in precision of 25 (29)% for F_0 (F_L) with respect to the most precise single measurement. A limit on anomalous right-handed vector (V_R), and left- and right-handed

tensor (g_L, g_R) tWb couplings and on corresponding Wilson coefficients is set.

Table 61.2: Measurement and 95% C.L. upper limits of the W helicity in top-quark decays. The table includes both preliminary, as of September 2021, and published results. A full set of published results is given in the Listings.

W Helicity	Source	$\int \mathcal{L}dt$ (fb^{-1})	Ref.	Method
$\mathcal{F}_0 = 0.722 \pm 0.081$	CDF+DØ Run II	2.7-5.4	[268]	$\cos\theta^*$ 2-param
$\mathcal{F}_0 = 0.682 \pm 0.057$	CDF+DØ Run II	2.7-5.4	[268]	$\cos\theta^*$ 1-param
$\mathcal{F}_0 = 0.726 \pm 0.094$	CDF Run II	8.7	[277]	ME 2-param
$\mathcal{F}_0 = 0.67 \pm 0.07$	ATLAS (7 TeV)	1.0	[269]	$\cos\theta^*$ 3-param
$\mathcal{F}_0 = 0.682 \pm 0.045$	CMS (7 TeV)	5.0	[270]	$\cos\theta^*$ 3-param
$\mathcal{F}_0 = 0.626 \pm 0.059$	ATLAS+CMS (7 TeV)	2.2	[271]	$\cos\theta^*$ 3-param
$\mathcal{F}_0 = 0.709 \pm 0.019$	ATLAS (8 TeV)	20.2	[272]	$\cos\theta^*$ 3-param
$\mathcal{F}_0 = 0.681 \pm 0.026$	CMS (8 TeV)	19.8	[273]	$\cos\theta^*$ 3-param
$\mathcal{F}_0 = 0.653 \pm 0.029$	CMS (8 TeV)	19.7	[274]	$\cos\theta^*$ 3-param
$\mathcal{F}_0 = 0.720 \pm 0.054$	CMS (8 TeV)	19.7	[275]	$\cos\theta^*$ 3-param
$\mathcal{F}_0 = 0.693 \pm 0.014$	ATLAS+CMS (8 TeV)	20	[276]	$\cos\theta^*$ 3-param
$\mathcal{F}_+ = -0.033 \pm 0.046$	CDF+DØ Run II	2.7-5.4	[268]	$\cos\theta^*$ 2-param
$\mathcal{F}_+ = -0.015 \pm 0.035$	CDF+DØ Run II	2.7-5.4	[268]	$\cos\theta^*$ 1-param
$\mathcal{F}_+ = -0.045 \pm 0.073$	CDF Run II	8.7	[277]	ME 2-param
$\mathcal{F}_+ = 0.01 \pm 0.05$	ATLAS (7 TeV)	1.0	[269]	$\cos\theta^*$ 3-param
$\mathcal{F}_+ = 0.008 \pm 0.018$	CMS (7 TeV)	5.0	[270]	$\cos\theta^*$ 3-param
$\mathcal{F}_+ = 0.015 \pm 0.034$	ATLAS+CMS (7 TeV)	2.2	[271]	$\cos\theta^*$ 3-param
$\mathcal{F}_+ = -0.008 \pm 0.014$	ATLAS (8 TeV)	20.2	[272]	$\cos\theta^*$ 3-param
$\mathcal{F}_+ = -0.004 \pm 0.015$	CMS (8 TeV)	19.8	[273]	$\cos\theta^*$ 3-param
$\mathcal{F}_+ = 0.018 \pm 0.027$	CMS (8 TeV)	19.7	[274]	$\cos\theta^*$ 3-param
$\mathcal{F}_+ = -0.018 \pm 0.022$	CMS (8 TeV)	19.7	[275]	$\cos\theta^*$ 3-param
$\mathcal{F}_+ = -0.008 \pm 0.007$	ATLAS+CMS (8 TeV)	20	[276]	$\cos\theta^*$ 3-param

61.3.2.4 *Top-Quark Electroweak Charges and Couplings*

The top quark is the only quark whose electric charge has not been measured through production at threshold in e^+e^- collisions. Furthermore, it is the only quark whose electromagnetic coupling has not been observed and studied until recently. Since the CDF and DØ analyses on top-quark production did not associate the b, $\bar{b}$, and $W^\pm$ uniquely to the top or antitop, decays such as $t \to W^+\bar{b}, \bar{t} \to W^-b$ were not excluded. A charge 4/3 quark of this kind is consistent with current electroweak precision data. The $Z \to \ell^+\ell^-$ and $Z \to b\bar{b}$ data, in particular the discrepancy between A_{LR} from SLC at SLAC and $A_{FB}^{0,b}$ of b-quarks and $A_{FB}^{0,\ell}$ of leptons from LEP at CERN, can be fitted with a top quark of mass $m_t = 270$ GeV/c^2, provided that the right-handed b quark mixes with the isospin +1/2 component of an exotic doublet of charge −1/3 and −4/3 quarks, $(Q_1, Q_4)_R$ [278,279]. Also the third component of the top quark's weak isospin has not been measured so far.

DØ studied the top-quark charge in double-tagged lepton+jets events, CDF did it in single tagged lepton+jets and dilepton events. Assuming the top- and antitop-quarks have equal but opposite electric charge, then reconstructing the charge of the b-quark through jet charge discrimination techniques, the $|Q_{top}| = 4/3$ and $|Q_{top}| = 2/3$ scenarios can be differentiated. For the exotic model of Chang *et al.* [279] with a top-quark charge $|Q_{top}| = 4/3$, CDF excluded the model at

99% C.L. [280] in 5.6 fb^{-1}, while DØ excluded the model at a significance greater than 5 standard deviations using 5.3 fb^{-1} and set an upper limit of 0.46 on the fraction of such quarks in the selected sample [281]. These results indicate that the observed particle is indeed consistent with being a SM $|Q| = 2/3$ quark.

In 2.05 fb^{-1} at $\sqrt{s} = 7$ TeV, ATLAS performed a similar analysis, reconstructing the b-quark charge either via a jet-charge technique or via the lepton charge in soft muon decays in combination with a kinematic likelihood fit. They measure the top-quark charge to be $0.64 \pm 0.02(stat.) \pm 0.08(syst.)$ from the charges of the top-quark decay products in single lepton $t\bar{t}$ events, and hence exclude the exotic scenario with charge $-4/3$ at more than 8σ [282].

In 4.6 fb^{-1} at $\sqrt{s} = 7$ TeV, CMS discriminates between the SM and the exotic top-quark charge scenario in the muon+jets final states in $t\bar{t}$ events. They exploit the charge correlation between high-p_t muons from W-boson decays and soft muons from B-hadron decays in b-jets. Using an asymmetry technique, where $A = -1$ represents the exotic $Q = -4/3$ scenario and $A = +1$ the SM $Q = +2/3$ scenario, they find $A_{meas} = 0.97 \pm 0.12(stat.) \pm 0.31(sys.)$, which agrees with the Standard Model expectation and excludes the exotic scenario at 99.9% C.L. [283].

The electromagnetic or the weak coupling of the top quark can be probed directly by investigating $t\bar{t}$ events with an additional gauge boson, such as $t\bar{t}\gamma$, $t\bar{t}W$, and $t\bar{t}Z$ events. The corresponding coupling can be extracted from the corresponding cross section or extracted from effective field theory (EFT) fits to various measured distributions and differential cross sections.

CDF performed a search for events containing a lepton, a photon, significant missing transverse momentum, and a jet identified as containing a b-quark and at least three jets and large total transverse energy in 6.0 fb^{-1}. They reported evidence for the observation of $t\bar{t}\gamma$ production with a cross section $\sigma_{t\bar{t}\gamma} = 0.18 \pm 0.08$ pb and a ratio of $\sigma_{t\bar{t}\gamma}/\sigma_{t\bar{t}} = 0.024 \pm 0.009$ [284].

ATLAS performed a first measurement of the $t\bar{t}\gamma$ cross section in pp collisions at $\sqrt{s} = 7$ TeV using 4.6 fb^{-1} of data. Events are selected that contain a large transverse momentum electron or muon and a large transverse momentum photon. The production of $t\bar{t}\gamma$ events was observed with a significance of 5.3 standard deviations. The resulting cross section times branching ratio into the single lepton channel for $t\bar{t}\gamma$ production with a photon with transverse momentum above 20 GeV is $\sigma^{fid.}(t\bar{t}\gamma) \times BR = 63 \pm 8(stat.)^{+17}_{-13}(syst.) \pm 1(lumi.)$ pb per lepton flavour [285], which is consistent with leading-order theoretical calculations.

At 8 TeV, ATLAS has used 20.2 fb^{-1} of data to measure the $t\bar{t}\gamma$ cross section with a photon above 15 GeV and $|\eta| < 2.37$. The fiducial cross section is measured to be 139 ± 18 fb [286], in good agreement with the NLO prediction [287]. Using 19.7 fb^{-1} of data at 8 TeV, CMS performed a similar measurement of the $t\bar{t}\gamma$ production cross section in the lepton+jets decay mode with a photon transverse momentum above 25 GeV and $|\eta|$ <1.44. They obtain a normalized cross section $\mathcal{R} = \sigma_{t\bar{t}+\gamma}/\sigma_{t\bar{t}} = (5.7 \pm 1.8) \times 10^{-4}$ in e+jets and $(4.7 \pm 1.3) \times 10^{-4}$ in μ+jets. The fiducial $t\bar{t}\gamma$ cross section is obtained by multiplying by the measured $t\bar{t}$ fiducial cross section of $244.9 \pm 1.4(stat.)^{+6.3}_{-5.5}(sys.) \pm 6.4(lumi.)$ pb. Extrapolating to the full phase space, the result is $\sigma_{t\bar{t}\gamma} \times$BR$=(515 \pm 108)$ fb, per lepton+jets final state [288], in good agreement with the theoretical prediction.

At $\sqrt{s} = 13$ TeV, using 36.1 fb^{-1} of single-lepton and dilepton events with exactly one photon, ATLAS measures the $t\bar{t}\gamma$ cross section. They employ neural network algorithms to separate the signal from the backgrounds. The fiducial cross-sections are measured to be $521 \pm 9(stat.) \pm 41(sys.)$ fb and $69 \pm 3(stat.) \pm 4(sys.)$ fb for the single-lepton and dilepton channels, respectively. The differential cross-sections are measured as a function of photon transverse momentum, photon absolute pseudorapidity, and angular distance between the photon and its closest lepton in both channels, as well as azimuthal opening angle and absolute pseudorapidity difference between the two leptons in the dilepton channel. All measurements are in agreement with the theoretical

predictions [289]. Very recently, ATLAS uses 139 fb^{-1} of $\sqrt{s}$ = 13 TeV $e\mu + \gamma$ events with at least two jets, out of which at least one is b-tagged, to measure the inclusive and differential cross-sections for the production of a top-quark pair in association with a photon. This analysis is sensitive to both processes, $t\bar{t}\gamma + tW\gamma$. The fiducial cross-section is measured to be $39.6^{+2.7}_{-2.3}$ fb in good agreement with the dedicated theoretical calculation provided by the authors of refs. [290,291], which predicts a value of $\sigma_{fid} = 38.50^{+0.56}_{-2.18}$ (scale)$^{+1.04}_{-1.18}$ (PDF) fb for the chosen fiducial phase space. Differential cross-sections as functions of several observables are compared to state-of-the-art Monte Carlo simulations and next-to-leading order theoretical calculations. These include cross-sections as functions of the photon transverse momentum and absolute pseudorapidity and angular variables related to the photon and the leptons and between the two leptons in the event. All measurements are in agreement with the predictions [292]. In 35.9 fb^{-1} of lepton-plus-photon-plus-jets events, CMS manages to establish the first evidence for the associated production of a single-top quark and a photon at $\sqrt{s}$ = 13 TeV. They employ a multivariate discriminant based on topological and kinematic event properties to separate signal from background processes. An excess above the background-only hypothesis is observed, with a significance of 4.4 standard deviations. A fiducial cross section is measured for isolated photons with transverse momentum greater than 25 GeV in the central region of the detector. The measured product of the cross section and branching fraction is $\sigma(pp \to t\gamma j)B(t \to \mu\gamma b) = 115 \pm 17(stat) \pm 30(syst)$ fb, which is consistent with the SM prediction [293]. Very recently, CMS used 137 fb^{-1} of data to measure the $t\bar{t}\gamma$ cross section. In the lepton-plus-jets channel, they perform measurements in a fiducial volume defined at the particle level. Events with an isolated, highly energetic lepton, at least three jets from the hadronization of quarks, among which at least one is b-tagged, and one isolated photon are selected. The inclusive fiducial $t\bar{t}\gamma$ cross section, for a photon with transverse momentum greater than 20 GeV and pseudorapidity $|\eta| < 1.4442$, is measured to be $\sigma_{t\bar{t}\gamma} = 800 \pm 7(stat) \pm 46(syst)$ fb, in good agreement with the prediction from the standard model at NLO in QCD [294]. The differential cross sections are also measured as a function of several kinematic observables and interpreted in the framework of the standard model effective field theory (EFT), leading to the most stringent direct limits to date on anomalous electromagnetic dipole moment interactions of the top quark and the photon. Using the same dataset, in the dilepton channel, an inclusive cross section of $174.4 \pm 2.5(stat) \pm 6.1(syst)$ fb is measured in a signal region with at least one b-tagged jet and exactly one photon with transverse momentum above 20 GeV [295]. In the same analysis, differential cross sections are measured as a function of several kinematic observables of the photon, leptons, and jet, and compared to standard model predictions. The measurements are also interpreted in the standard model effective field theory framework, and limits on the relevant Wilson coefficients are combined with a previous CMS measurement of the same production process using single-lepton events. Using 35.9 fb^{-1} of data with a single muon and a photon, CMS reports first evidence of events consistent with the production of a single top quark in association with a photon. A multivariate discriminant based on topological and kinematic event properties is employed to separate signal from background processes. An excess above the background-only hypothesis is observed, with a significance of 4.4 standard deviations [296]. A precision test of the vector and axial vector couplings in $t\bar{t}\gamma$ events or searches for possible tensor couplings of top-quarks to photons will only be feasible with an integrated luminosity of several hundred fb^{-1} in the future [297].

ATLAS and CMS have also studied the associate production of top-antitop quark pairs along with an electroweak gauge boson, where in the Standard Model the W-boson is expected to be produced via initial state radiation, while the Z-boson can also be radiated from a final-state top-quark and hence provides sensitivity to the top-quark neutral current weak gauge coupling, which implies a sensitivity to the third component of the top-quark's weak isospin, which has not been

measured so far.

CMS performed measurements of the $t\bar{t}W$ and $t\bar{t}Z$ cross section at $\sqrt{s} = 7$ TeV with 5 fb^{-1}, yielding $\sigma_{t\bar{t}V} = 0.43^{+0.17}_{-0.15}(stat.)^{+0.09}_{-0.07}(syst.)$ pb ($V = Z, W$) and $\sigma_{t\bar{t}Z} = 0.28^{+0.14}_{-0.11}(stat.)^{+0.06}_{-0.03}(syst.)$ fb, at about 3 standard deviations significance [298] and compatible with the SM expectations of $0.306^{+0.031}_{-0.053}$ pb and $0.137^{+0.012}_{-0.016}$ pb, respectively [299,300]. ATLAS performed a similar analysis with 4.7 fb^{-1} in the three-lepton channel and set an upper limit of 0.71 pb at 95% C.L. [301].

Using 20.3 fb^{-1} of 8 TeV data, ATLAS performs a simultaneous measurement of the $t\bar{t}W$ and $t\bar{t}Z$ cross section. They observe the $t\bar{t}W$ and $t\bar{t}Z$ production at the 5.0σ and 4.2σ level, respectively, yielding $\sigma_{t\bar{t}W} = 369^{+100}_{-91}$ fb and $\sigma_{t\bar{t}Z} = 176^{+58}_{-52}$ fb [302]. CMS performs an analysis where signal events are identified by matching reconstructed objects in the detector to specific final state particles from $t\bar{t}W$ and $t\bar{t}Z$ decays using 19.5 fb^{-1} of 8 TeV data. They obtain $\sigma_{t\bar{t}W} = 382^{+117}_{-102}$ fb and $\sigma_{t\bar{t}Z} = 242^{+65}_{-55}$ fb, yielding a significance of 4.8 and 6.4 standard deviation, respectively [303]. These measurements are used to set bounds on five anomalous dimension-six operators that would affect the $t\bar{t}W$ and $t\bar{t}Z$ cross sections.

The most recent measurements in these channels are made at 13 TeV from ATLAS and CMS in multilepton final states. ATLAS made a measurement using 36.1 fb^{-1} of events with two, three or four leptons. In multiple regions, the $t\bar{t}Z$ and $t\bar{t}W$ cross sections are simultaneously measured using a combined fit to all regions, yielding $\sigma_{t\bar{t}Z} = 0.95 \pm 0.08(stat) \pm 0.10(syst)$ pb and $\sigma_{t\bar{t}W} = 0.87 \pm 0.13(stat) \pm 0.14(syst)$ pb [304] to be compared with the NLO+NLL (QCD) and NLO (EW) SM predictions, $\sigma_{t\bar{t}W} = 579^{+14\%}_{-9\%}$ fb and $\sigma_{t\bar{t}Z} = 811^{+11\%}_{-10\%}$ fb [305]. Very recently, ATLAS uses 139 fb^{-1} in three and four lepton events to measure the inclusive and differential $t\bar{t}Z$ cross section. The inclusive cross section is measured to be $\sigma_{t\bar{t}Z} = 0.99 \pm 0.05(stat.) \pm 0.08(syst.)$ pb [306], in agreement with the most precise theoretical predictions. The differential measurements are presented as a function of a number of kinematic variables which probe the kinematics of the $t\bar{t}Z$ system. Overall, good agreement is observed between the unfolded data and the predictions. CMS uses 35.9 fb^{-1} of data to measure $\sigma_{t\bar{t}W} = 0.77^{+0.12}_{-0.11}(stat.)^{+0.13}_{-0.12}(syst.)$ pb and $\sigma_{t\bar{t}Z} = 0.99^{+0.09}_{-0.08}(stat.)^{+0.12}_{-0.10}(syst.)$ pb production cross sections, and significances over the background-only hypotheses of 5.5σ and 9.5σ, respectively [307], firmly establishing the observation of these processes. Very recently, CMS measured the inclusive $t\bar{t}Z$ cross section in 77.5 fb^{-1} of events with three or four charged leptons, and the Z boson is detected through its decay to an oppositely charged lepton pair. The production cross section is measured to be $\sigma(t\bar{t}Z) = 0.95 \pm 0.05(stat) \pm 0.06(syst)$ pb. This measurement includes differential cross sections as functions of the transverse momentum of the Z boson and the angular distribution of the negatively charged lepton from the Z boson decay as well as stringent direct limits on the anomalous tZ couplings [308].

The electroweak couplings can also be probed in single-top production in association with a Z boson. The $pp \to tZq$ process at the LHC probes both the WWZ coupling in the case where the Z emerges from the t-channel W in single-top production and, in the case where the Z is radiated from the top quark, the tZ coupling. A CMS search at 8 TeV using 19.7 fb^{-1} produced a hint of a tZq signal in tri-lepton events, with a significance compared to the background-only hypothesis of 2.4σ [309]. Very recently, CMS and ATLAS collaborations used 139 fb^{-1} in three-lepton events to measure $tZ(\to \ell^+\ell^-)q$. CMS obtains $\sigma_{tZq} = 87.9^{+7.5}_{-7.3}(stat)^{+7.3}_{-6.0}(syst)$ fb for $m(\ell\ell) > 30$ GeV [310]. The ratio between the cross sections for the top quark and the top antiquark production in association with a Z boson is measured as $2.37^{+0.56}_{-0.42}(stat)^{+0.27}_{-0.13}(syst)$. Differential measurements at parton and particle levels are performed for the first time. Additionally, the spin asymmetry, which is sensitive to the top quark polarization, is determined from the differential distribution of the polarization angle at parton level to be $0.58^{+0.15}_{-0.16}$ (stat) $\pm$ 0.06 (syst), in agreement with SM predictions at next-to-leading order. Using neural networks, ATLAS improves the background

rejection and extracts the signal. The measured cross-section for $m(\ell\ell) > 30$ GeV is $97 \pm 13(stat.) \pm 7(syst.)$ fb, consistent with the Standard Model prediction [311].

Searches for and now also measurements of the associate production of a top-antitop quark pair along with a Higgs boson, $t\bar{t}h$, with various subsequent decays provide sensitivity to the top-Higgs Yukawa coupling. For further details, see the review on "Higgs".

61.3.3 *Searches for Physics Beyond the Standard Model*

The top quark plays a special role in the SM. Being the only quark with a coupling to the Higgs boson of order one, it provides the most important contributions to the quadratic radiative corrections to the Higgs mass exposing the issue of the naturalness of the SM. It is therefore very common for models where the naturalness problem is addressed to have new physics associated with the top quark. In SUSY, for instance, naturalness predicts the scalar top partners to be the lightest among the squarks and to be accessible at the LHC energies (see the review "Supersymmetry: Theory"). In models where the Higgs is a pseudo-Goldstone boson, such as Little Higgs models, naturalness predicts the existence of partners of the top quarks with the same spin and color, but with different electroweak couplings, the so-called vectorial t'. Stops and t''s are expected to have sizeable branching ratios to top quarks. Another intriguing prediction of SUSY models with universal couplings at the unification scale is that for a top-quark mass close to the measured value, the running of the Yukawa coupling down to 1 TeV naturally leads to the radiative breaking of the electroweak symmetry [312]. In fact, the top quark plays a role in the dynamics of electroweak symmetry breaking in many models [313]. One example is topcolor [314], where a large top-quark mass can be generated through the formation of a dynamic $t\bar{t}$ condensate, X, which is formed by a new strong gauge force coupling preferentially to the third generation. Another example is topcolor-assisted technicolor [315], predicting the existence of a heavy Z' boson that couples preferentially to the third generation of quarks. If light enough such a state might be directly accessible at the present hadron collider energies, or if too heavy, lead to four-top interactions possibly visible in the $t\bar{t}t\bar{t}$ final state. This final state has been recently observed by CMS [316] and by ATLAS [119].

Current strategies to search for new physics in top quark events at hadron colliders are either tailored to the discovery of specific models or model independent. They can be broadly divided in two classes. In the first class new resonant states are looked for through decay processes involving the top quarks. Current searches for bosonic resonances in $t\bar{t}$ final states, or for direct stop and t' production, or for a charged Higgs in $H^+ \to t\bar{b}$ fall in the category. On the other hand, if new states are too heavy to be directly produced, they might still give rise to deviations from the SM predictions for the strength and Lorentz form of the top-quark couplings to other SM particles. Accurate SM predictions and measurements are therefore needed and the results be interpreted in the framework of an effective field theory [317–319] as done for example in recent analyses sensitive to the strength and structure of the top quark couplings by the ATLAS [94, 184, 276, 304, 320–323] and CMS [111, 121, 324–330] collaborations. Global effective field theory interpretations based on publicly available measurements in the top quark sector have also appeared [331–337].

61.3.3.1 *New Physics in Top Quark Production*

Theoretical [338,339] and experimental efforts have been devoted to the searches of $t\bar{t}$ resonances, both at the Tevatron and at the LHC. Most the analyses have been performed in the hypothesis that resonances are narrow, yet generalizations have been considered for specific scenarios. At the Tevatron, both the CDF and DØ collaborations have searchedfor resonant production of $t\bar{t}$ pairs in the lepton+jets channel [340, 341]. In both analyses, the data indicate no evidence of resonant production of $t\bar{t}$ pairs. They place upper limits on the production cross section times branching fraction to $t\bar{t}$ in comparison to the prediction for a narrow ($\Gamma_{Z'} = 0.012 M_{Z'}$) leptophobic topcolor Z' boson. Within this model, they exclude Z' bosons with masses below 915 (CDF-full data set)

and 835 (DØ, 5 fb^{-1}) GeV/c^2 at the 95% C.L. These limits turn out to be independent of couplings of the $t\bar{t}$ resonance (pure vector, pure axial-vector, or SM-like Z'). A similar analysis has been performed by CDF in the all-hadronic channel using 2.8 fb^{-1} of data [342]. At the LHC, both the CMS and ATLAS collaborations have searched for resonant production of $t\bar{t}$ pairs, employing different techniques and final-state signatures (all-hadronic, lepton+jets, dilepton) at $\sqrt{s}$ = 7, 8 and 13 TeV. In the low mass range, from the $t\bar{t}$ threshold to about one TeV/c^2, standard techniques based on the reconstruction of each of the decay objects (lepton, jets and b-jets, missing E_T) are used to identify the top quarks, while at higher invariant mass, the top quarks are boosted and the decay products more collimated and can appear as large-radius jets with substructure. Dedicated reconstruction techniques have been developed in recent years for boosted top quarks [343] that are currently employed at the LHC. Most of the analyses are model-independent (i.e., no assumption on the quantum numbers of the resonance is made) yet they assume a small width and no signal-background interference. Using lepton+jets and fully hadronic channels in a data set corresponding to an integrated luminosity of 35.9 fb^{-1} at 13 TeV, the CMS collaboration finds no significant deviations from the SM background [344]. In particular, the existence of a leptophobic topcolor particle Z' is excluded at the 95% confidence level for resonances in the mass range $0.6 < M_{Z'} < 3.8$ TeV/c^2, $0.5 < M_{Z'} < 5.25$ TeV/c^2, and $0.5 < M_{Z'} < 6.65$ TeV/c^2 for $\Gamma_{Z'} = 1\%, 10\%, 30\% M_{Z'}$, respectively [345]. Kaluza-Klein excitations of a gluon with $M_{G_{KK}} <$ 4.55 TeV/c^2 (at 95% confidence level) in the Randall-Sundrum model are also excluded. A dedicated analysis [346] searching for a scalar resonance, set bounds between 400 and 750 GeV in various scenarios. The ATLAS collaboration has performed a search for resonant $t\bar{t}$ production in the lepton+jets channel using 36.1 fb^{-1} of proton-proton (pp) collision data collected at a center-of-mass energy $\sqrt{s} = 13$ TeV [347]. A search for local excesses in the number of data events compared to the Standard Model expectation in the $t\bar{t}$ invariant mass spectrum is performed. No evidence for a $t\bar{t}$ resonance is found and 95% confidence-level limits on the production rate are determined for massive states predicted in several benchmark models. For instance, a narrow leptophobic topcolor Z' boson with a mass below 3.0 TeV/c^2 is excluded. A Kaluza-Klein excitation of the graviton is excluded for masses in the range 0.45 TeV/c^2 $< m_G <$ 0.65 TeV/c^2. A Kaluza-Klein excitation of the gluon in a Randall-Sundrum model is excluded for masses below 3.8 TeV/c^2. ATLAS has also conducted a search for resonances in the all-jet final state at 13 TeV corresponding to an integrated luminosity of 139 fb^{-1} [348]. The $t\bar{t}$ events are reconstructed by selecting two top quarks in their fully hadronic decay modes. A Z' in the topcolor-assisted-technicolor model is excluded at 95% confidence level for masses below 3.9 and 4.7 TeV for the decay widths of 1% and 3%, respectively.

Heavy charged bosons, such as W' or H^+, can also be searched for in $t\bar{b}, tj$ final states (for more information see the review "W'-boson searches" and "Higgs Bosons: theory and searches"), while heavy fermion resonances, such as vectorial or excited quarks, in final states such as tZ, tH, tW, bW. CMS has performed several searches in this context, the most stringent limits coming from those at $\sqrt{s} = 13$ TeV [349–356]. For instance, a $W' \to t\bar{b}$ has been searched for in all-hadronic final state in 137 fb^{-1}. No evidence has been found for left- and right-handed W' boson and masses below 3.4 TeV/c^2 are excluded at 95% confidence level [356]. Single production of a vector-like quark decaying to a W boson and a top quark, in fully hadronic final state also been searched in the same data set. No significant deviation from the SM background expectation is observed. The hypotheses of b* quarks with left-handed, right-handed, and vector-like chiralities are excluded at 95% confidence level for masses below 2.6, 2.8, and 3.1 TeV/c^2, respectively. These represent the most stringent exclusion limits for the single production of vector-like quarks in this channel. [357] In the same data set, searches for pair production of vector-like T or B quarks in fully hadronic final states have been performed. Lower limits are set on the mass at 95% confidence level equal to 1570 TeV/c^2 in the case where decays exclusively to a b quark and a Higgs boson, 1390 TeV/c^2

for when it decays exclusively to a b quark and a Z boson, and 1450 TeV/c^2 for when it decays equally in these two modes. [358]. ATLAS has performed searches for heavy bosons and fermions decaying to one top quark at $\sqrt{s}$ = 7, 8 and 13 TeV. A $W' \to t\bar{b}$ has been searched for at 13 TeV in lepton+jets in 36.1 fb^{-1}. No evidence has been found for a right-handed W' boson with a mass below 3.25 TeV/c^2 are excluded at 95% [359]. A $H^+ \to t\bar{b}$ has been searched for at 13 TeV in lepton+jets in 139 fb^{-1}. No significant excess above the background-only hypothesis is observed and exclusion limits are derived for the production cross-section times branching ratio as a function of its mass, ranging from 3.6 pb at 200 GeV/c^2 to 0.036 pb at 2000 GeV/c^2 at 95% confidence level. [360]. ATLAS has conducted a search for the single and pair production of a new charge +2/3 quark (T) decaying via $T \to Zt$ (and also -1/3 quark (B) decaying via $B \to Zb$) in a dataset corresponding to 139 fb^{-1} luminosity at $\sqrt{s}$ = 13 TeV [361]. No significant excess of events above the SM expectation is observed, and upper limits are derived for vector-like quarks of various masses in a two-dimensional plane of branching ratios. Under branching ratio assumptions corresponding to a weak-isospin singlet scenario, a T quark with mass lower than 1.27 TeV/c^2 (1.2 TeV/c^2 for a B quark) is excluded at the 95% confidence level. Under branching ratio assumptions corresponding to a particular weak-isospin doublet scenario, a T quark with mass lower than 1.46; TeV/c^2 (1.32 TeV/c^2 for a B quark) is excluded at the 95% confidence level. In the same dataset, ATLAS combines the searches for pair-produced vector-like partners of the top and bottom quarks in various decay channels ($T \to Zt/Wb/Ht, B \to Zb/Wt/Hb$). The observed data are found to be in good agreement with the SM background prediction in all individual searches. Therefore, combined 95% confidence-level upper limits are set on the production cross-section for a range of vector-like quark scenarios, significantly improving upon the reach of the individual searches. Model-independent limits are set assuming the vector-like quarks decay to SM particles. A singlet T is excluded for masses below 1.31 TeV/c^2 and a singlet B is excluded for masses below 1.22 TeV/c^2. Assuming a weak isospin (T, B) doublet and $|V_{Tb}| << |V_{tB}|$, T and B masses below 1.37 TeV/c^2 are excluded [362].

Vector-like partners of the top and bottom quarks have been searched also in single (electroweak) production, in several decay modes: $T \to tH$ [363], $T \to Wb$ [364], $T \to t(Z \to \nu\nu)$ [365] and $B \to bH$ with $H \to b\bar{b}$ [366] and $H \to \gamma\gamma$ [367].

In many models top-quark partners preferably decay to top quarks and weakly interacting neutral stable particles, i.e., possibly dark matter candidates, that are not detected. In addition, top quarks could be coupled to states that would mostly decay to dark matter or be invisible. In both cases, an observable especially sensitive to new physics effects in $t\bar{t}$ production is therefore the missing transverse momentum. CMS has presented a differential cross section measurement of top-quark pair and single production with missing transverse energy and corresponding interpretations in the context of dark matter (effective and simplified) models at 8 and 13 TeV [368–371]. The results obtained so far are consistent with the SM expectations. In particular the search performed at 13 TeV [371] is based on 35.9 fb^{-1} of integrated luminosity. Upper limits are derived on the production cross section and interpreted in terms of a simplified model with a scalar/pseudoscalar mediator. Scalar and pseudoscalar mediator particles with masses below 290 and 300 GeV/c^2, respectively, are excluded at 95% confidence level, assuming a dark matter particle mass of 1 GeV/c^2 and mediator couplings to fermions and dark matter particles equal to unity. A generic search for new phenomena with top quark pairs in final states with one isolated electron or muon, multiple jets, and large missing transverse momentum has been performed by ATLAS in a dataset corresponding to 139 fb^{-1} luminosity at $\sqrt{s}$ = 13 TeV. No significant excess above the SM background is observed, and limits at 95% confidence level are set in various models. The results exclude top squark masses up to about 1 TeV/c^2, and masses of the lightest neutralino up to about 500 GeV/c^2. Limits on dark-matter production are set for scalar (pseudoscalar) mediator masses up to about 250 (300)

GeV/c^2. [372].

ATLAS has also conducted searches for missing transverse momenta in association with single top quarks [373, 374].

Flavor-changing-neutral-currents (FCNC) are hugely suppressed in the SM as non zero contributions only arise at one-loop and are proportional to the splitting between the quark masses. In the case of the top quark $B(t \to Bq)$ with $B = g, \gamma, Z, H$ and $q = u, c$ are predicted to be order of 10^{-12} $(t \to cg)$ or much smaller [375]. Several observables are accessible at colliders to test and constrain such couplings. CMS has performed several studies on the search for FCNC in top-quark production. They have considered single-top quark production in the t-channel in 5 fb^{-1} integrated luminosity at 7 TeV and 19.7 fb^{-1} integrated luminosity at 8 TeV [376]. Events with the top quark decaying into a muon, neutrino and two or three jets are selected. The upper limits on effective coupling strength can be translated to the 95% upper limits on the corresponding branching ratios $B(t \to gu) \leq 2.0 \cdot 10^{-5}$, $B(t \to gc) \leq 4.1 \cdot 10^{-4}$. They have performed a search for a single top quark produced in association with a photon in 19.1 fb^{-1} integrated luminosity at 8 TeV [377]. The event selection requires the presence of one isolated muon and jets in the final state. The upper limits on effective coupling strength can be translated to the 95% upper limits on the corresponding branching ratios $B(t \to \gamma u) \leq 0.0161\%$, $B(t \to \gamma c) \leq 0.182\%$. A search for flavor-changing neutral currents in associated production of a top quark with a Higgs boson decaying into $b\bar{b}$ has also been presented by CMS, corresponding to an integrated luminosity of 35.9 fb^{-1} at 13 TeV. Two complementary channels are considered: top quark pair production, with FCNC decay of the top quark or antiquark, and single top associated production. A final state with one isolated lepton and at least three reconstructed jets, among which at least two are identified as b quark jets, is considered. No significant deviation is observed from predicted background and upper limits at 95% confidence level are set on the branching ratios of top quark decays, $B(t \to uH) < 0.47\%$ and $B(t \to cH) < 0.47\%$ [378], which are similar to the combined limits on all decay channels obtained with the full data set at 8 TeV [379]. More recently, a search for the signature of flavor-changing neutral current interactions of top quarks and Higgs bosons has been performed. corresponding to an integrated luminosity of 137 fb^{-1} at 13 TeV. Multivariate machine learning techniques have been used to separate signal and standard model background processes. No significant excess above the background prediction is observed, and upper limits on the $t \to Hq$ branching fractions are derived through a binned fit to the diphoton invariant mass spectrum. The observed 95% confidence level upper limits are found to be 1.9×10^{-4} for $\Gamma(t \to Hu)$ and 7.3×10^{-4} for $\Gamma(t \to Hc)$.

ATLAS has presented results on the search for single top-quark production via FCNC's in strong interactions using data collected at $\sqrt{s}$=8 TeV and corresponding to an integrated luminosity of 20.3 fb^{-1}. Flavor-changing-neutral-current events are searched for in which a light quark (u or c) interacts with a gluon to produce a single top quark, either with or without the associated production of another light quark or gluon. Candidate events of top quarks decaying into leptons and jets are selected and classified into signal- and background-like events using a neural network. The observed 95% C.L. limit is $\sigma_{qq \to t} \times B(t \to Wb) < 3.4$ pb that can be interpreted as limits on the branching ratios, $B(t \to ug) < 4 \cdot 10^{-5}$ and $B(t \to cg) < 1.7 \cdot 10^{-4}$ [380]. ATLAS has set limits on the coupling of a top quark, a photon, and an up or charm quark using 81 fb^{-1} of data 13 TeV. Events with a photon, an electron or muon, a b-tagged jet, and missing transverse momentum are selected. The data are consistent with the background-only hypothesis, and limits are set on the strength of the $tq\gamma$ coupling in an effective field theory. These are also interpreted as 95% CL upper limits on $t \to u\gamma$ branching ratio via a left-handed (right-handed) interaction of 2.8×10^{-5} (6.1×10^{-5}) and on the $t \to c\gamma$ branching ratio for of 22×10^{-5} (18×10^{-5}) [381]. Constraints on FCNC couplings of the top quark can also be obtained from searches for anomalous single top-quark production in e^+e^- collisions, via the process $e^+e^- \to \gamma, Z^* \to t\overline{q}$ and its charge-conjugate

($q = u, c$), or in $e^{\pm}p$ collisions, via the process $e^{\pm}u \to e^{\pm}t$. For a leptonic W decay, the topology is at least a high-p_T lepton, a high-p_T jet and missing E_T, while for a hadronic W-decay, the topology is three high-p_T jets. Limits on the cross section for this reaction have been obtained by the LEP collaborations [382] in e^+e^- collisions, and by H1 [383] and ZEUS [384] in $e^{\pm}p$ collisions. When interpreted in terms of branching ratios in top decay [385,386], the LEP limits lead to typical 95% C.L. upper bounds of $B(t \to qZ) < 0.137$. Assuming no coupling to the Z boson, the 95% C.L. limits on the anomalous FCNC coupling $\kappa_\gamma < 0.13$ and < 0.27 by ZEUS and H1, respectively, are stronger than the CDF limit of $\kappa_\gamma < 0.42$, and improve over LEP sensitivity in that domain. The H1 limit is slightly weaker than the ZEUS limit due to an observed excess of five-candidate events over an expected background of 3.2 ± 0.4. If this excess is attributed to FCNC top-quark production, this leads to a total cross section of $\sigma(ep \to e + t + X, \sqrt{s} = 319 \text{ GeV}) < 0.25$ pb [383,387].

61.3.3.2 *New Physics in Top-Quark decays*

The large sample of top quarks produced at the Tevatron and the LHC allows to measure or set stringent limits on the branching ratios of rare top-quark decays. For example, the existence of a light H^+ can be constrained by looking for $t \to H^+b$ decay, in particular with tau-leptons in the final state (for more information see the review "Higgs Bosons: theory and searches").

A first class of searches for new physics focuses on the structure of the Wtb vertex. Using up to 2.7 fb^{-1} of data, DØ has measured the Wtb coupling form factors by combining information from the W-boson helicity in top-quark decays in $t\bar{t}$ events and single top-quark production, allowing to place limits on the left-handed and right-handed vector and tensor couplings [388–390].

ATLAS has published the results of a search for CP-violation in the decay of single top quarks produced in the t-channel where the top quarks are predicted to be highly polarized, using the lepton+jets final state [391]. The data analyzed are from pp collisions at $\sqrt{s} = 7$ TeV and correspond to an integrated luminosity of 4.7 fb^{-1}. In the Standard Model, the couplings at the Wtb vertex are left-handed, right-handed couplings being absent. A forward-backward asymmetry with respect to the normal to the plane defined by the W-momentum and the top-quark polarization has been used to probe the complex phase of a possibly non-zero value of the right-handed coupling, signaling a source of CP-violation beyond the SM. The measured value of the asymmetry is $0.031 \pm 0.065(stat.)^{+0.029}_{-0.031}(syst.)$ in good agreement with the Standard Model.

A second class of searches focuses on FCNC's in the top-quark decays. Both, CDF and DØ, have provided the first limits for FCNC's in Run I and II. The most recent results from CDF give $B(t \to qZ) < 3.7\%$ and $B(t \to q\gamma) < 3.2\%$ at the 95% C.L. [392] while DØ [393, 394] sets $B(t \to qZ)(q = u, c \text{ quarks }) < 3.2\%)$ at 95% C.L., $B(t \to gu) < 2.0 \cdot 10^{-4}$, and $B(t \to gc) < 3.9 \cdot 10^{-3}$ at the 95% C.L. At the LHC, CMS has used a sample at a center-of-mass energy of 8 TeV corresponding to 19.7 fb^{-1} of integrated luminosity to perform a search for flavor changing neutral current top-quark decay $t \to Zq$. Events with a topology compatible with the decay chain $t\bar{t} \to Wb + Zq \to \ell\nu\ b + \ell\ell q$ are searched for. There is no excess seen in the observed number of events relative to the SM prediction; thus no evidence for flavor changing neutral current in top-quark decays is found. A combination with a previous search at 7 TeV excludes a $t \to Zq$ branching fraction greater than 0.05% at the 95% confidence level [395]. CMS has also performed a search for the production of a single top quark in association with a Z boson in the same data set at 8 TeV. Final states with three leptons (electrons or muons) and at least one jet are investigated. Exclusion limits at 95% confidence level on the branching fractions are found to be $B(t \to uZ) < 0.022\%$ and $B(t \to cZ) < 0.049\%$ [396].

The ATLAS collaboration has also searched for FCNC processes in 36.1 fb^{-1} of $t\bar{t}$ events at a center-of-mass energy of 13 TeV, with one top quark decaying through FCNC ($t \to qZ$) and the other through the SM dominant mode ($t \to bW$). Only the decays of the Z boson to charged

leptons and leptonic W boson decays were considered as signal, leading to a final state topology characterized by the presence of three isolated leptons, at least two jets and missing transverse energy from the undetected neutrino. No evidence for an FCNC signal was found. An upper limit on the $t \to qZ$ branching ratio of $B(t \to Zu(c)) < 1.7(2.4) \times 10^{-4}$ is set at the 95% confidence level [397]. The ATLAS collaboration has also searched for a tqZ coupling, in a study that includes events where a single top quark is produced as $gq \to tZ$ (with $q = u, c$) and top-quark pair events, with one top quark decaying through the $t \to qZ$ channel, 139 fb^{-1} of data at 13 TeV. The analysis selects events with three leptons (electrons or muons), a b-tagged jet, possible additional jets and missing transverse momentum. The data are consistent with the background-only hypothesis and 95% confidence-level limits on the branching ratios are set. These are 6.2×10^{-5} (13×10^{-5}) for $t \to Zu$ ($t \to Zc$) for a left-handed coupling, and 6.6×10^{-5} (12×10^{-5}) in the case of a right-handed coupling [398].

Another search for FCNCs is the interactions of a top-quark to a Higgs boson and a light parton, tqH, $q = u, c$. The CMS collaboration has performed a search using a sample at a center-of-mass energy of 13 TeV corresponding to 35.9 fb^{-1} of integrated luminosity, [399], combining single top quark FCNC production in association with the Higgs boson ($pp \to tH$), and top quark pair production with FCNC decay of the top quark ($t \to qH$). The combined analysis sets an upper limit on the $t \to u/cH$ branching ratios of $B(t \to u/cH) < 0.47\%$ at 95% confidence level. The ATLAS collaboration considers $t \to qH$, $q = u, c$ with 36.1 fb^{-1} of $t\bar{t}$ events at $\sqrt{s} = 13$ TeV. A combined measurement including $H \to bb$ and $H \to \tau\tau$ modes yields a 95% C.L. upper limit of 0.11% and 0.12% on the branching ratios of $B(t \to cH)$ and $B(t \to uH)$, respectively [400].

61.4 Outlook

Top-quark physics at hadron colliders has developed into precision physics. Various properties of the top quark have been measured with high precision, where the LHC has by now surpassed the Tevatron precision and reach in the majority of relevant observables. Several $\sqrt{s}$-dependent physics quantities, such as the production cross-section, have been measured at several energies at the Tevatron and the LHC. Up to now, all measurements are consistent with the SM predictions and allow stringent tests of the underlying production mechanisms by strong and weak interactions. Given the very large event samples available at the LHC, top-quark properties will be further determined in $t\bar{t}$ as well as in electroweak single top-quark production. At the Tevatron, the $t-$ and $s-$channels for electroweak single top-quark production have been measured separately. At the LHC, quick progress has been achieved in the last years making all three relevant channels measured with more than 5 sigma significance. Furthermore, $t\bar{t}\gamma$, $t\bar{t}Z$, and $t\bar{t}W$ together with $t\bar{t}H$ associated production have started to provide key information on the top-quark electroweak couplings. Corresponding effective field theory (EFT) fits for the coupling extraction are being developed. At the same time various models of physics beyond the SM involving top-quark production are being constrained. While a majority of the Run-II data recorded at 13 TeV has been analysed or is in an advanced stage, the beginning of the Run-III at $\sqrt{s} = 13.6$ to 14 TeV and an expected integrated luminosity of $160 - 200$ fb^{-1}, doubling the Run-I plus Run-II data set, is immanent. With the first results to be released, top-quark physics has the potential to shed light on open questions and new aspects of physics at the TeV scale.

CDF note references can be retrieved from
https://www-cdf.fnal.gov/physics/new/top/top.html,
and DØ note references from
https://www-d0.fnal.gov/Run2Physics/WWW/documents/Run2Results.htm,
and ATLAS note references from
https://twiki.cern.ch/twiki/bin/view/AtlasPublic/TopPublicResults,

and CMS note references from
https://twiki.cern.ch/twiki/bin/view/CMSPublic/PhysicsResultsTOP,
and plots provided by the LHC Top Working Group from
https://twiki.cern.ch/twiki/bin/view/LHCPhysics/LHCTopWGSummaryPlots.

References

[1] M. Czakon, P. Fiedler and A. Mitov, Phys. Rev. Lett. **110**, 252004 (2013), [arXiv:1303.6254].

[2] S. Catani *et al.*, JHEP **07**, 100 (2019), [arXiv:1906.06535].

[3] ATLAS,CMS, CDF, & D0 Collab, [arXiv:1403.4427].

[4] S. Cortese and R. Petronzio, Phys. Lett. **B253**, 494 (1991).

[5] S. S. D. Willenbrock and D. A. Dicus, Phys. Rev. **D34**, 155 (1986).

[6] J. Campbell, T. Neumann and Z. Sullivan, JHEP **02**, 040 (2021), [arXiv:2012.01574].

[7] M. Brucherseifer, F. Caola and K. Melnikov, Phys. Lett. **B736**, 58 (2014), [arXiv:1404.7116].

[8] E. L. Berger, J. Gao and H. X. Zhu, JHEP **11**, 158 (2017), [arXiv:1708.09405].

[9] N. Kidonakis, Phys. Rev. **D81**, 054028 (2010), [arXiv:1001.5034].

[10] N. Kidonakis, Phys. Rev. **D82**, 054018 (2010), [arXiv:1005.4451].

[11] T. M. P. Tait and C. P. Yuan, Phys. Rev. **D63**, 014018 (2000), [hep-ph/0007298].

[12] M. Jezabek and J. H. Kuhn, Nucl. Phys. **B314**, 1 (1989).

[13] I. I. Y. Bigi *et al.*, Phys. Lett. **B181**, 157 (1986).

[14] A. H. Hoang *et al.*, Phys. Rev. **D65**, 014014 (2002), [hep-ph/0107144].

[15] K. Hagiwara, Y. Sumino and H. Yokoya, Phys. Lett. **B666**, 71 (2008), [arXiv:0804.1014].

[16] B. Fuks *et al.*, Phys. Rev. D **104**, 3, 034023 (2021), [arXiv:2102.11281].

[17] A. Czarnecki and K. Melnikov, Nucl. Phys. **B544**, 520 (1999), [hep-ph/9806244]; K. G. Chetyrkin *et al.*, Phys. Rev. **D60**, 114015 (1999), [hep-ph/9906273].

[18] S. Frixione, P. Nason and B. R. Webber, JHEP **08**, 007 (2003), [hep-ph/0305252]; W. Kim and H. Shin, JHEP **07**, 070 (2007), [arXiv:0706.3563]; S. Frixione, P. Nason and G. Ridolfi, JHEP **09**, 126 (2007), [arXiv:0707.3088]; J. M. Campbell *et al.*, JHEP **04**, 114 (2015), [arXiv:1412.1828]; T. Ježo *et al.*, Eur. Phys. J. **C76**, 12, 691 (2016), [arXiv:1607.04538].

[19] S. Frixione *et al.*, JHEP **03**, 092 (2006), [hep-ph/0512250]; V. Marotta and A. Naddeo, JHEP **08**, 029 (2008), [arXiv:0810.4759]; S. Alioli *et al.*, JHEP **09**, 111 (2009), [Erratum: JHEP02,011(2010)], [arXiv:0907.4076]; E. Re, Eur. Phys. J. **C71**, 1547 (2011), [arXiv:1009.2450]; R. Frederix, E. Re and P. Torrielli, JHEP **09**, 130 (2012), [arXiv:1207.5391]; R. Frederix *et al.*, JHEP **06**, 027 (2016), [arXiv:1603.01178].

[20] S. Frixione and B. R. Webber, JHEP **06**, 029 (2002), [hep-ph/0204244].

[21] P. Nason, JHEP **11**, 040 (2004), [hep-ph/0409146].

[22] J. Mazzitelli *et al.*, Phys. Rev. Lett. **127**, 6, 062001 (2021), [arXiv:2012.14267].

[23] E. Todesco and J. Wenninger, Phys. Rev. Accel. Beams **20**, 8, 081003 (2017).

[24] V. M. Abazov *et al.* (D0), Phys. Rev. **D94**, 092004 (2016), [arXiv:1605.06168].

[25] T. Aaltonen *et al.* (CDF), Phys. Rev. **D88**, 091103 (2013), [arXiv:1304.7961].

[26] T. A. Aaltonen *et al.* (CDF, D0), Phys. Rev. **D89**, 7, 072001 (2014), [arXiv:1309.7570].

[27] T. A. Aaltonen *et al.* (CDF), Phys. Rev. **D89**, 9, 091101 (2014), [arXiv:1402.6728].

[28] T. Aaltonen *et al.* (CDF), Phys. Rev. Lett. **105**, 012001 (2010), [arXiv:1004.3224].

[29] V. M. Abazov *et al.* (D0), Phys. Rev. **D90**, 9, 092006 (2014), [arXiv:1401.5785].

[30] M. Czakon and A. Mitov, Comput. Phys. Commun. **185**, 2930 (2014), [arXiv:1112.5675].

[31] ATLAS Collab., ATLAS-CONF-2021-003.

[32] A. M. Sirunyan *et al.* (CMS), JHEP **03**, 115 (2018), [arXiv:1711.03143].

[33] CMS Collab., CMS-PAS-TOP-20-004 (2021).

[34] G. Aad *et al.* (ATLAS), Eur. Phys. J. **C74**, 10, 3109 (2014), [Addendum: Eur. Phys. J.C76,no.11,642(2016)], [arXiv:1406.5375].

[35] ATLAS Collab., ATLAS-CONF-2011-121 (2011).

[36] G. Aad *et al.* (ATLAS), JHEP **05**, 059 (2012), [arXiv:1202.4892].

[37] ATLAS Collab., ATLAS-CONF-2011-140.

[38] ATLAS Collab., ATLAS-CONF-2012-024.

[39] G. Aad *et al.* (ATLAS), Eur. Phys. J. **C73**, 3, 2328 (2013), [arXiv:1211.7205].

[40] G. Aad *et al.* (ATLAS), Phys. Lett. **B717**, 89 (2012), [arXiv:1205.2067].

[41] ATLAS Collab., ATLAS-CONF-2012-031.

[42] G. Aad *et al.* (ATLAS), Phys. Rev. **D91**, 5, 052005 (2015), [arXiv:1407.0573].

[43] S. Chatrchyan *et al.* (CMS), JHEP **11**, 067 (2012), [arXiv:1208.2671].

[44] S. Chatrchyan *et al.* (CMS), Phys. Lett. **B720**, 83 (2013), [arXiv:1212.6682].

[45] S. Chatrchyan *et al.* (CMS), JHEP **05**, 065 (2013), [arXiv:1302.0508].

[46] S. Chatrchyan *et al.* (CMS), Phys. Rev. **D85**, 112007 (2012), [arXiv:1203.6810].

[47] S. Chatrchyan *et al.* (CMS), Eur. Phys. J. **C73**, 4, 2386 (2013), [arXiv:1301.5755].

[48] ATLAS & CMS Collab., ATLAS-CONF-2012-134, CMS-PAS-TOP-12-003.

[49] G. Aad *et al.* (ATLAS), Eur. Phys. J. **C74**, 10, 3109 (2014), [Addendum: Eur. Phys. J.C76,no.11,642(2016)], [arXiv:1406.5375].

[50] G. Aad *et al.* (ATLAS), Phys. Rev. **D91**, 11, 112013 (2015), [arXiv:1504.04251].

[51] M. Aaboud *et al.* (ATLAS), Eur. Phys. J. **C78**, 487 (2018), [arXiv:1712.06857].

[52] M. Aaboud *et al.* (ATLAS), Phys. Rev. **D95**, 7, 072003 (2017), [arXiv:1702.08839].

[53] V. Khachatryan *et al.* (CMS), Eur. Phys. J. **C77**, 1, 15 (2017), [arXiv:1602.09024].

[54] S. Chatrchyan *et al.* (CMS), JHEP **02**, 024 (2014), [Erratum: JHEP02,102(2014)], [arXiv:1312.7582].

[55] V. Khachatryan *et al.* (CMS), JHEP **08**, 029 (2016), [arXiv:1603.02303].

[56] V. Khachatryan *et al.* (CMS), Phys. Lett. **B739**, 23 (2014), [arXiv:1407.6643].

[57] V. Khachatryan *et al.* (CMS), Eur. Phys. J. **C76**, 3, 128 (2016), [arXiv:1509.06076].

[58] ATLAS Collab., ATLAS-CONF-2014-054, CMS Collab., CMS-PAS-TOP-14-016.

[59] R. Aaij *et al.* (LHCb), Phys. Rev. Lett. **115**, 11, 112001 (2015), [arXiv:1506.00903].

[60] ATLAS Collab., ATLAS-CONF-2015-033.

[61] ATLAS collab., ATLAS-CONF-2015-049.

[62] M. Aaboud *et al.* (ATLAS), Phys. Lett. **B761**, 136 (2016), [Erratum: Phys. Lett.B772,879(2017)], [arXiv:1606.02699].

[63] G. Aad *et al.* (ATLAS), Eur. Phys. J. C **80**, 6, 528 (2020), [arXiv:1910.08819].

[64] G. Aad *et al.* (ATLAS), Phys. Lett. B **810**, 135797 (2020), [arXiv:2006.13076].

[65] V. Khachatryan *et al.* (CMS), Phys. Rev. Lett. **116**, 5, 052002 (2016), [arXiv:1510.05302].

[66] V. Khachatryan *et al.* (CMS), Eur. Phys. J. **C77**, 172 (2017), [arXiv:1611.04040].

[67] A. M. Sirunyan *et al.* (CMS), Eur. Phys. J. **C79**, 5, 368 (2019), [arXiv:1812.10505].

[68] A. M. Sirunyan *et al.* (CMS), JHEP **02**, 191 (2020), [arXiv:1911.13204].

[69] CMS Collab., CMS-PAS-TOP-15-005.

[70] A. M. Sirunyan *et al.* (CMS), JHEP **09**, 051 (2017), [arXiv:1701.06228].

[71] A. Tumasyan *et al.* (CMS) (2021), [arXiv:2108.02803].

[72] CMS Collab., CMS-PAS-TOP-16-013.

[73] A. M. Sirunyan *et al.* (CMS), Phys. Rev. Lett. **119**, 24, 242001 (2017), [arXiv:1709.07411].

[74] V. M. Abazov *et al.* (D0), Phys. Rev. Lett. **107**, 121802 (2011), [arXiv:1106.5436]; D. Acosta *et al.* (CDF), Phys. Rev. Lett. **95**, 102002 (2005), [hep-ex/0505091].

[75] V. Khachatryan *et al.* (CMS), Phys. Lett. **B736**, 33 (2014), [arXiv:1404.2292].

[76] M. Czakon, D. Heymes and A. Mitov, Phys. Rev. Lett. **116**, 8, 082003 (2016), [arXiv:1511.00549].

[77] T. Aaltonen *et al.* (CDF), Phys. Rev. Lett. **110**, 12, 121802 (2013), [arXiv:1211.5363].

[78] G. Aad *et al.* (ATLAS), Eur. Phys. J. **C73**, 1, 2261 (2013), [arXiv:1207.5644].

[79] G. Aad *et al.* (ATLAS), Phys. Rev. **D90**, 7, 072004 (2014), [arXiv:1407.0371].

[80] G. Aad *et al.* (ATLAS), JHEP **06**, 100 (2015), [arXiv:1502.05923].

[81] S. Chatrchyan *et al.* (CMS), Eur. Phys. J. **C73**, 3, 2339 (2013), [arXiv:1211.2220].

[82] M. Aaboud *et al.* (ATLAS), Phys. Rev. **D94**, 9, 092003 (2016), [arXiv:1607.07281].

[83] G. Aad *et al.* (ATLAS), Eur. Phys. J. **C76**, 10, 538 (2016), [arXiv:1511.04716].

[84] G. Aad *et al.* (ATLAS), Phys. Rev. **D93**, 3, 032009 (2016), [arXiv:1510.03818].

[85] V. Khachatryan *et al.* (CMS), Phys. Rev. **D94**, 5, 052006 (2016), [arXiv:1607.00837].

[86] A. M. Sirunyan *et al.* (CMS), Eur. Phys. J. **C77**, 7, 459 (2017), [arXiv:1703.01630].

[87] V. Khachatryan *et al.* (CMS), Phys. Rev. **D94**, 7, 072002 (2016), [arXiv:1605.00116].

[88] V. Khachatryan *et al.* (CMS), Eur. Phys. J. **C75**, 11, 542 (2015), [arXiv:1505.04480].

[89] V. Khachatryan *et al.* (CMS), Eur. Phys. J. **C76**, 3, 128 (2016), [arXiv:1509.06076].

[90] M. Aaboud *et al.* (ATLAS), Eur. Phys. J. **C77**, 5, 292 (2017), [arXiv:1612.05220].

[91] M. Aaboud *et al.* (ATLAS), JHEP **11**, 191 (2017), [arXiv:1708.00727].

[92] M. Aaboud *et al.* (ATLAS), Phys. Rev. **D98**, 1, 012003 (2018), [arXiv:1801.02052].

[93] G. Aad *et al.* (ATLAS), Eur. Phys. J. C **79**, 12, 1028 (2019), [Erratum: Eur.Phys.J.C 80, 1092 (2020)], [arXiv:1908.07305].

[94] ATLAS Collab., ATLAS-CONF-2021-031.

[95] G. Aad *et al.* (ATLAS), JHEP **01**, 033 (2021), [arXiv:2006.09274].

[96] CMS Collab., CMS-PAS-TOP-15-010.

[97] A. M. Sirunyan *et al.* (CMS), JHEP **04**, 060 (2018), [arXiv:1708.07638].

[98] V. Khachatryan *et al.* (CMS), Phys. Rev. **D95**, 9, 092001 (2017), [arXiv:1610.04191].

[99] A. M. Sirunyan *et al.* (CMS), JHEP **06**, 002 (2018), [arXiv:1803.03991].

[100] A. M. Sirunyan *et al.* (CMS), Phys. Rev. **D97**, 11, 112003 (2018), [arXiv:1803.08856].

[101] A. M. Sirunyan *et al.* (CMS), JHEP **02**, 149 (2019), [arXiv:1811.06625].

[102] A. M. Sirunyan *et al.* (CMS), Eur. Phys. J. C **80**, 7, 658 (2020), [arXiv:1904.05237].

[103] A. M. Sirunyan *et al.* (CMS), Phys. Rev. D **103**, 5, 052008 (2021), [arXiv:2008.07860].

[104] G. Aad *et al.* (ATLAS), Eur. Phys. J. **C76**, 1, 11 (2016), [arXiv:1508.06868].

[105] G. Aad *et al.* (ATLAS), JHEP **01**, 020 (2015), [arXiv:1407.0891].

[106] S. Chatrchyan *et al.* (CMS), Eur. Phys. J. **C74**, 3014 (2015), [Erratum: Eur. Phys. J.C75,no.5,216(2015)], [arXiv:1404.3171].

[107] V. Khachatryan *et al.* (CMS), Phys. Lett. **B746**, 132 (2015), [arXiv:1411.5621].

[108] G. Aad *et al.* (ATLAS), Phys. Rev. **D92**, 7, 072005 (2015), [arXiv:1506.05074].

[109] G. Aad *et al.* (ATLAS), Nature Phys. **17**, 7, 813 (2021).

[110] ATLAS Collab., ATLAS-CONF-2020-050.

[111] A. M. Sirunyan *et al.* (CMS), Phys. Rev. D **102**, 9, 092013 (2020), [arXiv:2009.07123].

[112] M. Aaboud *et al.* (ATLAS), JHEP **04**, 046 (2019), [arXiv:1811.12113].

[113] A. M. Sirunyan *et al.* (CMS), Phys. Lett. **B776**, 355 (2018), [arXiv:1705.10141].

[114] A. M. Sirunyan *et al.* (CMS), JHEP **07**, 125 (2020), [arXiv:2003.06467].

[115] A. M. Sirunyan *et al.* (CMS) (2019), [arXiv:1909.05306].

[116] A. M. Sirunyan *et al.* (CMS), Phys. Lett. B **803**, 135285 (2020), [arXiv:1909.05306].

[117] A. M. Sirunyan *et al.* (CMS), Phys. Lett. B **820**, 136565 (2021), [arXiv:2012.09225].

[118] R. Frederix, D. Pagani and M. Zaro, JHEP **02**, 031 (2018), [arXiv:1711.02116].

[119] G. Aad *et al.* (ATLAS), Eur. Phys. J. C **80**, 11, 1085 (2020), [arXiv:2007.14858].

[120] G. Aad *et al.* (ATLAS) (2021), [arXiv:2106.11683].

[121] A. M. Sirunyan *et al.* (CMS), Eur. Phys. J. C **80**, 2, 75 (2020), [arXiv:1908.06463].

[122] A. M. Sirunyan *et al.* (CMS), JHEP **11**, 082 (2019), [arXiv:1906.02805].

[123] V. M. Abazov *et al.* (D0), Phys. Rev. Lett. **103**, 092001 (2009), [arXiv:0903.0850]; V. M. Abazov *et al.* (D0), Phys. Rev. **D78**, 012005 (2008), [arXiv:0803.0739]; V. M. Abazov *et al.* (D0), Phys. Rev. Lett. **98**, 181802 (2007), [hep-ex/0612052].

[124] T. Aaltonen *et al.* (CDF), Phys. Rev. Lett. **103**, 092002 (2009), [arXiv:0903.0885]; T. Aaltonen *et al.* (CDF), Phys. Rev. **D81**, 072003 (2010), [arXiv:1001.4577].

[125] T. Aaltonen *et al.* (CDF), Phys. Rev. **D82**, 112005 (2010), [arXiv:1004.1181].

[126] A. Heinson and T. R. Junk, Ann. Rev. Nucl. Part. Sci. **61**, 171 (2011), [arXiv:1101.1275].

[127] Tevatron Electroweak Working Group, (2009), [arXiv:0908.2171].

[128] N. Kidonakis, Phys. Rev. **D83**, 091503 (2011), [arXiv:1103.2792].

[129] CDF Collab., CDF conference note 11113 (2014), DØ Collab., DØ conference note 6448 (2014).

[130] T. A. Aaltonen *et al.* (CDF, D0), Phys. Rev. Lett. **115**, 15, 152003 (2015), [arXiv:1503.05027].

[131] T. A. Aaltonen *et al.* (CDF, D0), Phys. Rev. Lett. **112**, 231803 (2014), [arXiv:1402.5126].

[132] G. Aad *et al.* (ATLAS), Phys. Rev. **D90**, 11, 112006 (2014), [arXiv:1406.7844].

[133] G. Aad *et al.* (ATLAS), Phys. Lett. **B717**, 330 (2012), [arXiv:1205.3130].

[134] S. Chatrchyan *et al.* (CMS), JHEP **12**, 035 (2012), [arXiv:1209.4533].

[135] M. Aaboud *et al.* (ATLAS), Eur. Phys. J. **C77**, 8, 531 (2017), [arXiv:1702.02859].

[136] M. Aaboud *et al.* (ATLAS), JHEP **04**, 124 (2017), [arXiv:1702.08309].

[137] V. Khachatryan *et al.* (CMS), JHEP **06**, 090 (2014), [arXiv:1403.7366].
[138] CMS Collab., CMS-PAS-TOP-15-007.
[139] M. Aaboud *et al.* (ATLAS), JHEP **04**, 086 (2017), [arXiv:1609.03920].
[140] A. M. Sirunyan *et al.* (CMS), Phys. Lett. **B772**, 752 (2017), [arXiv:1610.00678].
[141] A. M. Sirunyan *et al.* (CMS), Phys. Lett. B **800**, 135042 (2020), [arXiv:1812.10514].
[142] A. M. Sirunyan *et al.* (CMS), Phys. Lett. B **808**, 135609 (2020), [arXiv:2004.12181].
[143] C. D. White *et al.*, JHEP **11**, 074 (2009), [arXiv:0908.0631].
[144] S. Frixione *et al.*, JHEP **07**, 029 (2008), [arXiv:0805.3067].
[145] G. Aad *et al.* (ATLAS), Phys. Lett. **B716**, 142 (2012), [arXiv:1205.5764].
[146] S. Chatrchyan *et al.* (CMS), Phys. Rev. Lett. **110**, 022003 (2013), [arXiv:1209.3489].
[147] G. Aad *et al.* (ATLAS), JHEP **01**, 064 (2016), [arXiv:1510.03752].
[148] M. Aaboud *et al.* (ATLAS, CMS), JHEP **05**, 088 (2019), [arXiv:1902.07158].
[149] G. Aad *et al.* (ATLAS), Eur. Phys. J. C **81**, 8, 720 (2021), [arXiv:2007.01554].
[150] S. Chatrchyan *et al.* (CMS), Phys. Rev. Lett. **112**, 23, 231802 (2014), [arXiv:1401.2942].
[151] M. Aaboud *et al.* (ATLAS), JHEP **01**, 063 (2018), [arXiv:1612.07231].
[152] A. M. Sirunyan *et al.* (CMS), JHEP **10**, 117 (2018), [arXiv:1805.07399].
[153] A. Tumasyan *et al.* (CMS) (2021), [arXiv:2109.01706].
[154] ATLAS Collab., ATLAS-CONF-2011-118.
[155] G. Aad *et al.* (ATLAS), Phys. Lett. **B756**, 228 (2016), [arXiv:1511.05980].
[156] V. Khachatryan *et al.* (CMS), JHEP **09**, 027 (2016), [arXiv:1603.02555].
[157] M. Aaboud *et al.* (ATLAS, CMS), JHEP **05**, 088 (2019), [arXiv:1902.07158].
[158] CMS Collab., CMS-PAS-TOP-14-004.
[159] CMS Collab., CMS-PAS-TOP-13-001.
[160] A. M. Sirunyan *et al.* (CMS), Eur. Phys. J. C **80**, 5, 370 (2020), [arXiv:1907.08330].
[161] M. Aaboud *et al.* (ATLAS), Eur. Phys. J. C **78**, 3, 186 (2018), [arXiv:1712.01602].
[162] CMS Collab., CMS-PAS-TOP-19-003.
[163] M. Czakon, P. Fiedler and A. Mitov, Phys. Rev. Lett. **115**, 5, 052001 (2015), [arXiv:1411.3007].
[164] W. Hollik and D. Pagani, Phys. Rev. **D84**, 093003 (2011), [arXiv:1107.2606].
[165] W. Bernreuther and Z.-G. Si, Phys. Rev. **D86**, 034026 (2012), [arXiv:1205.6580].
[166] S. Jung *et al.*, Phys. Rev. **D81**, 015004 (2010), [arXiv:0907.4112].
[167] V. M. Abazov *et al.* (D0), Phys. Rev. Lett. **100**, 142002 (2008), [arXiv:0712.0851].
[168] T. Aaltonen *et al.* (CDF), Phys. Rev. Lett. **101**, 202001 (2008), [arXiv:0806.2472].
[169] T. A. Aaltonen *et al.* (CDF, D0), Phys. Rev. Lett. **120**, 4, 042001 (2018), [arXiv:1709.04894].
[170] G. Aad *et al.* (ATLAS), JHEP **02**, 107 (2014), [arXiv:1311.6724].
[171] G. Aad *et al.* (ATLAS), Eur. Phys. J. **C76**, 2, 87 (2016), [Erratum: Eur. Phys. J.C77,564(2017)], [arXiv:1509.02358].
[172] G. Aad *et al.* (ATLAS), Phys. Rev. **D94**, 3, 032006 (2016), [arXiv:1604.05538].
[173] S. Chatrchyan *et al.* (CMS), Phys. Lett. **B717**, 129 (2012), [arXiv:1207.0065].
[174] V. Khachatryan *et al.* (CMS), Phys. Rev. **D93**, 3, 034014 (2016), [arXiv:1508.03862].

[175] V. Khachatryan *et al.* (CMS), Phys. Lett. **B760**, 365 (2016), [arXiv:1603.06221].
[176] M. Czakon *et al.*, Phys. Rev. **D98**, 1, 014003 (2018), [arXiv:1711.03945].
[177] V. Khachatryan *et al.* (CMS), Phys. Lett. **B757**, 154 (2016), [arXiv:1507.03119].
[178] G. Aad *et al.* (ATLAS), Phys. Lett. **B756**, 52 (2016), [arXiv:1512.06092].
[179] G. Aad *et al.* (ATLAS), JHEP **05**, 061 (2015), [arXiv:1501.07383].
[180] S. Chatrchyan *et al.* (CMS), JHEP **04**, 191 (2014), [arXiv:1402.3803].
[181] M. Aaboud *et al.* (ATLAS, CMS), JHEP **04**, 033 (2018), [arXiv:1709.05327].
[182] ATLAS Collab., ATLAS-CONF-2019-026.
[183] CMS Collab., CMS-PAS-TOP-15-018.
[184] G. Aad *et al.* (ATLAS) (2021), [arXiv:2110.05453].
[185] F. Abe *et al.* (CDF), Phys. Rev. **D50**, 2966 (1994).
[186] A. Abulencia *et al.* (CDF), Phys. Rev. **D73**, 032003 (2006), [hep-ex/0510048].
[187] M. Aaboud *et al.* (ATLAS), Eur. Phys. J. **C79**, 4, 290 (2019), [arXiv:1810.01772].
[188] V. Khachatryan *et al.* (CMS), Phys. Rev. **D93**, 7, 072004 (2016), [arXiv:1509.04044].
[189] A. M. Sirunyan *et al.* (CMS), Eur. Phys. J. **C78**, 11, 891 (2018), [arXiv:1805.01428].
[190] S. Argyropoulos and T. Sjöstrand, JHEP **11**, 043 (2014), [arXiv:1407.6653].
[191] J. R. Christiansen and P. Z. Skands, JHEP **08**, 003 (2015), [arXiv:1505.01681].
[192] A. M. Sirunyan *et al.* (CMS), Phys. Rev. Lett. **124**, 20, 202001 (2020), [arXiv:1911.03800].
[193] V. M. Abazov *et al.* (D0), Nature **429**, 638 (2004), [hep-ex/0406031].
[194] K. Kondo, T. Chikamatsu and S. H. Kim, J. Phys. Soc. Jap. **62**, 1177 (1993).
[195] R. H. Dalitz and G. R. Goldstein, Phys. Rev. **D45**, 1531 (1992); R. H. Dalitz and G. R. Goldstein, Phys. Lett. **B287**, 225 (1992).
[196] V. M. Abazov *et al.* (D0), Phys. Rev. Lett. **113**, 032002 (2014), [arXiv:1405.1756].
[197] L. Sonnenschein, Phys. Rev. **D73**, 054015 (2006), [Erratum: Phys. Rev.D78,079902(2008)], [hep-ph/0603011].
[198] G. Aad *et al.* (ATLAS), Eur. Phys. J. **C75**, 7, 330 (2015), [arXiv:1503.05427].
[199] A. M. Sirunyan *et al.* (CMS), Phys. Rev. **D96**, 3, 032002 (2017), [arXiv:1704.06142].
[200] C. G. Lester and D. J. Summers, Phys. Lett. **B463**, 99 (1999), [hep-ph/9906349].
[201] A. M. Sirunyan *et al.* (CMS), Eur. Phys. J. **C79**, 4, 313 (2019), [arXiv:1812.10534].
[202] M. Aaboud *et al.* (ATLAS), JHEP **09**, 118 (2017), [arXiv:1702.07546].
[203] CMS Collab., CMS-PAS-TOP-19-009.
[204] The Tevatron Electroweak Working Group and Aaltonen, T., For the CDF and D0 Collab., arXiv:1608.01881, FERMILAB-CONF-16-298-E.
[205] B. Abbott *et al.* (D0), Phys. Rev. **D60**, 052001 (1999), [hep-ex/9808029]; F. Abe *et al.* (CDF), Phys. Rev. Lett. **82**, 271 (1999), [Erratum: Phys. Rev. Lett.82,2808(1999)], [hep-ex/9810029].
[206] T. Aaltonen *et al.* (CDF), Phys. Rev. **D92**, 3, 032003 (2015), [arXiv:1505.00500].
[207] T. A. Aaltonen *et al.* (CDF), Phys. Rev. **D90**, 9, 091101 (2014), [arXiv:1409.4906].
[208] A. M. Sirunyan *et al.* (CMS), Eur. Phys. J. **C77**, 5, 354 (2017), [arXiv:1703.02530].
[209] T. Aaltonen *et al.* (CDF), Phys. Lett. **B698**, 371 (2011), [arXiv:1101.4926].
[210] CMS Collab., CMS-PAS-TOP-12-030.

[211] T. Aaltonen *et al.* (CDF), Phys. Rev. **D80**, 051104 (2009), [arXiv:0906.5371].

[212] ATLAS Collab., ATLAS-CONF-2019-046.

[213] V. Khachatryan *et al.* (CMS), Phys. Rev. **D93**, 9, 092006 (2016), [arXiv:1603.06536].

[214] V. Khachatryan *et al.* (CMS), JHEP **12**, 123 (2016), [arXiv:1608.03560].

[215] CMS Collab., CMS-PAS-TOP-15-002.

[216] CMS Collab., CMS-PAS-TOP-16-002.

[217] V. M. Abazov *et al.* (D0), Phys. Rev. Lett. **100**, 192004 (2008), [arXiv:0803.2779]; S. Chatrchyan *et al.* (CMS), Phys. Lett. **B728**, 496 (2014), [Erratum: Phys. Lett.B738,526(2014)], [arXiv:1307.1907]; V. M. Abazov *et al.* (D0), Phys. Lett. **B703**, 422 (2011), [arXiv:1104.2887]; ATLAS Collab., ATLAS-CONF-2019-041; U. Langenfeld, S. Moch and P. Uwer, Phys. Rev. **D80**, 054009 (2009), [arXiv:0906.5273]; J. Fuster *et al.*, Eur. Phys. J. C **77**, 11, 794 (2017), [arXiv:1704.00540].

[218] G. Aad *et al.* (ATLAS) (2019), [arXiv:1905.02302].

[219] CMS Collab., CMS-PAS-TOP-13-006 (2016).

[220] CDF Collab., CDF conference note 11080 (2014).

[221] V. M. Abazov *et al.* (D0), Phys. Rev. **D91**, 11, 112003 (2015), [arXiv:1501.07912].

[222] CMS Collab., CMS-PAS-TOP-13-005.

[223] A. H. Hoang, Ann. Rev. Nucl. Part. Sci. **70**, 225 (2020), [arXiv:2004.12915].

[224] M. Beneke *et al.*, Phys. Lett. **B775**, 63 (2017), [arXiv:1605.03609].

[225] A. H. Hoang, C. Lepenik and M. Preisser, JHEP **09**, 099 (2017), [arXiv:1706.08526].

[226] A. H. Hoang *et al.*, Phys. Rev. Lett. **101**, 151602 (2008), [arXiv:0803.4214].

[227] ATLAS Collab., ATL-PHYS-PUB-2021-034.

[228] A. M. Sirunyan *et al.*, Physics Letters B **803**, 135263 (2020), [arXiv:1909.09193].

[229] S. Catani *et al.*, JHEP **08**, 08, 027 (2020), [arXiv:2005.00557].

[230] G. Aad *et al.* (ATLAS), Phys. Lett. **B716**, 1 (2012), [arXiv:1207.7214].

[231] S. Chatrchyan *et al.* (CMS), Phys. Lett. **B716**, 30 (2012), [arXiv:1207.7235].

[232] G. Degrassi *et al.*, JHEP **08**, 098 (2012), [arXiv:1205.6497].

[233] S. Alekhin, A. Djouadi and S. Moch, Phys. Lett. **B716**, 214 (2012), [arXiv:1207.0980].

[234] T. Aaltonen *et al.* (CDF), Phys. Rev. **D87**, 5, 052013 (2013), [arXiv:1210.6131].

[235] V. M. Abazov *et al.* (D0), Phys. Rev. **D84**, 052005 (2011), [arXiv:1106.2063].

[236] G. Aad *et al.* (ATLAS), Phys. Lett. **B728**, 363 (2014), [arXiv:1310.6527].

[237] S. Chatrchyan *et al.* (CMS), JHEP **06**, 109 (2012), [arXiv:1204.2807].

[238] S. Chatrchyan *et al.* (CMS), Phys. Lett. **B770**, 50 (2017), [arXiv:1610.09551].

[239] G. Mahlon and S. J. Parke, Phys. Rev. **D53**, 4886 (1996), [hep-ph/9512264]; G. Mahlon and S. J. Parke, Phys. Lett. **B411**, 173 (1997), [hep-ph/9706304].

[240] G.R. Goldstein, in *Spin 96: Proceedings of the 12th International Symposium on High Energy Spin Physics,* Amsterdam, 1996, ed. C.W. Jager (World Scientific, Singapore, 1997), p. 328.

[241] T. Stelzer and S. Willenbrock, Phys. Lett. **B374**, 169 (1996), [hep-ph/9512292].

[242] W. Bernreuther *et al.*, Nucl. Phys. **B690**, 81 (2004), [hep-ph/0403035].

[243] A. Brandenburg, Z. G. Si and P. Uwer, Phys. Lett. **B539**, 235 (2002), [hep-ph/0205023].

[244] CDF Collab., CDF conference note 10719 (2011).
[245] CDF Collab., CDF conference note 10211 (2010).
[246] V. M. Abazov *et al.* (D0), Phys. Lett. **B757**, 199 (2016), [arXiv:1512.08818].
[247] V. M. Abazov *et al.* (D0), Phys. Rev. **D95**, 1, 011101 (2017), [arXiv:1607.07627].
[248] V. M. Abazov *et al.* (D0), Phys. Rev. **D92**, 052007 (2015), [arXiv:1507.05666].
[249] G. Mahlon and S. J. Parke, Phys. Rev. **D81**, 074024 (2010), [arXiv:1001.3422].
[250] G. Aad *et al.* (ATLAS), Phys. Rev. **D90**, 11, 112016 (2014), [arXiv:1407.4314].
[251] G. Aad *et al.* (ATLAS), Phys. Rev. Lett. **114**, 14, 142001 (2015), [arXiv:1412.4742].
[252] G. Aad *et al.* (ATLAS), Phys. Rev. **D93**, 1, 012002 (2016), [arXiv:1510.07478].
[253] S. Chatrchyan *et al.* (CMS), Phys. Rev. Lett. **112**, 18, 182001 (2014), [arXiv:1311.3924].
[254] V. Khachatryan *et al.* (CMS), Phys. Lett. **B758**, 321 (2016), [arXiv:1511.06170].
[255] V. Khachatryan *et al.* (CMS), Phys. Rev. **D93**, 5, 052007 (2016), [arXiv:1601.01107].
[256] M. Aaboud *et al.* (ATLAS), Eur. Phys. J. C **80**, 8, 754 (2020), [arXiv:1903.07570].
[257] A. M. Sirunyan *et al.* (CMS), Phys. Rev. **D100**, 7, 072002 (2019), [arXiv:1907.03729].
[258] W. Bernreuther, D. Heisler and Z.-G. Si, JHEP **12**, 026 (2015), [arXiv:1508.05271].
[259] M. Aaboud *et al.* (ATLAS), JHEP **03**, 113 (2017), [arXiv:1612.07004].
[260] A. F. Falk and M. E. Peskin, Phys. Rev. **D49**, 3320 (1994), [hep-ph/9308241].
[261] T. A. Aaltonen *et al.* (CDF), Phys. Rev. Lett. **111**, 20, 202001 (2013), [arXiv:1308.4050].
[262] CMS Collab., CMS-PAS-TOP-16-019.
[263] M. Aaboud *et al.* (ATLAS), Eur. Phys. J. **C78**, 2, 129 (2018), [arXiv:1709.04207].
[264] ATLAS Collab., ATLAS-CONF-2019-038.
[265] V. M. Abazov *et al.* (D0), Phys. Rev. **D85**, 091104 (2012), [arXiv:1201.4156].
[266] G. L. Kane, G. A. Ladinsky and C. P. Yuan, Phys. Rev. **D45**, 124 (1992).
[267] A. Czarnecki, J. G. Korner and J. H. Piclum, Phys. Rev. **D81**, 111503 (2010), [arXiv:1005.2625].
[268] T. Aaltonen *et al.* (CDF, D0), Phys. Rev. **D85**, 071106 (2012), [arXiv:1202.5272].
[269] G. Aad *et al.* (ATLAS), JHEP **06**, 088 (2012), [arXiv:1205.2484].
[270] S. Chatrchyan *et al.* (CMS), JHEP **10**, 167 (2013), [arXiv:1308.3879].
[271] ATLAS and CMS Collab., ATLAS-CONF-2013-033, CMS-PAS-TOP-12-025.
[272] M. Aaboud *et al.* (ATLAS), Eur. Phys. J. **C77**, 4, 264 (2017), [Erratum: Eur. Phys. J.C79,no.1,19(2019)], [arXiv:1612.02577].
[273] V. Khachatryan *et al.* (CMS), Phys. Lett. **B762**, 512 (2016), [arXiv:1605.09047].
[274] CMS Collab., CMS-PAS-TOP-14-017.
[275] V. Khachatryan *et al.* (CMS), JHEP **01**, 053 (2015), [arXiv:1410.1154].
[276] G. Aad *et al.* (CMS, ATLAS), JHEP **08**, 08, 051 (2020), [arXiv:2005.03799].
[277] T. Aaltonen *et al.* (CDF), Phys. Rev. **D87**, 3, 031104 (2013), [arXiv:1211.4523].
[278] D. Choudhury, T. M. P. Tait and C. E. M. Wagner, Phys. Rev. **D65**, 053002 (2002), [hep-ph/0109097].

[279] D. Chang, W.-F. Chang and E. Ma, Phys. Rev. **D59**, 091503 (1999), [hep-ph/9810531]; D. Chang, W.-F. Chang and E. Ma, Phys. Rev. **D61**, 037301 (2000), [hep-ph/9909537].

[280] T. Aaltonen *et al.* (CDF), Phys. Rev. **D88**, 3, 032003 (2013), [arXiv:1304.4141].

[281] V. M. Abazov *et al.* (D0), Phys. Rev. **D90**, 5, 051101 (2014), [Erratum: Phys. Rev.D90,no.7,079904(2014)], [arXiv:1407.4837].

[282] G. Aad *et al.* (ATLAS), JHEP **11**, 031 (2013), [arXiv:1307.4568].

[283] CMS Collab., CMS-PAS-TOP-11-031.

[284] T. Aaltonen *et al.* (CDF), Phys. Rev. **D84**, 031104 (2011), [arXiv:1106.3970].

[285] G. Aad *et al.* (ATLAS), Phys. Rev. **D91**, 7, 072007 (2015), [arXiv:1502.00586].

[286] M. Aaboud *et al.* (ATLAS), JHEP **11**, 086 (2017), [arXiv:1706.03046].

[287] K. Melnikov, M. Schulze and A. Scharf, Phys. Rev. **D83**, 074013 (2011), [arXiv:1102.1967].

[288] A. M. Sirunyan *et al.* (CMS), JHEP **10**, 006 (2017), [arXiv:1706.08128].

[289] M. Aaboud *et al.* (ATLAS), Eur. Phys. J. **C79**, 5, 382 (2019), [arXiv:1812.01697].

[290] G. Bevilacqua *et al.*, JHEP **10**, 158 (2018), [arXiv:1803.09916].

[291] G. Bevilacqua *et al.*, JHEP **01**, 188 (2019), [arXiv:1809.08562].

[292] G. Aad *et al.* (ATLAS), JHEP **09**, 049 (2020), [arXiv:2007.06946].

[293] A. M. Sirunyan *et al.* (CMS), Phys. Lett. **B779**, 358 (2018), [arXiv:1712.02825].

[294] A. Tumasyan *et al.* (CMS) (2021), [arXiv:2107.01508].

[295] CMS Collab., CMS-PAS-TOP-21-004.

[296] A. M. Sirunyan *et al.* (CMS), Phys. Rev. Lett. **121**, 22, 221802 (2018), [arXiv:1808.02913].

[297] M. Cepeda *et al.* (HL/HE WG2 group) (2019), [arXiv:1902.00134].

[298] S. Chatrchyan *et al.* (CMS), Phys. Rev. Lett. **110**, 172002 (2013), [arXiv:1303.3239].

[299] J. M. Campbell and R. K. Ellis, JHEP **07**, 052 (2012), [arXiv:1204.5678].

[300] M. V. Garzelli *et al.*, JHEP **11**, 056 (2012), [arXiv:1208.2665].

[301] ATLAS Collab., ATLAS-CONF-2012-126.

[302] G. Aad *et al.* (ATLAS), JHEP **11**, 172 (2015), [arXiv:1509.05276].

[303] V. Khachatryan *et al.* (CMS), JHEP **01**, 096 (2016), [arXiv:1510.01131].

[304] M. Aaboud *et al.* (ATLAS), Phys. Rev. **D99**, 7, 072009 (2019), [arXiv:1901.03584].

[305] A. Broggio *et al.*, JHEP **08**, 039 (2019), [arXiv:1907.04343].

[306] G. Aad *et al.* (ATLAS), Eur. Phys. J. C **81**, 737 (2021), [arXiv:2103.12603].

[307] A. M. Sirunyan *et al.* (CMS), JHEP **08**, 011 (2018), [arXiv:1711.02547].

[308] A. M. Sirunyan *et al.* (CMS), JHEP **03**, 056 (2020), [arXiv:1907.11270].

[309] A. M. Sirunyan *et al.* (CMS), JHEP **07**, 003 (2017), [arXiv:1702.01404].

[310] CMS Collab., CMS-PAS-TOP-20-010.

[311] G. Aad *et al.* (ATLAS), JHEP **07**, 124 (2020), [arXiv:2002.07546].

[312] S. P. Martin 1–98 (1997), [Adv. Ser. Direct. High Energy Phys.18,1(1998)], [hep-ph/9709356].

[313] C. T. Hill and E. H. Simmons, Phys. Rept. **381**, 235 (2003), [Erratum: Phys. Rept.390,553(2004)], [hep-ph/0203079].

[314] C. T. Hill, Phys. Lett. **B266**, 419 (1991).

[315] C. T. Hill, Phys. Lett. **B345**, 483 (1995), [hep-ph/9411426].

[316] A. M. Sirunyan *et al.* (CMS) (2019), [arXiv:1908.06463].

[317] C. Zhang and S. Willenbrock, Phys. Rev. **D83**, 034006 (2011), [arXiv:1008.3869].

[318] J. A. Aguilar-Saavedra, Nucl. Phys. **B843**, 638 (2011), [Erratum: Nucl. Phys.B851,443(2011)], [arXiv:1008.3562].

[319] D. Barducci *et al.* (2018), [arXiv:1802.07237].

[320] M. Aaboud *et al.* (ATLAS), Phys. Rev. D **99**, 5, 052009 (2019), [arXiv:1811.02305].

[321] Technical report, CERN, Geneva (2019), all figures including auxiliary figures are available at https://atlas.web.cern.ch/Atlas/GROUPS/PHYSICS/CONFNOTES/ATLAS-CONF-2019-026, URL http://cds.cern.ch/record/2682109.

[322] Technical report, CERN, Geneva (2021), all figures including auxiliary figures are available at https://atlas.web.cern.ch/Atlas/GROUPS/PHYSICS/CONFNOTES/ATLAS-CONF-2021-027, URL http://cds.cern.ch/record/2773738.

[323] Technical report, CERN, Geneva (2021), all figures including auxiliary figures are available at https://atlas.web.cern.ch/Atlas/GROUPS/PHYSICS/CONFNOTES/ATLAS-CONF-2021-050, URL http://cds.cern.ch/record/2782534.

[324] A. M. Sirunyan *et al.* (CMS), JHEP **06**, 146 (2020), [arXiv:1912.09540].

[325] A. M. Sirunyan *et al.* (CMS), Eur. Phys. J. C **79**, 11, 886 (2019), [arXiv:1903.11144].

[326] Technical report, CERN, Geneva (2021), URL https://cds.cern.ch/record/2776770.

[327] A. M. Sirunyan *et al.* (CMS), JHEP **03**, 095 (2021), [arXiv:2012.04120].

[328] CMS Collab., CMS-PAS-TOP-18-007 (2020).

[329] Technical report, CERN, Geneva (2019), URL https://cds.cern.ch/record/2668721.

[330] A. Tumasyan *et al.* (CMS) (2021), [arXiv:2107.13896].

[331] A. Buckley *et al.*, JHEP **04**, 015 (2016), [arXiv:1512.03360].

[332] N. P. Hartland *et al.*, JHEP **04**, 100 (2019), [arXiv:1901.05965].

[333] I. Brivio *et al.* (2019), [arXiv:1910.03606].

[334] G. Durieux *et al.*, JHEP **12**, 98 (2019), [Erratum: JHEP 01, 195 (2021)], [arXiv:1907.10619].

[335] J. Ellis *et al.*, JHEP **04**, 279 (2021), [arXiv:2012.02779].

[336] J. J. Ethier *et al.* (2021), [arXiv:2105.00006].

[337] V. Miralles *et al.* (2021), [arXiv:2107.13917].

[338] V. Barger, T. Han and D. G. E. Walker, Phys. Rev. Lett. **100**, 031801 (2008), [hep-ph/0612016].

[339] R. Frederix and F. Maltoni, JHEP **01**, 047 (2009), [arXiv:0712.2355].

[340] T. Aaltonen *et al.* (CDF), Phys. Rev. Lett. **110**, 12, 121802 (2013), [arXiv:1211.5363].

[341] D. Acosta *et al.* (CDF), Phys. Rev. Lett. **94**, 211801 (2005), [hep-ex/0501050].

[342] T. Aaltonen *et al.* (CDF), Phys. Rev. **D84**, 072003 (2011), [arXiv:1108.4755].

[343] A. Altheimer *et al.*, J. Phys. **G39**, 063001 (2012), [arXiv:1201.0008].

[344] A. M. Sirunyan *et al.* (CMS), JHEP **04**, 031 (2019), [arXiv:1810.05905].

[345] A. M. Sirunyan *et al.* (CMS), JHEP **07**, 001 (2017), [arXiv:1704.03366].

[346] A. M. Sirunyan *et al.* (CMS), JHEP **04**, 171 (2020), [arXiv:1908.01115].

[347] M. Aaboud *et al.* (ATLAS), Eur. Phys. J. **C78**, 7, 565 (2018), [arXiv:1804.10823].

[348] G. Aad *et al.* (ATLAS), JHEP **10**, 061 (2020), [arXiv:2005.05138].

[349] A. M. Sirunyan *et al.* (CMS), Phys. Lett. **B777**, 39 (2018), [arXiv:1708.08539].

[350] A. M. Sirunyan *et al.* (CMS), Phys. Lett. **B781**, 574 (2018), [arXiv:1708.01062].

[351] A. M. Sirunyan *et al.* (CMS), JHEP **08**, 073 (2017), [arXiv:1705.10967].

[352] A. M. Sirunyan *et al.* (CMS), Phys. Lett. **B772**, 634 (2017), [arXiv:1701.08328].

[353] V. Khachatryan *et al.* (CMS), Phys. Lett. **B771**, 80 (2017), [arXiv:1612.00999].

[354] A. M. Sirunyan *et al.* (CMS), JHEP **04**, 136 (2017), [arXiv:1612.05336].

[355] A. M. Sirunyan *et al.* (CMS), JHEP **05**, 029 (2017), [arXiv:1701.07409].

[356] A. M. Sirunyan *et al.* (CMS), Phys. Lett. B **820**, 136535 (2021), [arXiv:2104.04831].

[357] A. M. Sirunyan *et al.* (CMS) (2021), [arXiv:2104.12853].

[358] A. M. Sirunyan *et al.* (CMS), Phys. Rev. D **102**, 112004 (2020), [arXiv:2008.09835].

[359] M. Aaboud *et al.* (ATLAS), Phys. Lett. **B788**, 347 (2019), [arXiv:1807.10473].

[360] G. Aad *et al.* (ATLAS), JHEP **06**, 145 (2021), [arXiv:2102.10076].

[361] Technical report, CERN, Geneva (2021), all figures including auxiliary figures are available at https://atlas.web.cern.ch/Atlas/GROUPS/PHYSICS/CONFNOTES/ATLAS-CONF-2021-024, URL `http://cds.cern.ch/record/2773300`.

[362] M. Aaboud *et al.* (ATLAS), Phys. Rev. Lett. **121**, 21, 211801 (2018), [arXiv:1808.02343].

[363] Technical report, CERN, Geneva (2021), all figures including auxiliary figures are available at https://atlas.web.cern.ch/Atlas/GROUPS/PHYSICS/CONFNOTES/ATLAS-CONF-2021-040, URL `http://cds.cern.ch/record/2779174`.

[364] M. Aaboud *et al.* (ATLAS), JHEP **05**, 164 (2019), [arXiv:1812.07343].

[365] M. Aaboud *et al.* (ATLAS), JHEP **05**, 041 (2019), [arXiv:1812.09743].

[366] ATLAS Collab., ATLAS-CONF-2021-018 (2021).

[367] ATLAS Collab., ATLAS-CONF-2018-024 (2018).

[368] CMS Collab. CMS-PAS-TOP-12-042 (2013).

[369] V. Khachatryan *et al.* (CMS), JHEP **06**, 121 (2015), [arXiv:1504.03198].

[370] A. M. Sirunyan *et al.* (CMS), Eur. Phys. J. **C77**, 12, 845 (2017), [arXiv:1706.02581].

[371] A. M. Sirunyan *et al.* (CMS), JHEP **03**, 141 (2019), [arXiv:1901.01553].

[372] G. Aad *et al.* (ATLAS), JHEP **04**, 165 (2021), [arXiv:2102.01444].

[373] G. Aad *et al.* (ATLAS), Eur. Phys. J. C **81**, 860 (2021), [arXiv:2011.09308].

[374] Technical report, CERN, Geneva (2021), all figures including auxiliary figures are available at https://atlas.web.cern.ch/Atlas/GROUPS/PHYSICS/CONFNOTES/ATLAS-CONF-2021-036, URL `http://cds.cern.ch/record/2777863`.

[375] J. A. Aguilar-Saavedra, Acta Phys. Polon. **B35**, 2695 (2004), [hep-ph/0409342].

[376] V. Khachatryan *et al.* (CMS), JHEP **02**, 028 (2017), [arXiv:1610.03545].

[377] CMS Collab., CMS-PAS-TOP-14-003.

[378] CMS Collab., CMS-PAS-TOP-17-003.

[379] V. Khachatryan *et al.* (CMS), JHEP **02**, 079 (2017), [arXiv:1610.04857].

[380] G. Aad *et al.* (ATLAS), Eur. Phys. J. **C76**, 2, 55 (2016), [arXiv:1509.00294].

[381] G. Aad *et al.* (ATLAS), Phys. Lett. **B800**, 135082 (2020), [arXiv:1908.08461].

[382] A. Heister *et al.* (ALEPH), Phys. Lett. **B543**, 173 (2002), [hep-ex/0206070]; J. Abdallah *et al.* (DELPHI), Phys. Lett. **B590**, 21 (2004), [hep-ex/0404014]; P. Achard *et al.* (L3), Phys. Lett. **B549**, 290 (2002), [hep-ex/0210041]; G. Abbiendi *et al.* (OPAL), Phys. Lett. **B521**, 181 (2001), [hep-ex/0110009].

[383] F. D. Aaron *et al.* (H1), Phys. Lett. **B678**, 450 (2009), [arXiv:0904.3876].

[384] H. Abramowicz *et al.* (ZEUS), Phys. Lett. **B708**, 27 (2012), [arXiv:1111.3901].

[385] M. Beneke *et al.*, in "1999 CERN Workshop on standard model physics (and more) at the LHC, CERN, Geneva, Switzerland, 25-26 May: Proceedings," 419–529 (2000), [hep-ph/0003033], URL `http://weblib.cern.ch/abstract?CERN-TH-2000-100`.

[386] V. F. Obraztsov, S. R. Slabospitsky and O. P. Yushchenko, Phys. Lett. **B426**, 393 (1998), [hep-ph/9712394].

[387] T. Carli, D. Dannheim and L. Bellagamba, Mod. Phys. Lett. **A19**, 1881 (2004), [hep-ph/0402012].

[388] V. M. Abazov *et al.* (D0), Phys. Rev. Lett. **102**, 092002 (2009), [arXiv:0901.0151].

[389] V.M. Abazov *et al.* (DØ Collab.), DØ conference note 5838 (2009).

[390] V. M. Abazov *et al.* (D0), Phys. Lett. **B708**, 21 (2012), [arXiv:1110.4592].

[391] ATLAS Collab., ATLAS-CONF-2013-032.

[392] T. Aaltonen *et al.* (CDF), Phys. Rev. Lett. **101**, 192002 (2008), [arXiv:0805.2109].

[393] V. M. Abazov *et al.* (D0), Phys. Lett. **B701**, 313 (2011), [arXiv:1103.4574].

[394] V. M. Abazov *et al.* (D0), Phys. Lett. **B693**, 81 (2010), [arXiv:1006.3575].

[395] S. Chatrchyan *et al.* (CMS), Phys. Rev. Lett. **112**, 17, 171802 (2014), [arXiv:1312.4194].

[396] A. M. Sirunyan *et al.* (CMS), JHEP **07**, 003 (2017), [arXiv:1702.01404].

[397] M. Aaboud *et al.* (ATLAS), JHEP **07**, 176 (2018), [arXiv:1803.09923].

[398] M. Aaboud *et al.* (ATLAS), Phys. Rev. D **98**, 11, 112010 (2018), [arXiv:1806.10555].

[399] A. M. Sirunyan *et al.* (CMS), JHEP **06**, 102 (2018), [arXiv:1712.02399].

[400] M. Aaboud *et al.* (ATLAS), JHEP **05**, 123 (2019), [arXiv:1812.11568].